UNIVERZITA KARLOVA V PRAZE

Přírodovědecká fakulta

Katedra parazitologie

Studijní program: Biologie

Studijní obor: Parazitologie

Bc. Michal Stoklasa

Organely mitochondriálního původu u diplomonád

Mitochondrion-related organelles in diplomonads

Diplomová práce

Školitel: prof. RNDr. Jan Tachezy, Ph.D.

Praha, 2019

Prohlášení:

Prohlašuji, že jsem závěrečnou práci zpracoval/a samostatně a že jsem uvedl/a všechny použité informační zdroje a literaturu. Tato práce ani její podstatná část nebyla předložena k získání jiného nebo stejného akademického titulu.

V Praze, 03.01.19

Podpis

Poděkování:

Především bych rád poděkoval svému školiteli prof. RNDr. Janu Tachezymu Ph.D. za jeho zpětnou vazbu a odborné rady během sepisování této práce a zároveň i za to, že mi umožnil na půl roku přerušit práci v laboratoři kvůli mému pobytu v Číně, který nijak nesouvisel s výzkumnou činností. Dále bych chtěl poděkovat členům naší laboratoře, jmenovitě hlavně Evě Nývltové, která se mě ujala už během bakalářského studia a naučila mě většinu metod použitých v této práci, Zdeňkovi Vernerovi za trpělivé zodpovídání mých všemožných dotazů a za jeho analytický přístup, díky kterému mi bylo všechno hned srozumitelnější a naší laborantce Míše Marcinčíkové za veškerou poskytnutou pomoc a vstřícnost. Nakonec děkuji svojí rodině, kamarádům a spolužákům za veškerou podporu.

Abstract

Order Diplomonadida includes parasitic and free-living species that adapted to the oxygen-poor environment. They possess reduced form of mitochondria (hydrogenosome or mitosome). These organelles lack Krebs cycle and membrane electron-transport chain. ATP synthesis by oxidative phosphorylation and other mitochondrial metabolic pathways are modified or entirely absent. Main difference between hydrogenosome and mitosome is synthesis of hydrogen using the enzyme hydrogenase and ATP synthesis by substrate level phosphorylation in hydrogenosomes that are absent in mitosomes. The most studied diplomonads are a human pathogen *Giardia intestinalis* possessing the mitosomes and a salmon parasite *Spironucleus salmonicida* with hydrogenosomes. This thesis was focused on determining the type of mitochondrial organelles in angelfish parasite *Spironucleus vortens* and free living *Hexamita sp.* It has not been described whether they possess the hydrogenosomes or the mitosomes so far.

In both protists transmission electron microscopy revealed presence of double membrane vesicles, possibly their mitochondrial organelles. Homologous *S. vortens* anti-hydrogenase and anti-HydE antibodies were produced and tested in order to determine their cellular localization. Using the western blot analysis and immunofluorescence microscopy, hydrogenase was detected in the cytosol whereas HydE in mitochondrial organelles of *S. vortens*. Moreover, expression of HydE, HydG and IscU recombinant proteins was performed. All three proteins were detected in the organellar fraction. These results suggest that *S. vortens* possesses mitochondrial organelles with characteristics corresponding to the mitosomes.

Hexamita sp. genomic DNA and total RNA was sequenced and the genome was partially assembled. Sequences of proteins involved in ATP synthesis, production of hydrogen, conversion of serine into glycine, H-cluster synthesis and Fe-S cluster synthesis were predicted to reside in the mitochondrial organelle of *Hexamita*. Based on this genome, mitochondrial organelle of *Hexamita sp.* was described as the hydrogenosome.

Abstrakt

Řád Diplomonadida zahrnuje parazitické i volně žijící prvoky, kteří se přizpůsobili prostředí s nedostatkem kyslíku. Jejich mitochondriální organely (hydrogenosom nebo mitosom) jsou redukované, neobsahují Krebsův cyklus nebo elektron-transportní řetězec a některé metabolické dráhy (jako například tvorba ATP pomocí oxidativní fosforylace) jsou zde modifikované nebo úplně chybí. Hlavními rozdíly mezi těmito dvěma organelami je hydrogenosomální produkce vodíku díky enzymu zvaném hydrogenáza a absence tvorby ATP substrátovou fosforylací v mitosomech. Nejvíce prostudované jsou mitosomy lidského patogena *Giardia intestinalis* a hydrogenosomy parazita lososů *Spironucleus salmonicida*. Tato práce byla zaměřena na střevního parazita skalár *Spironucleus vortens* a volně žijícího prvoka *Hexamita sp*. s cílem identifikovat typ jejich mitochondriálních organel, u kterých zatím není jasné, jestli mají spíše metabolismus hydrogenosomu či mitosomu.

Oba prvoci byli pozorováni transmisní elektronovou mikroskopií, pomocí které byly detekovány dvoumembránové váčky, patrně jejich mitochondriální organely. Dále byla připravena homologní protilátka proti hydrogenáze a hydrogenázové maturáze HydE u *S. vortens*. Hydrogenáza byla pomocí western blotu a imunofluorescenční mikroskopie detekována v cytosolu tohoto prvoka. Na druhou stranu HydE byl lokalizován v mitochondriálních organelách. Provedena byla také overexprese tří proteinů, HydE, HydG a IscU v buňkách *S. vortens*. Všechny tři proteiny byly detekovány v organelách. Tyto výsledky naznačují, že *S. vortens* pravděpodobně obsahuje mitosomy.

U prvoka *Hexamita sp.* byla sekvencována DNA a celková RNA, následně byla sestavena částečná sekvence genomu. V genomu byly nalezeny sekvence mitochondriálních proteinů účastnících se tvorby ATP, syntézy vodíku, H-clusteru a Fe-S center a proteinu katalyzujícího přeměnu serinu na glycin. Na základě této analýzy byla mitochondriální organela *Hexamita sp.* predikována jako hydrogenosom.

1. Introduction

Mitochondrion is one of the key organelles present in virtually all eukaryotic cells that has a vital role in many biochemical processes. Main function of mitochondrion is aerobic respiration that leads to adenosine triphosphate (ATP) production. This molecule is used as the source of energy for variety of metabolic pathways occurring inside the cell. However, there are other crucial mitochondrial processes, such as iron-sulfur (Fe-S) cluster biogenesis, biosynthesis of heme, lipids and steroids, apoptosis, amino acid and nucleotide metabolism, protein synthesis and β-oxidation of fatty acids.

Several species adapted to oxygen-limited environment that led to reductive evolution of their mitochondria. These mitochondrion-derived organelles have lost to various extend typical mitochondrial functions, such as respiratory chain, Krebs cycle or fatty acid metabolism. The two most reduced mitochondria called hydrogenosome and mitosome have even lost its own genome, furthermore, mitosome does not have any ATP production pathways. Diplomonadida is one of the groups adapted to anaerobiosis. Apart from having modified mitochondria, diplomonads possess double karyomastigont (karyomastigont = nucleus, 4 basal bodies of flagella and associated microtubules) and lack typical Golgi and peroxisomes. The most studied organisms from this group are *Giardia intestinalis* (human pathogen causing diarrhea) possessing mitosomes and *Spironucleus salmonicida* (salmon parasite) having the hydrogenosomes. However, much less data is available on other diplomonads. This thesis is focused mainly on fish parasite *Spironucleus vortens* and free-living protist *Hexamita sp*. As other diplomonads, these species possess unusual mitochondria, however very limited experimental data are available to define whether these organelles represent hydrogenosomes or mitosomes (Sterud and Poynton, 2002; Millet et al., 2013).

2. Review of literature

2.1. Types of mitochondria

Process of transformation of prokaryotic to eukaryotic cell called eukaryogenesis proceeded around 1,5 - 2 mld. years ago (Knoll et al., 2006). Several different hypotheses about the specific timing of mitochondrial origin were introduced. According to the 'mitochondria-early' hypotheses, origin of mitochondria could have triggered the whole eukaryogenesis or at least was one of the first steps in the prokaryotic cell transformation (Martin and Müller, 1998; Martin et al., 2015). On the other hand, 'mitochondria-late' hypotheses suggest, that some features of the eukaryotic cell had already evolved before acquisition of mitochondria (Cavalier-Smith, 1989; Martijn and Ettema, 2013; López-García et al., 2017).

Mitochondria originated via the process of endosymbiosis (Sagan, 1967; Schwartz and Dayhoff, 1978; Yang et al., 1985). The most recent analyses proposed that the host cell lineage was a close relative to a newly discovered group of Archaea, called Asgards (Spang et al., 2015; Zaremba-Niedzwiedzka et al., 2017). On the other hand, mitochondrial endosymbiont was related to the α-proteobacteria, however which specific lineage of these bacteria was the closest relative of mitochondria is still matter of discussion (Rodríguez-Ezpeleta and Embley, 2012; Wang and Wu, 2015; Martijn et al., 2018). After the engulfment, the autonomous endosymbiont had to undergo many specific changes in order to transform into the organelle such as genome reduction and endosymbiotic gene transfer to the nucleus, incorporation of the protein transport machinery into the outer and inner membrane and exchange and coordination of biochemical pathways between symbiont and host (Roger et al., 2017). Due to these transformation processes, most of the proteins targeted to contemporary mitochondria are encoded in the cell's nucleus and they are transported into the organelle post-translationally.

Several eukaryotic lineages live in an oxygen-poor environment and had to adapt their metabolism to the lack of oxygen, including the reduction of the mitochondrial biochemical pathways. Based of biochemical pathways and presence of the genome, mitochondria were classified into 5 different groups: aerobic mitochondria, anaerobic mitochondria, H_2-producing mitochondria, hydrogenosomes and mitosomes (Muller et al., 2012). However, the recently studied mitochondria in free-living protists like *Dysnectes brevis* don't fit into any of these categories and it seems that the reduced mitochondrial organelles exist as a functional

continuum from the aerobic mitochondrion to the mitosome (Leger et al., 2017). In the case of *Monocercomonoides sp.*, mitochondria have been lost completely (Karnkowska et al., 2016).

2.1.1. Aerobic mitochondrion

Vast majority of contemporary eukaryotes possess aerobic mitochondria. It is generally accepted that aerobic mitochondria derived from α-proteobacterial symbiont during the evolution of the eukaryotic cell (Sagan, 1967; Spang et al., 2015; Zaremba-Niedzwiedzka et al., 2017). All the other types of mitochondria are most likely derived from this aerobic type although anaerobic character of original mitochondria is still discussed (Martin and Müller, 1998; Martin et al., 2015).

The organelle is surrounded by two membranes (outer and inner) dividing mitochondrion into two parts, intermembrane space and matrix. Inner membrane forms specific folds called cristae, which enlarge the membrane surface to accommodate the respiratory chain. The mitochondrial membranes contain translocases TOM (translocase of the outer membrane) and TIM (translocase of the inner membrane), which are used for the import of mitochondrial pre-proteins from cytosol into organellar membrane, intermembrane space or matrix. Matrix mitochondrial pre-proteins usually have the N-terminal mitochondrial targeting sequences which enables the transport to the organelle (Neupert and Herrmann, 2007). Inside mitochondria, the targeting sequence is cleaved by mitochondrial processing peptidase (Yaffe et al., 1985).

Several biochemical pathways responsible for energy fixation in the form of ATP are present inside the organelle. ATP is then exported to the other compartments of the eukaryotic cell. First step of the eukaryotic cell energy metabolism occurs in the cytosol, where glycolysis takes place. In this process, glucose is catabolized into pyruvate, the main mitochondrial substrate. Then, pyruvate is transported into mitochondrial matrix via the pyruvate transporter (Herzig et al., 2012).

In matrix, pyruvate is oxidatively decarboxylated via pyruvate dehydrogenase (PDH) and forms acetyl-CoA, CO_2 and electrons. Acetyl-CoA then enters the citric acid cycle (Krebs cycle). This set of chemical reactions is responsible for decarboxylation and oxidation of citric acid while water, carbon dioxide and electrons are the end products of this cycle. The electrons

are crucial for the function of the electron transport chain (respiratory chain). NADH and $FADH_2$ coenzymes are used for the transport of electrons from the citric acid cycle to this chain. Electron transport chain is formed by 4 protein complexes, NADH: ubiquinone oxidoreductase (Complex I), succinate dehydrogenase (Complex II), ubiquinol-cytochrome c oxidoreductase (Complex III), cytochrome c oxidase (Complex IV) and is localized on the inner mitochondrial membrane.

The key molecule in this complicated process is oxygen. Oxygen is absorbed by the eukaryotic cell, transported into mitochondrial matrix and used as the final electron acceptor.

Ubiquinone and cytochrome c in the respiratory chain are responsible for the transport of electrons from reduced coenzymes to oxygen with formation of H_2O as byproduct. Protein complexes I, III and IV are transporting protons from matrix into intermembrane space which generates proton gradient. Finally, this gradient is used by ATP synthase (Complex V) for the ATP production by the oxidative phosphorylation.

Another source of energy is β-oxidation of fatty acids, which is one of the typical mitochondrial biochemical pathways. In order to cross both mitochondrial membranes, fatty acids have to bind carnitine in the cytosol. Carnitine serves as a carrier and is able to carry the fatty acid through the carnitine transporter into the matrix, where β-oxidation takes place. For every β-oxidation, two carbons are cleaved from the fatty acid and one acetyl-CoA is formed together with NADH and $FADH_2$ coenzymes. Acetyl-CoA enters the Krebs cycle and coenzymes are used for the electron transport to the respiratory chain complexes.

Apart from energy fixation, aerobic mitochondria are responsible for various biosynthetic pathways such as steroid, heme and biotin synthesis (Ajioka et al., 2006; Miller, 1995), metabolism of lipids and amino acids or formation of Fe-S clusters (Lill et al., 2005).

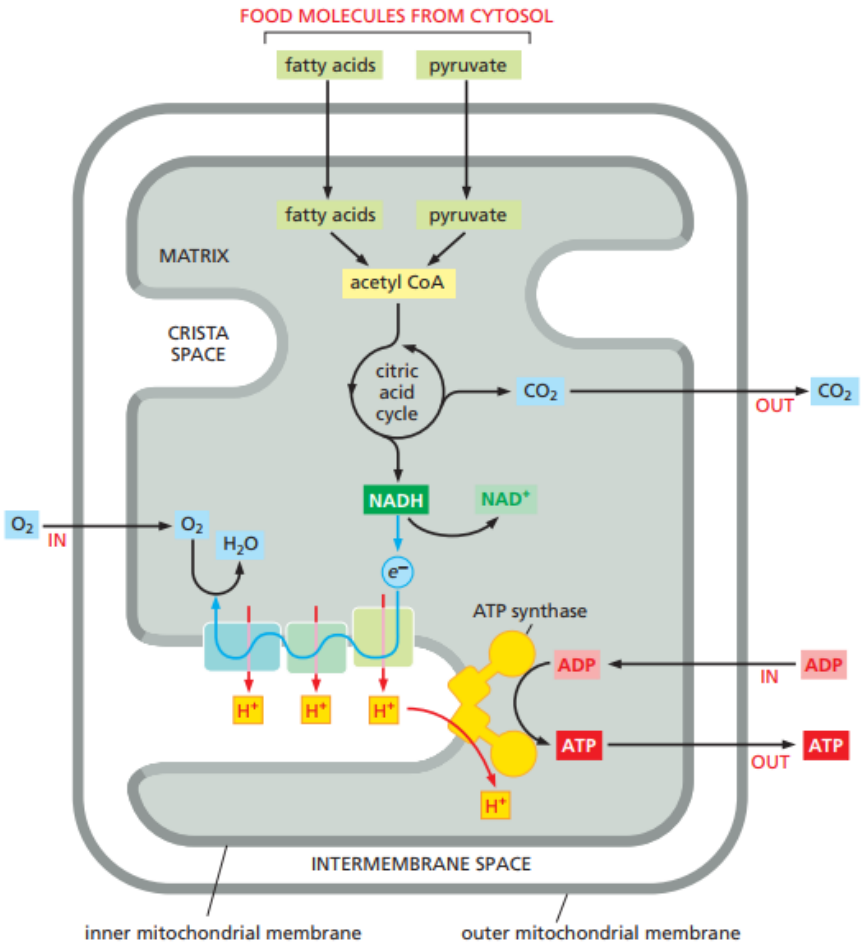

Figure 1. Overview of the energy metabolism in the aerobic mitochondria (Alberts et al., 2014).

2.1.2. Anaerobic mitochondrion

Organisms with anaerobic type of mitochondria are able to adapt its metabolism according to the amount of oxygen present in the environment. In the oxygen-rich surroundings, mitochondria work as the typical aerobic one. If the oxygen depletion occurs, some of the mitochondrial functions are changed. Fumarate, succinate and nitrate are used as the final electron acceptors instead of oxygen (Tielens, 1994; Kobayashi et al., 1996; Tielens et al., 2002). This type of mitochondrion does not use ubiquinone as the electron transporter, but instead possesses rhodoquinone, which transports the electrons from complex I to the fumarate reductase (the enzyme responsible for conversion of fumarate into one of the end products, succinate) (Takamiya et al., 1999). The other two metabolic end products in anaerobic mitochondria are acetate and propionate (Komuniecki et al., 1989; Muller et al., 2012).

Alternatively, pyruvate can be metabolized by pyruvate:$NADP^+$ oxidoreductase (PNO) or pyruvate formate lyase (PFL) (Inui et al., 1987; Mus et al., 2007). We can typicaly find anaerobic mitochondria in parasitic helminths (like *Ascaris lumbricoides* or *Fasciola hepatica*) and sea annelids (Tielens, 1994; Muller et al., 2012; Parvatham and Veerakumari, 2013). Surprisingly, anaerobic mitochondria were also discovered in two aerobic protists, *Euglena gracilis* and *Chlamydomonas reinhardtii* (Hoffmeister et al., 2004; Cardol, 2005). These organisms are able to switch their mitochondrial metabolism from aerobic to anaerobic one when they temporarily encounter low-oxygen environments.

2.1.3. H_2-producing mitochondrion

This organelle is basically a hybrid between anaerobic mitochondria and hydrogenosome. The electron transport chain is partially present (Complex I and II) and is used for generating the proton gradient. In case of *Brevimastigomonas*, several subunits of Complex V has also been found (Gawryluk et al., 2016). Furthermore, the organelle possess hydrogenase, anaerobic enzyme, which uses protons as a terminal electron acceptor and produces molecular hydrogen (Boxma et al., 2005). The organellar genome is still present. Pyruvate can be metabolized by PDH complex, PNO, PFL or pyruvate:ferredoxin oxidoreductase (PFO) (Lantsman et al., 2008; Muller et al., 2012; Youssef et al., 2013; Stairs et al., 2014). In H_2-producing mitochondria (and hydrogenosomes as well), ATP is generated by a process called substrate level phosphorylation. An acetate:succinate CoA-transferase (ASCT) and succinyl-CoA synthetase (SCS) enzymes are involved in this reaction (Stechmann et al., 2008) (Figure 2A). However, ATP can be also generated by acetyl-CoA synthetase (ACS) through conversion of acetyl-CoA to acetate (Figure 2B). This metabolic process occurs mainly in the cytosol (via ACS1), in case of *Cantina marsupialis* has been also localised into the mitochondrial organelle (Noguchi et al., 2015).

Organisms with this type of organelle are for example ciliate *Nyctotherus ovalis*, protist from the group Stramenopila *Blastocystis hominis* (Akhmanova et al., 1998; Stechmann et al., 2008), *Pygsuia biforma* (Maguire and Richards, 2014; Stairs et al., 2014), *Brevimastigomonas moltovehiculus* (Gawryluk et al., 2016), *Orpinomyces sp.* strain C1A (Youssef et al., 2013), *Acanthamoeba castellanii* (Gawryluk et al., 2014) or *C. marsupialis* (Noguchi et al., 2015).

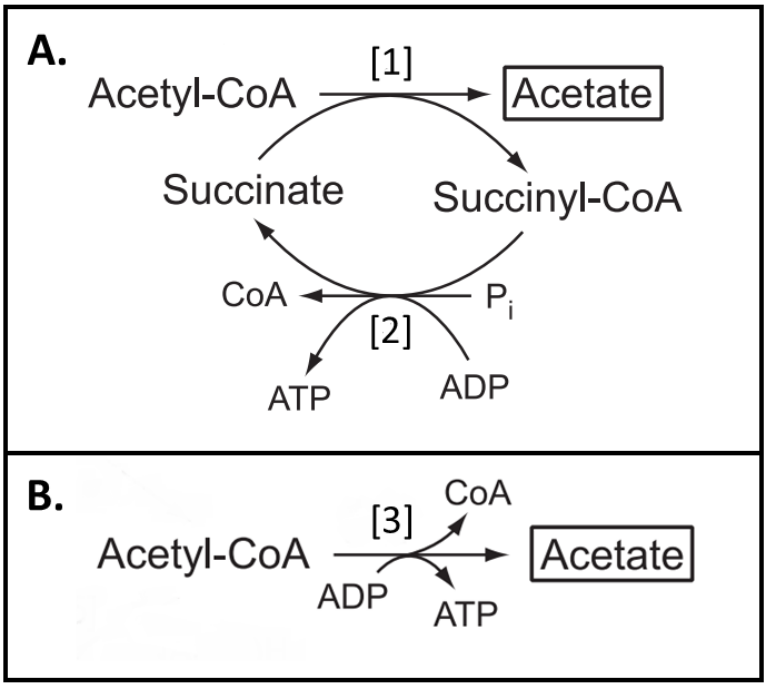

Figure 2. Two types of ATP synthesis in H_2-producing mitochondria and hydrogenosomes A. ATP synthesis via substrate-level phosphorylation process. **B.** Generating of ATP directly via conversion of acetyl-CoA into acetate. **[1]** = acetate:succinate CoA-transferase (ASCT) **[2]** = succinyl-CoA synthetase (SCS) **[3]** = acetyl-CoA synthetase (ACS) (Muller et al., 2012).

2.1.4. Hydrogenosome

Hydrogenosome was discovered in 1973 in a cattle parasite *Tritrichomonas foetus* (Lindmark and Müller, 1973). The organelle was named after the metabolic end product, hydrogen, which is synthesized by the enzyme hydrogenase. PFO oxidatively decarboxylates pyruvate into acetyl-CoA, carbon dioxide and reduced ferredoxin. [FeFe] hydrogenase utilizes electrons and transfers them from reduced ferredoxin to redox partners of the enzyme (protons), forming the hydrogen molecule (Vignais et al., 2001). ATP is in most cases synthesized by substrate-level phosphorylation using ASCT and SCS (Cerkasov et al., 1978; Muller, 1993). In *Spironucleus salmonicida,* ACS2 enzyme is used for the ATP fixation in hydrogenosomes (Jerlström-Hultqvist et al., 2013).

Hydrogenosomes do not possess any complexes of electron transport chain or citric acid cycle and the genome is entirely absent (Muller, 1993; Clemens and Johnson, 2000; Hrdy et al., 2004). However two soluble proteins of complex I (NuoE and NuoF) were discovered in hydrogenosome of *T. vaginalis*, they are responsible for the electron transport from NADH to

[2Fe2S] ferredoxin (Hrdy et al., 2004). Inner membrane does not form cristae. However, small intermembrane calcium containing vesicles can be observed in hydrogenosomes of *T. vaginalis* and *T. foetus* (Benchimol, 2009).

Hydrogenosomes can be found in other anaerobic protists like *Mastigamoeba balamuthii* (Gill et al., 2007), *Sawyeria marylandensis* (Barberà et al., 2010), *Piromyces sp.*, *Neocallimastix frontalis* (Akhmanova et al., 1999) or in one of the diplomonads, *Spironucleus salmonicida* (Jerlström-Hultqvist et al., 2013). Specific type of the hydrogenosome with no ATP synthesis has been predicted in the excavate flagellate *Dysnectes brevis* (Leger et al., 2017). This organellar condition could be the direct evolutionary transition between hydrogenosome and mitosome.

2.1.5. Mitosome

The mitosome (syn. crypton) is the most reduced mitochondrion-related organelle and was described for the first time in 1999 in pathogenic amoeba, *Entamoeba histolytica*.(Mai et al., 1999; Tovar et al., 1999).

Mitosomes do not synthesize ATP, the energy is generated exclusively in the cytosol. Hydrogenase or PFO (if present) are localized to the cytosol (Emelyanov and Goldberg, 2011). Organellar DNA is absent, therefore (just like in the hydrogenosome) all proteins are imported into the organelle from the cytosol.

The only known function of the mitosome is Fe-S cluster assembly. One exception is *E. histolytica*, where formation of the Fe-S clusters takes place in the cytosol (Dolezal et al., 2010; Nyvltova et al., 2013). In this case, the organelle has another specific function, the sulfate activation pathway (Mi-ichi et al., 2009). Sulfate has the positive effect on the cell growth and proliferation. Moreover, sulfate in the form of 3-phosphoadenosine-5-phosphosulfate is crucial for the production of sulfolipids and for the incorporation of sulfate into cysteine or methionine molecules (Mi-ichi et al., 2011).

Apart from *E. histolytica*, there are other protists possessing mitosome, for example apicomplexan *Cryptosporidium parvum* (LaGier, 2003), rhizarian *Mikrocytos mackini* (Burki et al., 2013), microsporidia species *Trachypleistophora hominis*, *Encephalitozoon cuniculii* and

Amphiamblys sp. (Katinka et al., 2001; Williams et al., 2002; Mikhailov et al., 2016) and diplomonad *Giardia intestinalis* (Tovar et al., 2003).

2.2. Fe-S cluster assembly

Iron-sulfur (Fe-S) clusters are cofactors necessary for the function of various proteins involved in regulation of gene expression, electron transfer and oxygen sensing (Kiley and Beinert, 1998). Many of these proteins can be found in aerobic mitochondria (NADH: ubiquinone oxidoreductase, succinate dehydrogenase or ubiquinol-cytochrome c oxidoreductase) as well as in their anaerobic forms like hydrogenosomes (hydrogenase, PFO, ferredoxin or NADH dehydrogenase). Characteristics of iron allow the broad redox potential of the clusters, ranging from -500mV up to +500mV (Capozzi et al., 1998). Iron atom is present in the form of Fe^{2+} or Fe^{3+} and it is coordinated by 4 S^{2-} atoms. There are many various types of Fe-S clusters, the most common are rhombic [2Fe2S] type and cubane [4Fe4S] type (assembled from two [2Fe2S] units) (Beinert, 2000; Johnson et al., 2005). Reduced Fe and S are rather toxic for the cells, consequently they are not present within cytosol in free soluble form (Fontecave et al., 2005). Therefore, specific machineries are necessary for their transport and assembly into Fe-S clusters inside the cell.

There are four different types of Fe-S cluster machinery: Nitrogen fixation pathway (NIF), Sulfur mobilization pathway (SUF), Iron-sulfur cluster assembly pathway (ISC) and Cytosolic Iron-sulfur cluster assembly pathway (CIA). First three originated from bacteria and the eukaryotes either inherited them from the bacterial endosymbiont (SUF, ISC) or were obtained by lateral gene transfer (SUF, NIF). CIA pathway can be found exclusively in eukaryotes within the cytosol and it is necessary for the incorporation of the Fe-S clusters into cytosolic and nuclear proteins. (Lill and Mühlenhoff, 2005).

ISC assembly pathway is the most important system of the Fe-S cluster production and maturation in bacteria and eukaryotes as well. Almost every eukaryotic cell possesses ISC pathway in its mitochondrial organelles that was inherited from α-proteobacteria (Lill and Mühlenhoff, 2005; Tachezy et al., 2001). ISC system is also responsible for maintaining the homeostasis of iron in the cell (Kispal et al., 1997).

We can divide ISC pathway in eukaryotes into early ISC machinery (with homologous proteins to prokaryotes, forming the [2Fe2S] clusters) and late ISC machinery responsible for the [4Fe4S] cluster assembly, which is not present in bacteria (Braymer and Lill, 2017). The pathway components are encoded in the nucleus and must be transported into the mitochondria.

First step of Fe-S cluster assembly requires the complex of proteins IscS-Isd11-Acp1. Cysteine desulfurase IscS (called Nfs1 in yeast) catalyzes the conversion of L-cysteine (source of sulfur for the cluster assembly) into alanine and sulfur in the form of persulfide (-SSH). Persulfide is bound to a catalytic cysteine residue of IscS (Zheng et al., 1993, 1994; Kato et al., 2002). Isd11 and Acp1 proteins are necessary for the stabilization of the Nfs1 and can be found only in the eukaryotes (Adam et al., 2006; Wiedemann et al., 2006; Van Vranken et al., 2016; Braymer and Lill, 2017).

IscU (Isu1 and Isu2 in yeast) is the main scaffold domain, which requires sulfur from the IscS-Isd11-Acp1 complex. S^0 atom is transferred to IscU and then reduced to S^{-2}. Ferredoxin (Yah1) is providing the electrons for this reaction (Nakamura et al., 1999). Mitochondrial membrane channels Mrs3 and Mrs4 are necessary for the iron (Fe^{2+}) import into the organelle (Foury and Roganti, 2002). However, it is still not clear which atom is bound first to the cluster formation site, whether iron or sulfur. Frataxin is another important protein in the pathway but its specific function is still unclear (Layer et al., 2006). It has been suggested that it might be a donor of iron for the Fe-S clusters (Pastore et al., 2007), it could help cysteine desulfurase with the L-cysteine conversion (Pandey et al., 2013), or it could transport sulfur from IscS to the IscU scaffold (Parent et al., 2015). IscU and IscS interact with each other directly and *de novo* synthesis of [2Fe2S] clusters is enabled after the conformational change (Urbina et al., 2001).

After the formation of [2Fe2S] cluster on IscU, the cluster is transported to the apoprotein (protein without Fe-S cluster). Fe-S cluster is released from the IscU scaffold by Ssq1 chaperone (Hsp70 type of chaperone). ATP is required for this step. Co-chaperone Jac1 is catalyzing ATPase activity of Ssq1 and Mge1 protein serves as the exchange factor, it exchanges ADP for ATP on Ssq1. Monothiol glutaredoxin 5 (Grx5) then transports released Fe-S center into the mitochondrial apoproteins (Uzarska et al., 2013).

IscU can also form [4Fe4S] clusters together with the complex of late ISC machinery proteins, Isa1-Isa2-Iba57 (Gelling et al., 2008; Mühlenhoff et al., 2011; Sheftel et al., 2012; Adrover et al., 2015; Braymer and Lill, 2017). Grx5 protein transports the cluster on this protein complex and $[4Fe4S]^{2+}$ is formed from two [2Fe2S] clusters (Kim et al., 2010; Brancaccio et

al., 2014). Carriers like Nfu1, Ind1 or Bol proteins facilitate transport of the complete [4Fe4S] clusters into specific apoproteins (Bych et al., 2008; Py et al., 2012; Melber et al., 2016).

Atm1 ABC half transporter resides in the inner mitochondrial membrane and is responsible for export of possibly activated sulfur to the cytosolic CIA pathway (Leighton and Schatz, 1995; Kispal et al., 1999; Srinivasan et al., 2014). For a graphical overview of ISC pathway, see Figure 3.

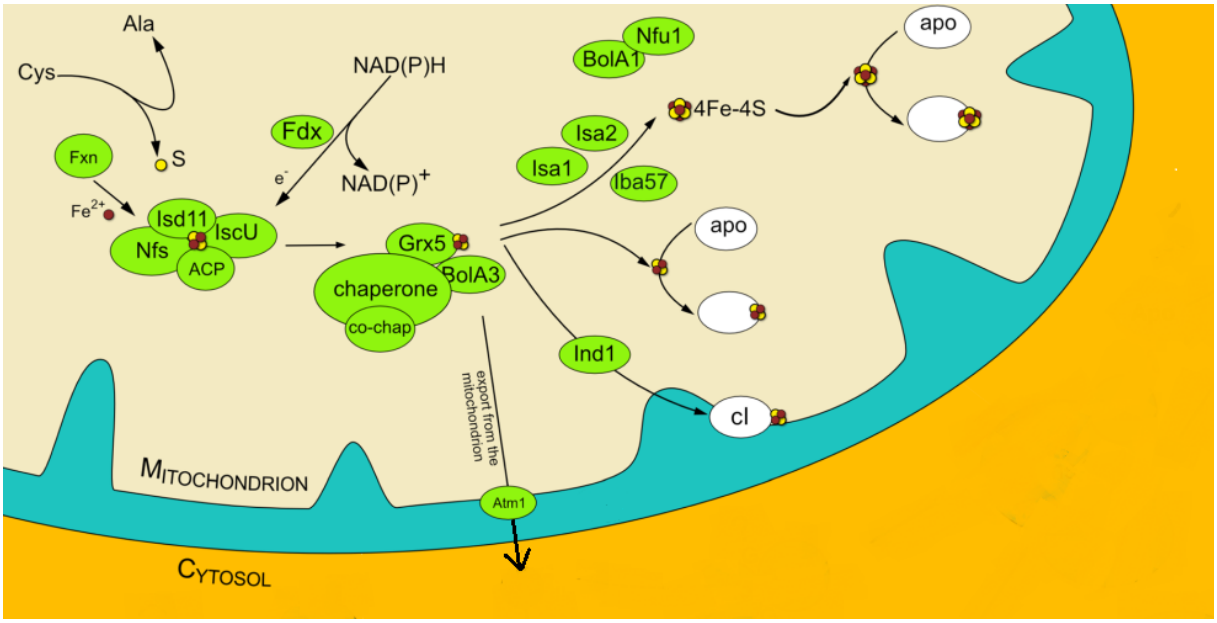

Figure 3. Overview of the ISC pathway in the mitochondria (Peña-Diaz and Lukeš, 2018).

NIF pathway is used by bacteria for synthesis of complex clusters for nitrogen-fixation protein – nitrogenase (Dean et al., 1993). In eukaryotes, this pathway have been found only in Archamoebae *E. histolytica* and its free-living relative *M. balamuthii* (Ali et al., 2004; Gill et al., 2007). In the amoebae, proteins of the NIF pathway were most likely acquired from ε-proteobacteria by lateral gene transfer (LGT) and it replaces the ISC pathway. Two NIF subunits (NifS and NifU) have dual localization in the cytosol and hydrogenosomes of *Mastigamoeba*, in *Entamoeba* have been localized only to the cytosol (Dolezal et al., 2010; Nyvltova et al., 2013; Nývltová et al., 2015).

SUF pathway is used by various bacteria and archaebacteria during iron starvation conditions or oxidative stress instead of ISC pathway (Nachin et al., 2001; Fontecave et al., 2005). In eukaryotes, SUF system is typically localized into plastids evolved from cyanobacteria (Takahashi and Tokumoto, 2002). Moreover, in *Blastocystis hominis* possesses fused protein Suf-CB that is situated into cytosol and it might contribute to the Fe-S clusters

biosynthesis under the oxidative stress in addition to the ISC and CIA pathway (Tsaousis et al., 2012). Suf-CB protein has been also observed in mitochondrial organelles of *Pygsuia biforma* (Stairs et al., 2014). *Monocercomonoides* is the only known eukaryote without mitochondria, therefore the Fe-S cluster assembly takes place only in cytosol. This organism also replaced the ISC pathway with the SUF machinery (Karnkowska et al., 2016).

2.3. Types of hydrogenase

The main function of the hydrogenase is to catalyze following chemical reaction: $2H^+ + 2e^- \leftrightarrow H_2$. Some hydrogenases are able to form hydrogen, some are more active in the opposite direction in order to form protons and electrons, and most of them can catalyze the reaction in both directions. Even though this enzyme is more typical for the metabolism of prokaryotes, we can find hydrogenase in various unicellular eukaryotic organisms (Vignais and Billoud, 2007; Tsaousis et al., 2014).

Hydrogenases could be classified according to the type of specific electron acceptors and donors including cytochromes, NAD, coenzyme F_{420} or ferredoxins (Vignais and Billoud, 2007; Yagi and Higuchi, 2013). Nowadays, however, hydrogenases are divided into three different groups according to type of metal atoms in their active site.

[NiFe] hydrogenases are the most studied and can be found only in prokaryotes. As the name suggests, they have a Ni and Fe atom at their active site. The enzyme is a heterodimer composed from two subunits. Larger α-subunit (cca 60 kDa) contains the active site of the enzyme and the β-subunit is hosting various Fe-S clusters (Higuchi et al., 1997; Garcin et al., 1999; Vignais and Billoud, 2007; Shomura et al., 2011). Most of the [NiFe] hydrogenases have a role in the H_2 consumption (Vignais et al., 2001).

[Fe]-hydrogenase, also called Hmd (5,10-methenyltetrahydromethanopterin hydrogenase), has been found only in several methanogenic archea so far (Vignais and Billoud, 2007). It is a homodimer (38kDa) with only one atom of Fe in the active site. Surprisingly, this enzyme lacks any Fe-S clusters (Pilak et al., 2006).

Finally, [FeFe] hydrogenases can be found in anaerobic bacteria and protists. Its function is mainly to produce hydrogen (Vignais et al., 2001). These enzymes can form monomers, heterodimers, trimers and/or tetradimers. Catalytic subunit contains several Fe-S

cluster domains and conserved domain within the active site, called H-cluster. This H-domain is formed by two parts: [4Fe-4S] cluster, used for electron transport and Fe-Fe center, which is the place for reverse oxidation of the hydrogen. The domain contains 3 conserved sites in the protein sequence, CCP, PCxxKxxE and MxCxxGCxxG (Meyer, 2007). For the purposes of this thesis, we will focus only on the maturation processes of the [FeFe] hydrogenase.

2.4. [FeFe] hydrogenase maturases

There are three accessory proteins crucial for the proper H-cluster synthesis. Two of them are radical S-adenosylmethionine (SAM) enzymes, specifically HydE and HydG and the third one (HydF) belongs to the GTPase family (Posewitz et al., 2004). HydF protein has two main functions: It serves as scaffold for the [2Fe-2S] cluster, which is precursor of Fe-Fe center and it also transports this center directly into H-cluster. Binding of CO, CN^- and dithiolate bridging ligand, as well as GTPase hydrolysis are necessary for the proper function of this enzyme (Nicolet et al., 2010; E. M. Shepard et al., 2010). HydE is possibly involved in the synthesis of dithiolate ligand and binds the ligand to [2Fe-2S] precursor (Nicolet et al., 2008). Precursor of the dithiolate ligand is tyrosine. HydG catalyzes conversion of tyrosine to p-cresol and dehydroglycine (DHG), which is crucial for the dithiolate ligand formation. In addition to that, HydG is also responsible for synthesis of CO and CN^- ligands (Driesener et al., 2010; Eric M. Shepard et al., 2010). This process is the final step in the assembly of the [FeFe] center and after transportation into the active site of the hydrogenase by HydF, the hydrogenase is fully maturated for the hydrogen production.

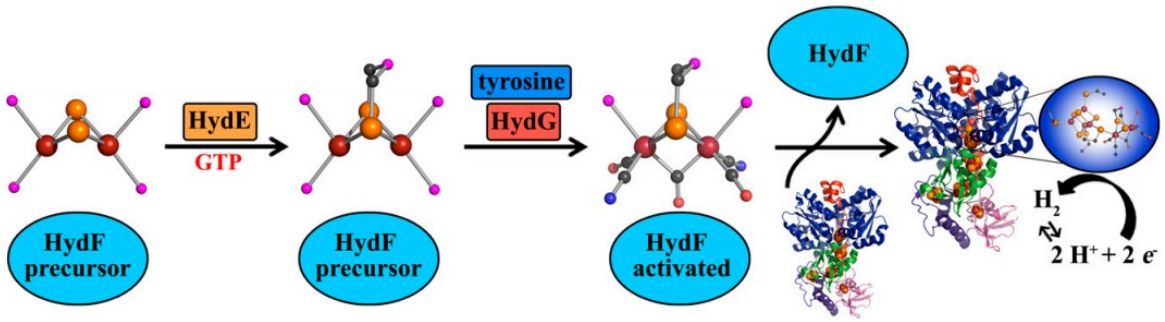

Figure 4. Biosynthesis of the H-cluster (E. M. Shepard et al., 2010).

2.5. Mitochondrion-related organelles in Diplomonadida group

Organisms from the order Diplomonadida are parasitic protists or free-livnig commensals that inhabit oxygen-poor niches. They have a single or mostly double karyomastigont (karyomastigont = nucleus, 4 basal bodies and flagella and associated microtubules), lack peroxisomes and typical Golgi. This order is divided into three main families: *Enteromonadidae* (polyphyletic taxon that includes protists with a single karyomastigont), *Hexamitidae* and *Giardiidae*. The typical characteristics of *Hexamitidae* is presence of two cytostomes. The members of this family include *Trepomonas*, *Hexamita* and *Spironucleus*. Family *Giardiidae* include *Octomitus* and *Giardia*, in which the cytostomes are absent. Moreover, *Giardia* species possess a ventral disc used for the adhesion to the gut epithelium.

All studied diplomonads except *Giardia* species use alternative genetic code, where UAA and UAG codons (normally stop codons) encode glutamine (Keeling and Doolittle, 1996, 1997; Kolisko et al., 2008). The only common characteristics of the mitochondrial organelles in diplomonads is the presence of ISC pathway (Leger et al., 2017).

I will focus on the differences in mitochondrion-derived organelles in diplomonads, specifically in *Trepomonas*, *S. salmonicida*, *S. vortens* and *G. intestinalis*. *Carpediemonas*-like organism *Dysnectes brevis* will be also included, since it is considered as one of the closest relatives to the order Diplomonadida (Figure 5) (Takishita et al., 2012). No study about *Hexamita sp*. mitochondrial organelle has been published so far.

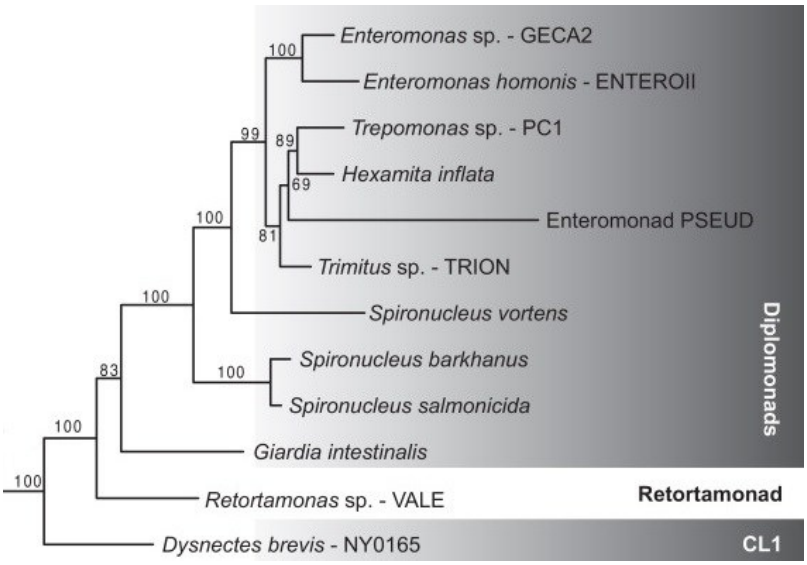

Figure 5. Phylogenetic tree of certain Metamonads based on SSU rRNA and six other proteins (α-tubulin, β-tubulin, Hsp70, Hsp90, EF-1α and EF2). Maximum likelihood phylogeny was used (Takishita et al., 2012).

2.5.1. *Dysnectes brevis*

Functions of mitochondrial organelle of the free-living protist *Dysnectes brevis* have been predicted recently. These organelles could surprisingly illuminate transition from the hydrogenosome into the mitosome. The transcriptomic data revealed several genes for the protein transport including TOM component Tom40, two TIM components Tim 17 and Tim 44 and two PAM components Pam 18 and Hsp70 (Leger et al., 2017). Interestingly, both subunits of mitochondrial processing peptidase are present, which suggests that some mitochondrial proteins may have N-terminal targeting sequence. No data about Fe-S cluster assembly in *Dysnectes* have been published.

Genes for mitochondrial [2Fe2S] ferredoxin, hydrogenase and its three maturases have been identified in the transcriptome, moreover, HydE and HydF possess mitochondrial targeting sequences. This could support the hypothesis about hydrogen production inside the mitochondrial organelle in *D. brevis*. Surprisingly, two subunits of complex I, NuoE and NuoF that were originally found in *T. vaginalis*, were also reported in *Dysnectes* (Hrdy et al., 2004; Leger et al., 2017). Furthermore, a glycine cleavage system (GCS) and its four components (GCSH, GCST, GCSP and GCSL) were also discovered in the transcriptome. In general, GCS is responsible for reversible metabolization of glycine into ammonium and CO_2 with associated reduction of NAD^+. Another protein possibly present in mitochondrial organelle is serine

hydroxymethyltransferase (SHMT) which is responsible for conversion of serine into glycine (the reaction may occur reversibly) (Leger et al., 2017; Fernandes et al., 2018).

It has been proposed, that NuoE and NuoF could transfer the electrons from NADH (produced by GCS) to ferredoxin and reoxidate the NADH cofactors. [FeFe] hydrogenase can then utilize electrons from ferredoxin and transport them to the protons, forming the hydrogen molecules. This whole process might function independently on pyruvate metabolism and it was predicted that hydrogen production functions only as an electron acceptor for amino acid metabolism.

Regarding the ATP synthesis, only the cytosolic ACS1 has been found in the transcriptome, which suggests that this mitochondrion organelle has lost its energy metabolism. Therefore *D. brevis* organelle may represent, a transitional state between the hydrogenosomes and mitosomes (Leger et al., 2017).

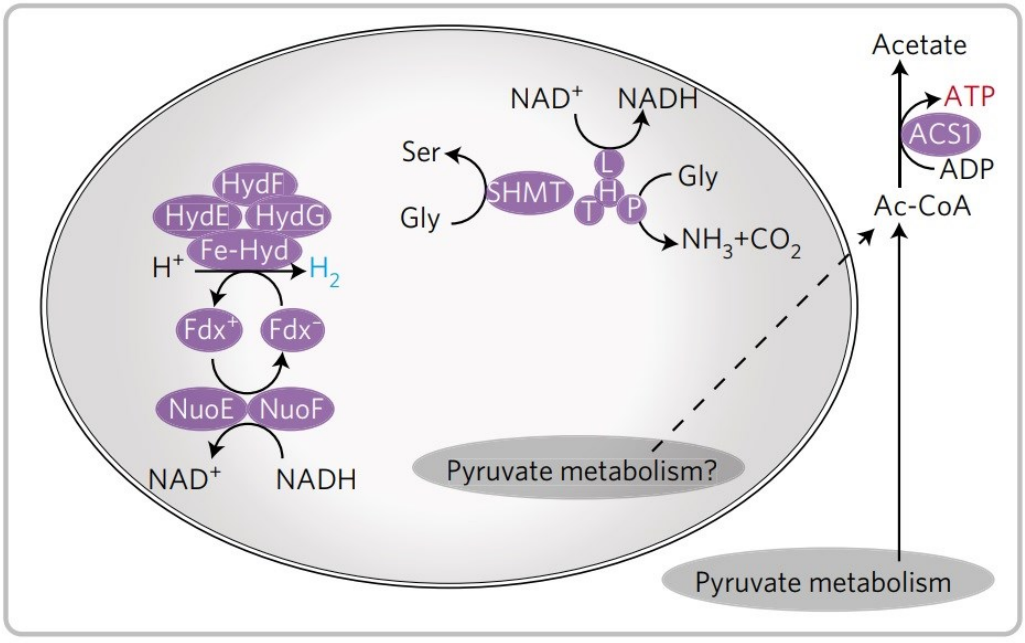

Figure 6. Mitochondrial organelle of *D. brevis* representing the intermediate state between the hydrogenosome and the mitosome (Leger et al., 2017).

2.5.2. *Trepomonas sp.*

Only a single transcriptomic study of this secondary free-living protist has been performed so far (Xu et al., 2016). According to the available bioinformatic data, the mitochondrial organelle of the *Trepomonas sp.* might contain hydrogenase, all three hydrogenase maturases, ferredoxin and SHMT (Leger et al., 2017). However, GCS proteins are possibly not present, therefore source of electrons for hydrogen production is unclear. Only cytosolic form of ACS1 was found in the transcriptome which suggests, that synthesis of ATP might occur only in cytosol.

2.5.3. *Spironucleus salmonicida*

S. salmonicida is a parasite causing infections in various salmon fish (Kent et al., 1992; Jørgensen and Sterud, 2006). Five different PFO genes and seven hydrogenases were found in the genome of this parasite. Only in the case of PFOR5 and two hydrogenases (FeHyd5 and FeHyd6), the mitochondrial localization was confirmed by the immunostaining and epitope tagging, the other paralogs are cytosolic (Jerlström-Hultqvist et al., 2013). All three hydrogenase maturases were localized to the mitochondria, together with acetyl-CoA synthetase (ACS2), whereas ACS1 is most likely present in the cytosol. These components allow a typical hydrogenosomal energy metabolism using pyruvate as a substrate that is converted into acetyl-CoA and subsequently into acetate, enabling the ATP synthesis. In addition. Cpn60, SHMT and GCSH (other three GCS proteins are absent), main components of the ISC pathway (like IscU, IscS, Jac1, frataxin, two ferredoxins and Nfu) and several proteins from the protein import machinery (Tom40, Pam18 and Hsp70) have been localized to the mitochondria (Jerlström-Hultqvist et al., 2013). All hydrogenosomal proteins lack the N-terminal targeting sequence, that is consistent with absence of both subunits for the mitochondrial processing peptidase. Altogether, characteristics of the mitochondrial organelle of *S. salmonicida* correspond to the hydrogenosome (Jerlström-Hultqvist et al., 2013).

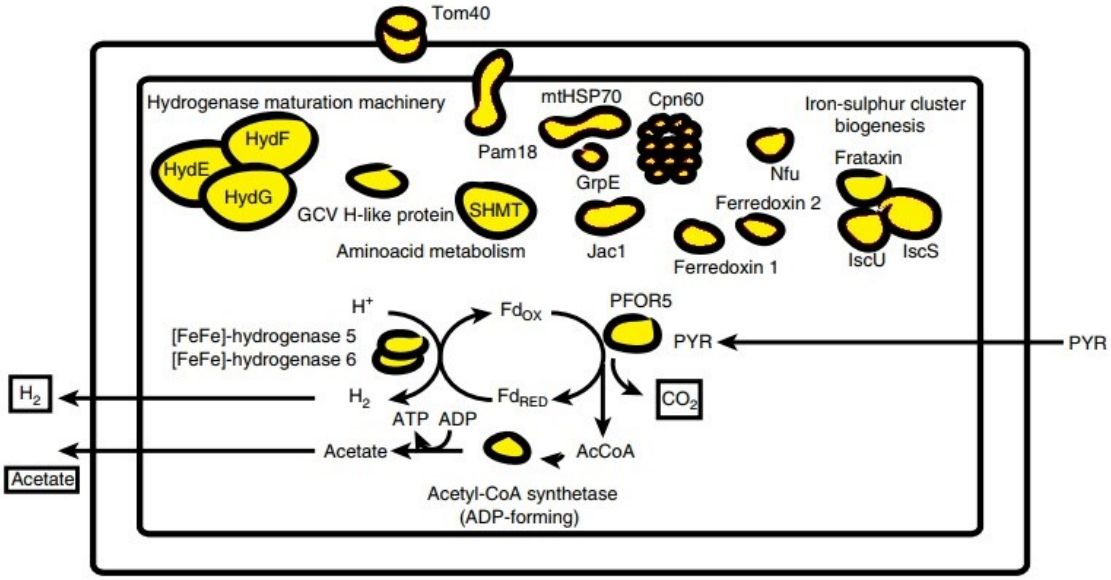

Figure 7. Hydrogenosomal metabolism of *S. salmonicida* (Jerlström-Hultqvist et al., 2013).

2.5.4. *Spironucleus vortens*

Hole-in-the-head disease in ornamental fish is associated with the presence of *S. vortens* (Paull and Matthews, 2001). It has been discovered that *S. vortens* produces hydrogen in rather high quantity (77 nmol/min/10^7 cells) (Millet et al., 2010). Four different heterologous antibodies against hydrogenase, frataxin, Isu1 and ferredoxin were tested for the possible mitochondrial localization. (Millet et al., 2013). The study suggests that *S. vortens* possess two different types of mitochondrion-derived double-membraned organelles in terms of size and antibody localization. Anti-hydrogenase antibody was detected in larger (200-1000 nm) organelles and anti-Isu1 and anti-frataxin antibody was localized in smaller (100-150 nm) mitochondria (Millet et al., 2013; Williams et al., 2013).

Hydrogenase, all three maturases, Tom40, IscU and IscS were found in the genome of *S. vortens* (Leger et al., 2017). ACS1 is possibly responsible for ATP synthesis in the cytosol, mitochondrial ACS2 has not been found in the genome. However, the cellular localization and consequently the type of mitochondrial-derived organelle has not been clarified.

2.5.5. *Giardia intestinalis*

G. intestinalis is an intestinal parasite causing a malabsorption of nutrients and greasy diarrhea in mammals including humans (Adam, 2001). *Giardia* possesses ventral adhesive disc, which is used for the adhesion to the gut epithelium. Furthermore, the most reduced mitochondrial organelle (the mitosome) has been discovered in this protist. The only known function of mitosomes is Fe-S cluster biosynthesis (Tovar et al., 2003). There are two different types of mitosomes according to their cell localization. Central mitosomes form a rod-like structure between nuclei, under basal bodies. Peripheral mitosomes are scattered throughout the cytosol, mostly in the caudal part of *Giardia* (Martincová et al., 2012; Voleman et al., 2017).

ISC pathway proteins IscS, IscU, Isa, Hsp70, Jac1, Nfu, glutaredoxin and [2Fe2S] ferredoxin are localized to the mitosomes of *Giardia* (Tovar et al., 2003; Rada et al., 2009; Jedelský et al., 2011; Rout et al., 2016). However, frataxin is absent from the genome (Jedelský et al., 2011). IscU and ferredoxin proteins possess the N-terminal targeting sequence, while IscS and chaperones Hsp70 and Cpn60 contain internal targeting signals (Dolezal et al., 2005; Santos et al., 2018).

Surprisingly, three proteins of the CIA pathway (Cia2, Nbp35-1 and Nbp35-2) have dual localization, they are present in the cytosol and in the mitosomes (Pyrih et al., 2016). In the organelle, Cia2 was localized to the intermembrane space and both Nbp35 proteins seem to be associated with the outer mitosomal membrane. This unexpected localization of CIA components may reflect a specific interaction between ISC and CIA machineries in *Giardia*.

GCS proteins are absent from the genome (Leger et al., 2017). Mitochondrial transport proteins MOP35, Hsp70, Pam 16, Pam18, Tom40, Tim17 and Tim44 were localized to the mitosomes (Martincova et al., 2015; Pyrihová et al., 2018).

3. The aims of the thesis

This study is focused on characterization of mitochondrial organelles in *Spironucleus vortens* and *Hexamita sp.* and their comparison with other diplomonads.

Specific aims of the thesis:

1) To select suitable orthologous proteins that are known to reside in mitochondrion-related organelles of other anaerobes, to develop specific antibodies against them and to investigate their cellular localization in *S. vortens* using the immunofluorescence microscopy and subcellular fractionation
2) Alternatively, to develop a single and double transfectants of *S. vortens* expressing selected proteins for localization studies
3) To sequence DNA and RNA of *Hexamita sp*. using next generation sequencing and to analyze the genomic data with focus on the identification of genes coding mitosomal/hydrogenosomal proteins and to estimate the type of *Hexamita sp*. mitochondrial organelles
4) To reconstruct the evolution of mitochondria in diplomonads based on available data and the results of this thesis.

4. Materials and methods

4.1. Cultivation of the organisms

4.1.1. Cultivation of protists

S. vortens (strain ATCC_50386) was isolated from a lip lesion in angelfish *Pterophyllum scalare* and was obtained from American Type Culture Collection (ATCC). *Hexamita sp.* was isolated from a lake in Řevnice, Czech Republic by prof. J. Kulda. Both organisms were cultivated in 10 ml of modified TYI-S-33 medium (pH 6,8) under anaerobic conditions at 24°C (Diamond et al., 1978). *S. vortens* was maintained in KIMAX glass culture tubes. In case of *Hexamita sp.,* Nunclon^{TM} Delta Surface tubes were used. *S. vortens* was transferred every 2-3 days in fresh media, *Hexamita sp.* every 5-7 days. Culture of *S. vortens* is axenic, whereas *Hexamita sp.* culture is monoxenic, containing the proteobacteria *Stenotrophomonas maltophilia*.

4.1.2. Cultivation of *Escherichia coli*

Bacterial strains TOP10 or XL-1 Blue of *E. coli* were used. The cells were incubated on the shaker (220 rpm) in Luria-Bertani broth (LB) medium (Bertani, 1951), at 37°C. Transformed cells were grown on LB plates with 100 µl of 5-bromo-4-chloro-3-indolyl-β-D-galactoside - X-gal (20 mg/ml) and 30 µl of screening antibiotics, Kanamycin (50 µg/ml) or Ampicillin (100 µg/ml) according to the specific cloning vectors. For long-term storage of *E. coli* cells, we used LB medium with 20 % glycerol and cells were stored at -80°C.

4.2. Cultivation media

Modified TYI-S-33 medium (pH 6,8) (Diamond et al., 1978):

Trypticase Peptone (Sigma)	20 g
Yeast extract (Sigma)	10 g
Glucose (Sigma)	10 g
NaCl (Sigma)	2 g
K_2HPO_4 (Sigma)	1 g
KH_2PO_4 (Sigma)	0,6 g
L-Cysteine (Sigma)	1 g
Ascorbic acid (Sigma)	0,2 g
Ammonium iron(III) citrate (Sigma)	22,8 mg
Distilled H_2O	total volume 890 ml
Inactivated Adult Bovine Serum (Sigma)	100 ml
Penicillin-Streptomycin (100 000 IU/ml) (Sigma)	10 ml

After dissolving all components in distilled H_2O, pH was adjusted with 3M NaOH to 6,8. Then, serum and antibiotics were added and medium sterilized by filtration (VWR® Vacuum Filter).

LB medium:

LB medium (Sigma)	20 g
Distilled H_2O	final volume 500 ml

LB plates:

LB agar (Sigma)	17 g
Distilled H_2O	final volume 500 ml

SOC medium (pH 7):

Tryptone (Sigma)	2 g
Yeast extract (Sigma)	0,5 g
NaCl (Sigma)	0,058 g
250 mM KCl (Sigma)	1 ml
Distilled H_2O	final volume 100 ml

20 % glucose (sterile)	1,8 ml (added after sterilization)
2 M $MgCl_2$ (sterile)	0,5 ml (added after sterilization)
Stored in -20°C.	

4.3. Buffers and Solutions

4.3.1. Solutions used for DNA fragment cloning

5-bromo-4-chloro-3-indolyl-β-D-galactoside (X-gal):

X-gal (ThermoFisher)	100 mg
N,N‘-dimethylformamide (Sigma)	2 ml

Antibiotics:

Ampicillin (Sigma)	100 mg/ml
Kanamycin (Sigma)	50 mg/ml
Penicillin-Streptomycin (Sigma)	100 000 IU/ml
Puromycin	50 µg/ml
G418 (Geneticin)	100 µg/ml

DNA electrophoresis buffer (Ogden and Adams, 1987):

1x Tris-Acetate-EDTA (TAE) (Bio-Rad)

DNA staining dye:

SYBR® Safe DNA gel stain (ThermoFisher)

4.3.2. SDS PAGE and Western blot analysis

SDS PAGE buffer:

1x Tris-Glycine-SDS (TGS) (Bio-Rad)

Blotting buffer:

10x concentrated SDS buffer (Bio-Rad)	100 ml
Methanol (Lach-Ner)	200 ml
Distilled H_2O	700 ml

Blocking buffer:

Dry milk (Nutristar)	10 g
Tween 20 (Sigma)	500 µl
Phosphate buffered saline (PBS)	total volume 200 ml

10x PBS:

NaCl (Sigma)	80 g
KCl (Sigma)	2 g
NaH_2PO_4 * 12 H_2O (Sigma)	14,4 g
KH_2PO_4 (Sigma)	2,4 g
Distilled H_2O	total volume 1 l

Coomassie Brilliant Blue solution (CBB):

Coomassie Brilliant Blue (Sigma)	200 mg
Denatured ethanol (Lach-Ner)	225 ml
Distilled H_2O	225 ml
Acetic acid (Lach-Ner)	50 ml

Destain solution:

Denatured ethanol (Lach-Ner)	250 ml
Acetic acid (Lach-Ner)	100 ml
Distilled H_2O	650 ml

Ponceau S:

Ponceau S (Merck)	0,5 %
Acetic acid (Lach-Ner)	1 %

Substrate for alkaline phosphatase:

Sigma Fast BCIP/NBT tablet	1 piece

Distilled H_2O	10 ml

Substrate for horse radish peroxidase:

Western HRP substrate Forte (Merck)	1 ml per membrane

4.3.3. Antibodies

Primary antibodies:

- anti-5xHis monoclonal antibody (mouse IgG) (QiaGen) (1:1000)
- anti-HA monoclonal antibody (mouse IgG) (Exbio) (1:400)
- anti-V5 monoclonal antibody (rabbit IgG) (Exbio) (1:1000)
- anti-hydrogenase (*S. vortens*) polyclonal antibody (rabbit) (Davids Biotechnologie) (1:500)
- anti-HydG (*S. vortens*) polyclonal antibody (rabbit) (Moravian Biotechnology)
- anti-HydE (*S. vortens*) polyclonal antibody (rat) (Jan Mach, Charles University)

Secondary antibodies:

- antibody against mouse IgG conjugated with alkaline phosphatase produced in goat (ICN/CAPPEL) (1:2000)
- antibody against rat IgG conjugated with alkaline phosphatase produced in goat (ICN/CAPPEL) (1:2000)
- antibody against rabbit IgG conjugated with alkaline phosphatase produced in goat (ICN/CAPPEL) (1:2000)
- antibody against mouse IgG conjugated with horse radish peroxidase produced in goat (Novex ECL) (1:2000)
- antibody against rat IgG conjugated with horse radish peroxidase produced in goat (Novex ECL) (1:2000)
- antibody against rabbit IgG conjugated with horse radish peroxidase produced in goat (Novex ECL) (1:2000)
- Alexa Fluor 594 dye mouse/rat/rabbit (ThermoFisher) 1:1000
- Alexa Fluor 488 dye mouse/rat/rabbit (ThermoFisher) 1:1000

4.3.4. Immunofluorescence

2x PEM buffer (pH 6,9) (Mooberry et al., 1999):

PIPES (Sigma)	30,2 g
0,5mM EGTA (Sigma)	2 ml
1M $MgSO_4$ (Sigma)	100 µl

Add NaOH until the buffer get transparent color. Adjust pH to 6,9 and fill in distilled water up to 500 ml. Use the autoclave for sterilization.

PEMBALG:

1x PEM buffer	100 ml
BSA (Sigma)	1 g
Lysin (Sigma)	1,8 g
Cold water fish skin gelatin (Sigma)	0,5 g

4.3.5. Fractionation of the *S. vortens*, *Hexamita sp.* and *G. intestinalis*

Sacharose-Tris (ST) buffer (pH 7,2):

Sacharose (Sigma)	42,85 g
Tris base (Sigma)	0,6 g
KCl (Sigma)	18,5 mg
Distilled H_2O	total volume 500 ml

Stored at -20°C.

Protease inhibitors:

Tosyl-L-lysine-chlormethylketone (TLCK) (Sigma)	25 mg/ml
Leupeptin (Sigma)	5 mg/ml
E-64 (Sigma)	10 mM

4.3.6. Purification of recombinant proteins under denaturation conditions (Purification of HIS-tagged proteins)

Lysis buffer (pH 8):

100 mM NaH_2PO_4 (Lach-Ner)

10 mM Tris-HCl (Sigma)

8 M Urea (Sigma)

Wash buffer (pH 6,3):

100 mM NaH_2PO_4 (Lach-Ner)

10 mM Tris-HCl (Sigma)

8 M Urea (Sigma)

Elution buffer D (pH 5,9):

100 mM NaH_2PO_4 (Lach-Ner)

10 mM Tris-HCl (Sigma)

8 M Urea (Sigma)

Elution buffer E (pH 4,5):

100 mM NaH_2PO_4 (Lach-Ner)

10 mM Tris-HCl (Sigma)

8 M Urea (Sigma)

4.3.7. DNA isolation using phenol-chloroform extraction (Chomczynski and Sacchi, 1987)

Lysis buffer:

Guanidium thiocyanate (Sigma)	35,5 g
0,5 M Ethylenediaminetetraacetic acid (EDTA) (Sigma)	1 ml
β – mercaptoethanol (Sigma)	350 µl
Sodium lauroyl sarcosinate (Sigma)	250 mg
1 M Tris-HCl (pH 8) (Sigma)	5 ml
Distilled H_2O	total volume 50 ml

5M NaCl

NaCl (Sigma)	29,2 g
Distilled H_2O	total volume 100 ml

TE buffer

1 M Tris (pH 7,4) (Sigma)	1 ml
0,5 M EDTA (pH 8) (Sigma)	200 µl
Distilled H_2O	total volume 50 ml

4.4. Methods

4.4.1. Cell fractionation

We used following protocol to obtain the cytosolic and organellar fractions:

1) Transfer $1x10^7$ cells into 15ml VWR® Centrifuge Tube
2) Spin down at 1000 x g / 10 min / 4°C (Hettich Universal 32R centrifuge)
3) Discard the supernatant
4) Resuspend the pellet in 30 ml of ST buffer
5) Spin down the cells at 1000 x g / 10 min / 4°C
6) Resuspend the pellet in 1 ml of ST buffer and transfer it to the Eppendorf tube
7) Add TLCK and Leupeptin to final concentrations 50µg/ml and 10 µg/ml, respectively
8) In case of *S. vortens* add also 10 mM of E-64 protease
9) Sonicate on ice for 30 seconds, 1 second pulses and amplitude 40 (QSonica Q125 sonicator)
10) Check the cells under microscope after sonication and stop when about 95% of the cells are disrupted
11) Take 100 µl aliquot of lysate and store
12) Spin the homogenized cells at 2500 g / 10 min / 4°C to remove whole cells and cell debris

13) Transfer the supernatant into the 2ml Beckman polycarbonate centrifuge tube and spin at 100 000 x g / 35 min / 4°C (Beckman Optima MAX-XP centrifuge, MLA-150 fixed angle rotor)
14) Collect supernatant (cytosolic fraction) and pellet (organellar fraction)

4.4.2. Immunofluorescence microscopy

4.4.2.1. Protocol for immunofluorescence slides preparation using methanol-acetone

1) Spin 10 ml of cells at 900 x g / 5 min. / 4°C (Hettich Universal 32R centrifuge)
2) Discard supernatant and resuspend the pellet in 10 ml of PEM buffer
3) Spin the cells at 900 x g / 5 min. / 4°C (Hettich Universal 32R centrifuge)
4) Discard supernatant and resuspend the pellet gently in 450 µl of PEM buffer by 1 ml Pasteur pipette
5) Place the cells in PEM buffer onto silanized microscope slides (150 µl per slide) and let it dry for 30 minutes
6) incubate the slides in methanol at -20 °C for 5 minutes
7) immediately incubate the slides in acetone at -20 °C for 5 minutes

Following steps proceed in the moister chamber at room temperature:

8) Add 100 µl of PEMBALG buffer, incubate 60 minutes
9) Remove buffer, add primary antibody in PEMBALG, incubate for 90 minutes
10) Remove buffer, wash in PEM buffer 3x (5, 10 and 15 minutes)
11) Remove buffer, add secondary antibody in PEMBALG, incubate for 60 minutes in the dark
12) Remove buffer, wash in PEM buffer 3x (5, 10 and 15 minutes)
13) Add Vectashield Antifade Mounting Medium with 4′,6-Diamidine-2′-phenylindole dihydrochloride (DAPI)
14) Cover the slides with cover slip (170 µm thick) and fix it with nail polish
15) Slides are prepared for the immunofluorescence microscopy, store at 4°C

4.4.2.2. Protocol for immunofluorescence slides preparation using formaldehyde:

1) Add 1% formaldehyde to 10 ml of the cell culture and incubate at the temperature of cultivation (24°C) for 30 minutes
2) Spin the cells at 900 x g / 5 min. / 4°C (Hettich Universal 32R centrifuge)
3) Discard supernatant and resuspend the pellet in 10 ml of PEM buffer
4) Spin the cells at 900 x g / 5 min. / 4°C (Hettich Universal 32R centrifuge)
5) Discard supernatant and resuspend the pellet gently in 450 µl of PEM buffer by 1 ml Pasteur pipette
6) Place the cells in PEM buffer onto silanized microscope slides (150 µl per slide) and let it dry for 30 minutes

Following steps will proceed in moister chamber at room temperature:

7) Permeabilize the cells using PEM buffer with 1% Triton TX-100 for 10 minutes
8) Remove the PEM with Triton from the slides and wash in PEM buffer 3x for 5 minutes
9) Next steps are the same as steps 8-15 in methanol-acetone protocol

4.4.3. Genomic DNA isolation using phenol-chloroform extraction

Day 1

1) Spin the cells (500 ml culture) at 900 x g / 5 min. / 4°C (Hettich Universal 32R centrifuge)
2) Discard the supernatant and wash the pellet in 40 ml of sterile PBS
3) Spin the cells at 900 x g / 5 min. / 4°C (Hettich Universal 32R centrifuge)
4) Discard the supernatant and resuspend the pellet in 2-5 ml of sterile PBS
5) Transfer the cells into small sterile beaker with magnetic stirrer
6) Stir the solution slowly and add Lysis buffer (2-5 ml) until the solution gets transparent
7) Slowly add isopropanol (10 ml), collect precipitated DNA with Pasteur pipette and put it into 50ml Sigma centrifuge tube with 20 ml of 75% ethanol + 20mM NaCl

8) Spin at 9000 x g / 5 min. / 4°C
9) Wash 3x in 75% ethanol + 20mM NaCl and spin at 9000 x g / 5 min. / 4°C in between
10) Remove as much ethanol as possible from the centrifuge tube by pipetting
11) Dry the DNA pellet in the flow box for 20 minutes
12) Add 1 ml of TE buffer, 0,5% SDS and proteinase K (100 µg/ml)
13) Seal the centrifuge tube with Parafilm and incubate at 56°C overnight in hybridization oven while shaking

Day 2

1) Add 4 ml of TE buffer and 100 µl of 5M NaCl
2) Prepare Phenol-chloroform solution – put 10 ml of chloroform and 10 ml of phenol into the 50 ml Sigma centrifuge tube and mix
3) Add 5 ml of phenol-chloroform solution to the centrifuge tube with DNA and TE buffer
4) Shake by hand for 30 seconds and spin at 9000 x g / 5 min. / 20°C

There are 3 different phases in the centrifuge tube after spinning: upper phase with DNA, middle white phase (proteins) and lower phase (phenol).

5) Transfer the upper phase into a new centrifuge tube
6) Repeat step 3-5 three times
7) Transfer the upper phase into a new centrifuge tube and add 2,5x more of 96% ethanol
8) Incubate in -20°C overnight

Day 3

1) Spin at 9000 x g / 5 min. / 20°C
2) Wash the pellet 2x with 75% ethanol + 20mM NaCl
3) Dry the DNA pellet
4) Add 1 ml of TE buffer and RNAse (100 µg/ml)
5) Incubate in hybridization oven at 37°C for 6 hours with rotation speed 10 rpm
6) Add 4 ml of TE buffer and 100 µl of 5M NaCl

7) Repeat the phenol-chloroform extraction (Day 2, steps 2-8)

Day 4

1) Spin at 9000 x g / 5 min. / 20°C, remove supernatant and dry the pellet in flow box
2) Resuspend pellet in 200-500 µl of TE buffer
3) Store the DNA in -80°C

4.4.4. Transfection of *S. vortens*

1) Prepare 100 ml of the well-grown cells
2) Use the Beckman Z2 Coulter® Particle Count and Size Analyzer for counting the number of cells (100 µl of cells diluted in 10 ml of isotonic buffer, size of the cells from 5 to 15 and set the dilution factor to 100)
3) Incubate the cells on ice for 15 min., then spin at 1000 x g / 5 min. / 4°C (Hettich Universal 32R centrifuge)
4) Discard the supernatant, resuspend the pellet in cold fresh TYI-S-33 medium to final concentration $3 \cdot 10^7$ cells per 1 ml
5) Add 300 µl of the solution into 4 mm electroporation cuvette (Bio-Rad)
6) Add 40 µg of plasmid DNA, mix gently and leave it on ice for 10 min.
7) Proceed with electroporation (GenePulser Xcell, Bio-Rad)

Following electroporation protocols were used:

a) exponential protocol – 350 V, 1500 uF, ∞ Ω
b) exponential protocol – 400 V, 1000 uF, 700 Ω
c) time-constant protocol – 350 V, 175 ms

8) Immediately immerse the cuvettes with cells in ice for 10 min.
9) Transfer the cells into fresh TYI-S-33 medium with Penicillin and Streptomycin added
10) Add Puromycin (50 µg/ml) or Geneticin (G418) (100 µg/ml) after 24 hours
11) Select transfeceted cells for 1-2 weeks
12) Test expression of the recombinant protein in lysate and cellular fractions of *S. vortens* using the Western blot

4.4.5. SDS-PAGE

Protein samples were prepared for the SDS-PAGE by dissolving in the SDS sample buffer and denaturation at 95°C for 5 minutes. 13,5% polyacrylamide gel with SDS was used for the protein separation under denaturing conditions. We used PageRuler™ Plus Prestained Protein Ladder (ThermoFisher) for the molecular weight determination. Mini-PROTEAN Tetra Cell was used for the SDS-PAGE.

4.4.6. Western blot analysis (Laemmli, 1970)

1) Soak the polyacrylamide gel together with 2 papers and nitrocellulose membrane (of the same size as gel) in the blotting buffer
2) Stack the components on the blotting machine (semi-dry blot Biometra) in the following order: from the bottom 1 filter paper, nitrocellulose membrane, gel and 1 filter paper
3) Blot at 3 mA per cm^2 for 35 minutes
4) Stain the membrane by Ponceau S (5%) for 30 seconds in order to visualize the proteins
5) Destain by washing in distilled H_2O
6) Incubate the membrane in the blocking buffer for 1 hour at room temperature or overnight at -4°C
7) Incubate the membrane with primary antibody in the blocking buffer for 1 hour at the room temperature or overnight at 4 °C
8) Wash the membrane 3x for 5 minutes in the blocking buffer
9) Incubate the membrane with secondary antibody in the blocking buffer for 30-60 minutes at room temperature
10) Wash the membrane 2x for 5 minutes in the blocking buffer and 1x for 5 minutes in PBS
11) Incubate the membrane with substrate for horse radish peroxidase or alkaline phosphatase
12) Amersham Imager 600 was used for the image capturing

4.4.7. Gene cloning

4.6.7.1. Amplification of the genes

S. vortens genes for hydrogenase, HydG and HydE (all sequences are listed in Appendix 1) were amplified by PCR (polymerase chain reaction). Genomic DNA of *S. vortens* was used as a template, that was obtained by High Pure PCR Template Preparation kit (Roche). Primers with required restriction sites were designed in *Geneious*® software (Biomatters).

List of primers for the gene amplification:

hydrogenase, restriction sites **NdeI, HindIII**	
forward	5'-**CATATG**TGCATCGAGATCATCTACG-3'
reverse	5'-**AAGCTT**CTCGGTCGAGAGCTGCTT-3'
HydG, restriction sites **NdeI, HindIII**	
forward	5'-**CATATG**AACCCGCAGCTCGTACGC-3'
reverse	5'-**AAGCTT**GCCGACTCCCATCGTGTC-3'
HydE, restriction sites **VspI (AseI), XhoI**	
forward	5'-**ATTAAT**ATGGCTCTTCAAACCACGC-3'
reverse	5'-**CTCGAG**CCGGCCGCCGGGAGGTA-3'

PCR reaction protocol:

5x Q5 reaction buffer (NEB)	5 µl
5x Q5 High GC enhancer (NEB)	5 µl
10 mM dNTPs (ThermoFisher)	0,5 µl
10 µM forward primer	1,25 µl
10 µM reverse primer	1,25 µl
genomic DNA (150 ng/µl)	1 µl
Q5® High-fidelity DNA polymerase (NEB)	0,25 µl
MiliQ H_2O	10,75 µl

Thermal cycler program:

Nr. of cycles	**1x**	**25x**			**1x**	
Temperature (°C)	98	98	47 - 72	72	72	4
Time (sec)	30	10	25	30	120	∞

4.6.7.2. DNA electrophoresis and PCR product purification

DNA samples were analyzed by a horizontal electrophoresis in 1x TAE buffer using the 1% agarose gel. SYBR® Safe dye (Invitrogen) was used for the DNA visualization. Samples were mixed with 6x concentrated sample buffer (Fermentas). The electrophoresis run under 130 V. GeneRuler™ DNA Ladder Mix was used as a standard. DNA was visualized by UV transilluminator. Bend of a predicted size was cut off from the gel by sterile scalpel. QIAquick Gel Extraction Kit (250) (Quiagen) was used for DNA purification.

4.6.7.3. Ligation into pJET vector

We subcloned genes of interest (hydrogenase, HydG and HydE) into pJET1.2/blunt vector (Ampicillin resistance) and used for transformation of *E. coli* TOP10 with this plasmid for a gene expression. The correct insertion was verified by sequencing.

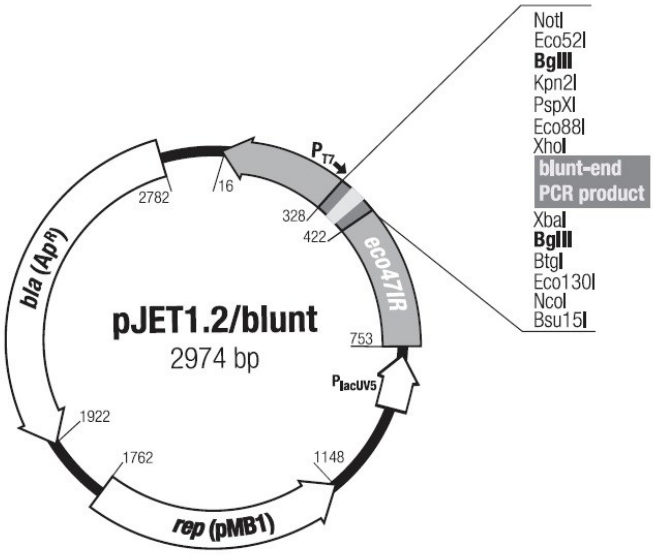

Figure 8. pJET1.2/blunt Vector Map (from CloneJET PCR Cloning Kit User Guide)

4.6.7.4. *E. coli* transformation (TOP10 and BL21-DE3 strains)

1) Incubate frozen competent bacteria on ice until they thaw (5-10 min.)
2) Add the plasmid (ligation sample) and leave it for 20 min. on ice
3) Thaw the SOC medium
4) Incubate bacteria with plasmid in water bath (42°C) for 35 sec.
5) Incubate for 2 min. on ice
6) Add 250 µl of SOC medium
7) Incubate at 37°C for 30-60 min.
8) Add 30 µl of antibiotics and 10 µl of X-gal
9) Distribute the transformed cells on the LB plate
10) Incubate at 37°C overnight
11) Store the plates at 4°C

4.6.7.5. Isolation of plasmid DNA

Plasmids with genes of our interest were isolated from 5 ml of bacterial culture using the Miniprep High Pure Plasmid Isolation Kit (Roche) or from 100 ml of bacterial culture using the Midiprep High Pure Plasmid Isolation Kit (Roche) according to the manufacturer protocols.

4.6.7.6. Restriction reaction

Plasmid	10 µg
Digest buffer	3 µl
Restriction enzyme Nr. 1	1 µl
Restriction enzyme Nr. 2	1 µl
MiliQ H_2O	total volume 30 µl

Reaction was incubated at 37°C overnight. Results of restriction were checked by the horizontal DNA electrophoresis using the 1% agarose gel.

4.6.7.7. Ligation of genes into expression vector

pET42b (Kanamycin resistance) was used as a vector for expression of recombinant hydrogenase, HydG and HydE. The correct insertion was verified by sequencing.

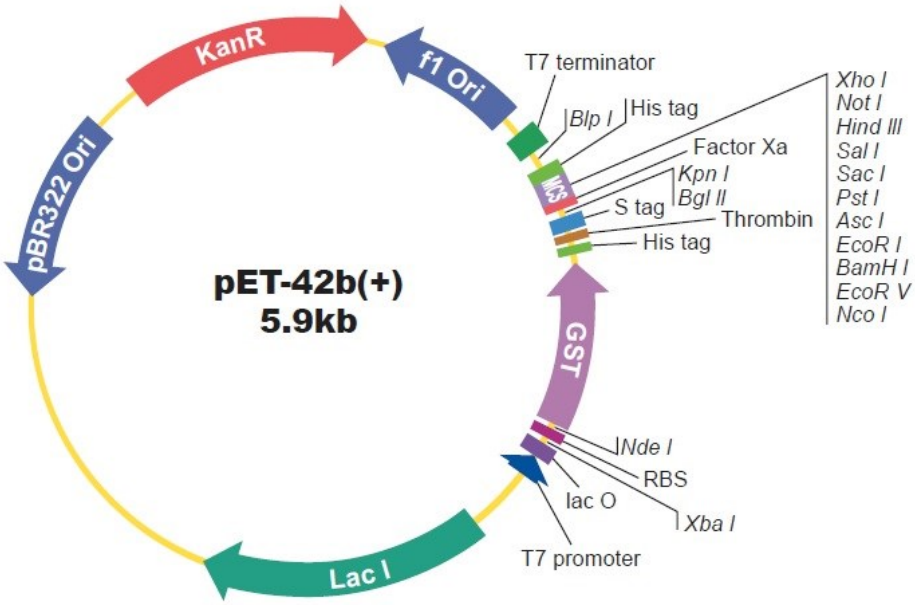

Figure 9. pET-42b Vector Map (from GenScript database)

4.6.7.8. Recombinant protein expression

E. coli BL21(DE3) strain was used for the production of the recombinant proteins with polyhistidine tag at C-terminus.

1) 100 ml of transformed bacterial culture cultivate with 100 µl of Kanamycin (50 µg/ml) overnight in LB medium on the shaker at 37°C, 220 rpm. Add into 2 l of LB media and incubated with shaking 220 rpm at 37°C
2) When OD (optical density) value reaches 600 (after 1-3 hours), add 250 µM IPTG and 400 mM ammonium iron(II) sulfate
3) Incubate on the shaker for 4-8 hours
4) Spin at 3000 x g / 8 min. / 4°C
5) Discard the supernatant and resuspend pellet in 40 ml of PBS buffer
6) Spin at 4500 x g / 10 min. / 4°C
7) Discard the supernatant, pellet is ready for the protein purification (can be stored at -20°C)

4.6.7.9. Recombinant His-tagged protein purification under denaturing conditions

Recombinant proteins were purified by affinity chromatography using PerfectPro NiNTA agarose (Qiagen) according to the manufacturer protocol:

1) Resuspend the pellet in 30 ml of lysis buffer
2) Sonicate the cells (amplitude 60, 1 second pulses, 90 seconds, sonicator Vibra Cell)
3) Spin at 100 000 x g / 35 min. / 4°C
4) Add 500 µl of PerfectPro NiNTA agarose (Qiagen) to the supernatant, mix by inverting the falcon several times and transfer the mixture to the column
5) Collect the flow-through
6) Wash the column 2x with the 4 ml of Wash buffer, collect the flow-through

7) Wash the column 5x with the 500 µl of Elution buffer D, collect the flow-through
8) Wash the column 5x – 8x with the 500 µl of Elution buffer E, collect the flow-through
9) Analyze the fractions by SDS-PAGE and Western blot

4.4.8. Single transfection of *S. vortens*

We obtained three genes (HydG, HydE and IscU) subcloned in pSvor_PAC_3xHA_C plasmid from laboratory of prof. S. Svard (Uppsala, Sweden). The plasmid contained the ampicillin gene (AmpR) for the selection in bacteria and *pac* gene for puromycin selection in *S. vortens*. Pac resistance gene was inserted between alpha-tubulin upstream and downstream regions (cloned between KpnI/XhoI and NcoI/HindIII restriction sites). The multiple cloning site was flanked by a 3xHA tag and termination was handled by a short stretch of the ribosomal protein S15A 3'UTR (cloned between ApaI/SacI sites). The C-terminal 3xHA tag was cloned between NotI and ApaI sites (for a detailed map of pSvor_PAC_3xHA_C with constructed cassette and restriction sites see Figure 10). HydG, HydE and IscU with their 5' upstream region containing native promoters were cloned into pSvor_PAC_3xHA_C using MluI and NotI restriction sites.

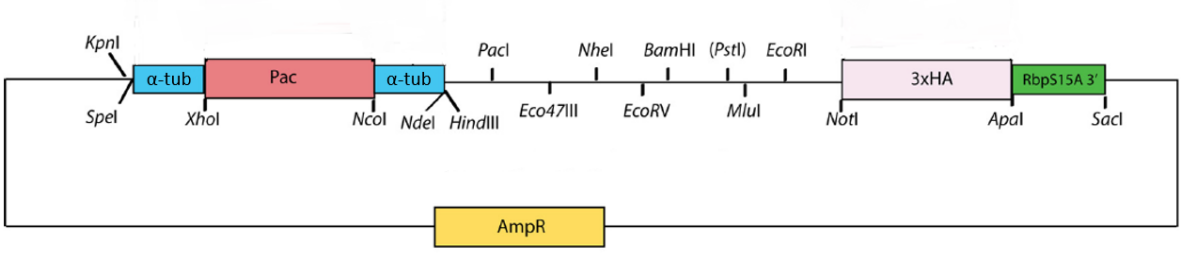

Figure 10. Detailed map of pSvor_PAC_3xHA_C vector showing constructed cassette and restriction sites (Jerlström-Hultqvist et al., 2013).

4.4.9. Double transfection of *S. vortens*

For double transfection, we obtained empty pSpiro_NptII_NEO plasmid (Uppsala, Sweden). Instead of *pac* gene, this vector contains gene for neomycin (G418 resistance) that is flanked by fructose bisphosphate aldolase (FBA) 3'UTR and 5'UTR. The genes for HydG, HydE and IscU with their 5' upstream regions containing native promoters (333, 239 and 206 base pairs respectively) were subcloned into this plasmid. The 3xHA tag was replaced with V5 tag (Figure 11).

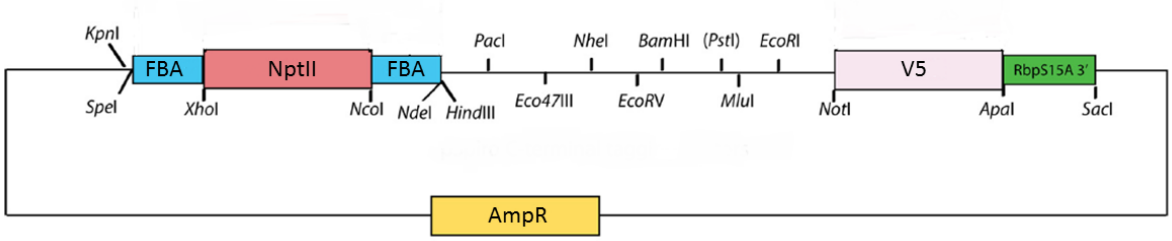

Figure 11. Detailed map of pSpiro_NptII_NEO_V5 vector showing constructed cassette and restriction sites. Adjusted from Jerlström-Hultqvist et al., 2013.

Primers used for the gene amplification and cloning into pSpiro_NptII_NEO:

HydE	
HydE Vor DS F - **MluI**	5'-**ACGCGT**GATGATGAAGAACTCACTCGT-3'
HydE Vor DS R - **NotI**	5'-**GCGGCCGC**TTACAATTACACTTATGCGGC-3'
HydG	
HydG DS F - **MluI**	5'-**ACGCGT**CACCACGTCGCGGTAGT-3'
HydG V5 DS R – **ApaI/V5tag/NotI**	5'-**GGGCCC**AGTAGAATCTAAGCCTAATAAAGG ATTAGGAATAGGTTTGCCC**GCGGCCGC**GAACA ACTGGCCACGCTT-3'
HydG Inner primer	5'-AAGGACAAGGAGCTGCG-3'
IscU	
IscU Vor DS F – **MluI**	5'-**ACGCGT**GAAGGGCTTTTCATTTGG-3'
IscU V5 DS R - **ApaI/V5tag/NotI**	5'-**GGGCCC**AGTAGAATCTAAGCCTAATAAAGGATT AGGAATAGGTTTGCCC**GCGGCCGC**CTTCTTAGACT TCTTATTTTTGTC-3'

4.4.10. Preparation of polyclonal antibodies

4.6.10.1. Anti-Hydrogenase polyclonal antibody

Purified recombinant protein (4mg) was sent for the immunization of rabbit to Davids Biotechnologie (Regensburg, Germany) in soluble form (4 M Urea). Preimmune serum and serum after the final 4th immunization was tested on the western blot. We obtained 80 ml of blood serum with polyclonal antibody after the 4th immunization. Azide was added to the serum in the final concentration of 0,01%, several aliquots (500 μl) were stored at 4°C, the stock was kept at -80°C (same storage process was used for the other two antibodies).

4.6.10.2. Anti-HydG polyclonal antibody

Two milligrams of purified protein were submitted for the immunization to Moravian Biotechnology (Brno, Czech Republic) in soluble form (2 M Urea). Two rabbits were selected for the immunization. Preimmune serum and serum after the final 4th immunization was tested on the western blot. After the last immunization, we obtained 80 ml of blood serum with polyclonal antibody.

4.6.10.3. Anti-HydE polyclonal antibody

Sample from the protein purification containing 2 mg of HydE protein was mixed with SDS sample buffer and loaded on the 13,5% acrylamide preparative gel. After separation, the gel was stained with CBB and destained with Destain solution. Gel containing the protein was cut out with scalpel, homogenized in Dounce homogenizer and used for the rat immunization (Jan Mach Ph.D., Department of Parasitology, Charles University, Prague). Preimmune serum was tested before immunization to test nonspecific reaction of the serum with cell lysate of *S. vortens*.

4.4.11. Transmission electron microscopy (TEM)

For transmission electron microscopy (TEM), pellets of *S. vortens* and *Hexamita sp*. were fixed for 24 h in 2,5% glutaraldehyde in 0,1 M cacodylate buffer (pH 7,2) and post fixed in 2% OsO4 in the same buffer. Fixed *S.vortens*/*Hexamita sp.* was dehydrated through an ascending ethanol and acetone series and embedded in Araldite - Poly/Bed® 812 mixture. Thin sections were cut on a Reichert-Jung Ultracut E ultramicrotome and stained using uranyl acetate and lead citrate. Sections were examined and photographed using JEOL JEM-1011 electron microscope. Fine structure measurements were performed using a Veleta camera and iTEM 5.1 software (Olympus Soft Imaging Solution GmbH).

4.4.12. Sequencing of *Hexamita spp.* genome

Genomic DNA for sequencing was obtained by a phenol-chloroform extraction. NucleoSpin RNA extraction kit (Roche) was used for the genomic RNA isolation. Purity of RNA was verified by Agilent 2100 Bioanalyzer (Agilent technologies) in OMICS-Genomics laboratory, Biotechnology and Biomedicine Center in Vestec – BIOCEV. Two different next generation sequencing methods were used: PacBio SMRT (single molecule real time sequencing) at the Uppsala Genome Center (Sweden) and MiSeq Illumina sequencing at the OMICS-Genomics laboratory (BIOCEV, Czech Republic).

4.4.13. Bioinformatic analysis tools

Hexamita sp. genomic and transcriptomic data were assembled in Laboratory of prof. S. Svard, Uppsala University, Sweden. BLASTp program was used for finding the hypothetical mitochondrial proteins in genomic data of *Hexamita sp.* Sequence alignments were constructed in Geneious v8.0.1 and BioEdit v7.0.5 software. Mitochondrial targeting sequences were predicted by TargetP (Emanuelsson et al., 2007), MitoFates (Fukasawa et al., 2015) and PSORT II Prediction servers (Nakai and Horton, 1999). Promega BioMath Calculator was used for the estimation of protein molecular weight (https://www.promega.com/a/apps/biomath/?calc=dnaprotein).

4.7. Supplementary data

Supplementary data 1 contain partial sequences of hydrogenase, HydE and HydG used for the preparation of homologous polyclonal antibodies, complete sequences of HydG, HydE and IscU used for the overexpression experiments. Moreover, these data include three complete protein sequences of hydrogenase discovered in the draft genome of *S. vortens* provided by Laboratory of prof. S. Svard (Uppsala University, Sweden) and seven sequences of *S. salmonicida* hydrogenase paralogs.

Partial sequences of *S. vortens* hypothetical mitochondrial proteins found in the Joint Genome Institute (JGI) genome database are listed in Supplementary data 2.

Supplementary data 3 contain seven partial sequences of hydrogenase found in the JGI genome of *S. vortens* and their alignment with the three complete hydrogenase sequences of *S. vortens* provided by Laboratory of prof. S. Svard (Uppsala University, Sweden).

Internal database of mitochondrial protein sequences from *Saccharomyces cerevisiae* and hydrogenosomal protein sequences from *S. salmonicida* provided by C. Stairs (Uppsala University, Sweden) can be found in Supplementary data 4.

Supplementary data 5 is a list of proteins which were or were not found in the genome of *Hexamita sp.* The table cover complete sequences of the proteins and the results from PSORTII, TargetP and MitoFates programs illustrating the possibility of having the mitochondrial targeting presequence. Higher probability predictions are highlighted in blue (threshold was set at 0.3). Hypothetical mitochondrial proteins are highlighted in green, the cytosolic ones in red, proteins with possible dual localization are colored in orange.

All supplementary data are uploaded on the CD attached to this thesis.

5. Results

5.1. Characterization of mitochondrial organelle in *Spironucleus vortens*

5.1.1. Transmission electron microscopy (TEM)

First, we investigated the ultrastructure of the cells with aim to identify their mitochondrial organelles using TEM. Two nuclei, cytostomes, flagella and various number of vacuoles were observed (Figure 12A). Endoplasmic reticulum was scattered in the cell with no specific pattern and distribution (Figure 12B). In addition, the cells possess organelles of 400 - 500 nm in diameter. The web of filamentous material forming circular patterns with the same electron density as cytosol was visible inside of these vesicles (Figure 13B, 13D and 13F). Two membranes surrounding the organelle were observed at higher magnifications (Figure 13B), which is the main characteristics of mitochondrial organelle. Comparison of the membrane thickness between vacuole and observed mitochondria is present in Figure 13D. Only one to three mitochondrial organelles were found on the single section of *S. vortens*, suggesting relatively low number of these organelles within the cell.

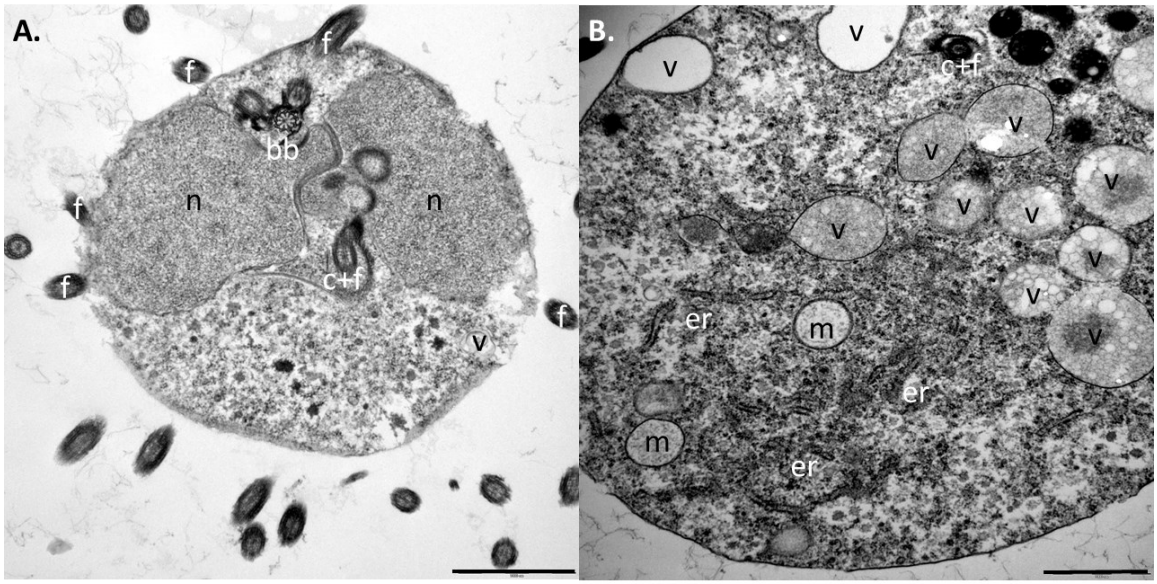

Figure 12. TEM of *S. vortens*. A. Overview of the whole cell of *S. vortens* – lateral section (scale bar = 2000 nm); **B.** Cell section of *S. vortens* with clearly visible endoplasmic reticulum and various vesicles (scale bar = 1000 nm); **n** = nucleus, **v** = vacuole, **c** = cytostome, **bb** = basal body of flagellum, **f** = flagellum, **er** = endoplasmic reticulum, **m** = double-membrane mitochondrial organelle.

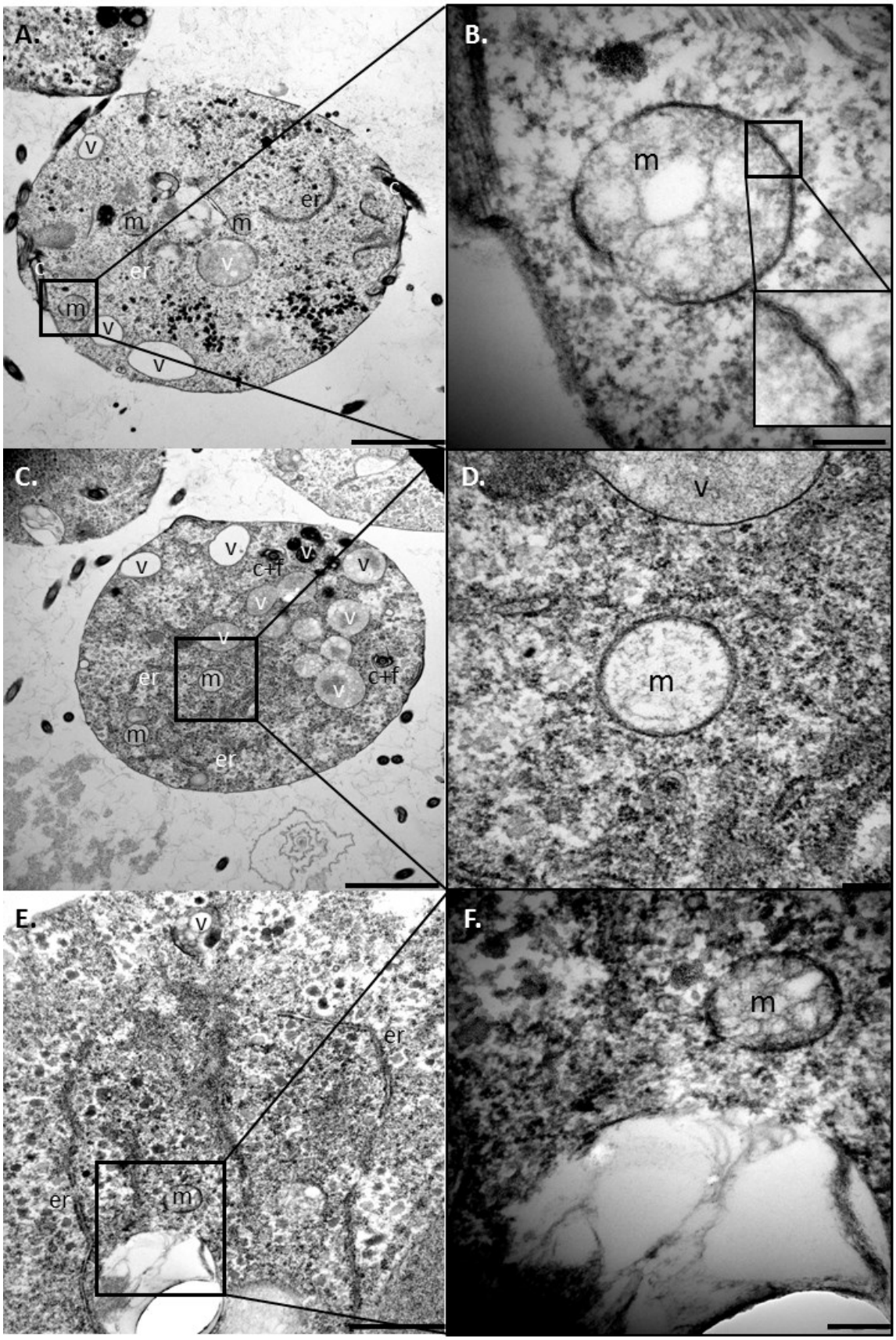

Figure 13. TEM of *S. vortens* with sections containing mitochondrial organelles. A.+C. *S. vortens* cell overview (scale bar = 2000 nm). **E.** Cell section with detail of endoplasmic reticulum and one mitochondrial organelle (scale bar = 1000 nm). **B.+D.+F.** Cell section with detail of double-membrane mitochondrial organelle (scale bar = 200 nm). **v** = vacuole, **c** = cytostome, **f** = flagellum, **er** = endoplasmic reticulum, **m** = double-membrane mitochondrial organelle.

5.1.2. Prediction of putative mitosomal proteins in *S. vortens* genome

I analyzed partially assembled genome of *S. vortens*, available at JGI genome database to find suitable mitochondrial candidates for the preparation of homologous polyclonal antibodies against corresponding recombinant proteins. The genome was downloaded from the JGI website (https://genome.jgi.doe.gov/portal/Spivo0/Spivo0.home.html) and imported into Geneious v8.0.1 software. Amino acid sequences of *S. salmonicida* hydrogenosomal proteins were selected as a query (GeneBank accession numbers AFV80041 - AFV80087), tblastn program was used against the JGI *S. vortens* genome database. Only hits with e-value lower than $1x10^{-5}$ were considered relevant. Partial sequences of IscU, IscS, ferredoxin, hybrid cluster protein, frataxin, Tom40, Tim14, hydrogenase, all three hydrogenase maturases, DnaK, Hsp70, Cpn60, SHMT, PFO ACS1 were found in the *S. vortens* genome (Supplementary data 2).

S. vortens as well as the other diplomonads (except for *G. intestinalis*) uses alternative genetic code – stop codons TAG and TAA are translated as glutamine and the only signal for termination is TGA (Keeling and Doolittle, 1997; Kolisko et al., 2008). Moreover, predicted proteins lack mitochondrial targeting sequence.

For the purposes of antibody preparation, partial gene sequences of three suitable candidates (hydrogenase, HydG and HydE) were selected for recombinant protein production. Hydrogenase and HydG sequence did not have any TAG or TAA codons encoding glutamine, HydE sequence had one TAG codon inside (see Supplementary data 1).

5.1.3. Hydrogenase of *S. vortens*

5.1.3.1. Comparison of the hydrogenase sequences in *S. vortens*

Seven orthologs of hydrogenase from *S. salmonicida* were used as query to search for hydrogenase in *S. vortens* (Supplementary data 1). I obtained seven different partial sequences of hydrogenase (Supplementary data 3). These sequences were sent to the prof. S. Svard at Uppsala University who resequenced genome of *S. vortens* (unpublished data) for comparison. Three orthologous genes of hydrogenase were found in this draft genome of *S. vortens* (complete protein sequences were provided by Xu FeiFei from Laboratory of prof. S. Svard, Uppsala University, Sweden). For the alignment of seven partial and three complete hydrogenase sequences in *S. vortens*, see Supplementary data 3. Seven hydrogenases of *S.*

salmonicida were aligned to three complete hydrogenase sequences of *S. vortens* in order to confirm the presence of conserved motifs (Fe-S clusters and H cluster) in the sequences (Figure 14). Hydrogenase 1, 2 and 3 from *S. vortens* are 469, 480 and 468 base pairs long which strongly correspond with the length of cytosolic hydrogenase 1 (468 bp) and hydrogenosomal hydrogenase 5 (467 bp) in *S. salmonicida*. Other two shorter *S. salmonicida* cytosolic hydrogenases 3 and 7 have 404 and 427 base pairs respectively.

According to the PSORT analysis (Gavel program), mitochondrial presequence was predicted in Hydrogenase 2 of *S. vortens* (Figure 14). However, TargetP program analysis showed only 0.209 score with reliability prediction class 3 (1 means the strongest prediction, 5 indicates the weakest) and MitoFates program predicted the probability of presequence with score 0.013. Predicted cleavage site is located between DRN and FS amino acids and the alignment illustrates, that this site is not unique for Hydrogenase 2 and is present with certain modifications in all hydrogenase sequences listed in the alignment. Moreover, based on the percentage identity of amino acid residues, all three hydrogenases from *S. vortens* are most identical with the cytosolic Hydrogenase 1 from *S. salmonicida* (Table 1), which also have similar number of base pairs. Percentage identity of amino acid residues between the hydrogenases of *S. vortens* ranged from 46,7 % to 59,5 % (Table 2).

The alignment also demonstrates that length of the sequences does not correspond with the cell localization. Hydrogenase 2, Hydrogenase 4 and Hydrogenase 6 of *S. salmonicida* are approximately 50 base pairs longer than other hydrogenases in the alignment and only Hydrogenase 6 is targeted to the mitochondrial organelle. Considering the shorter hydrogenase sequences, only Hydrogenase 5 from *S. salmonicida* has been localized to the hydrogenosome.

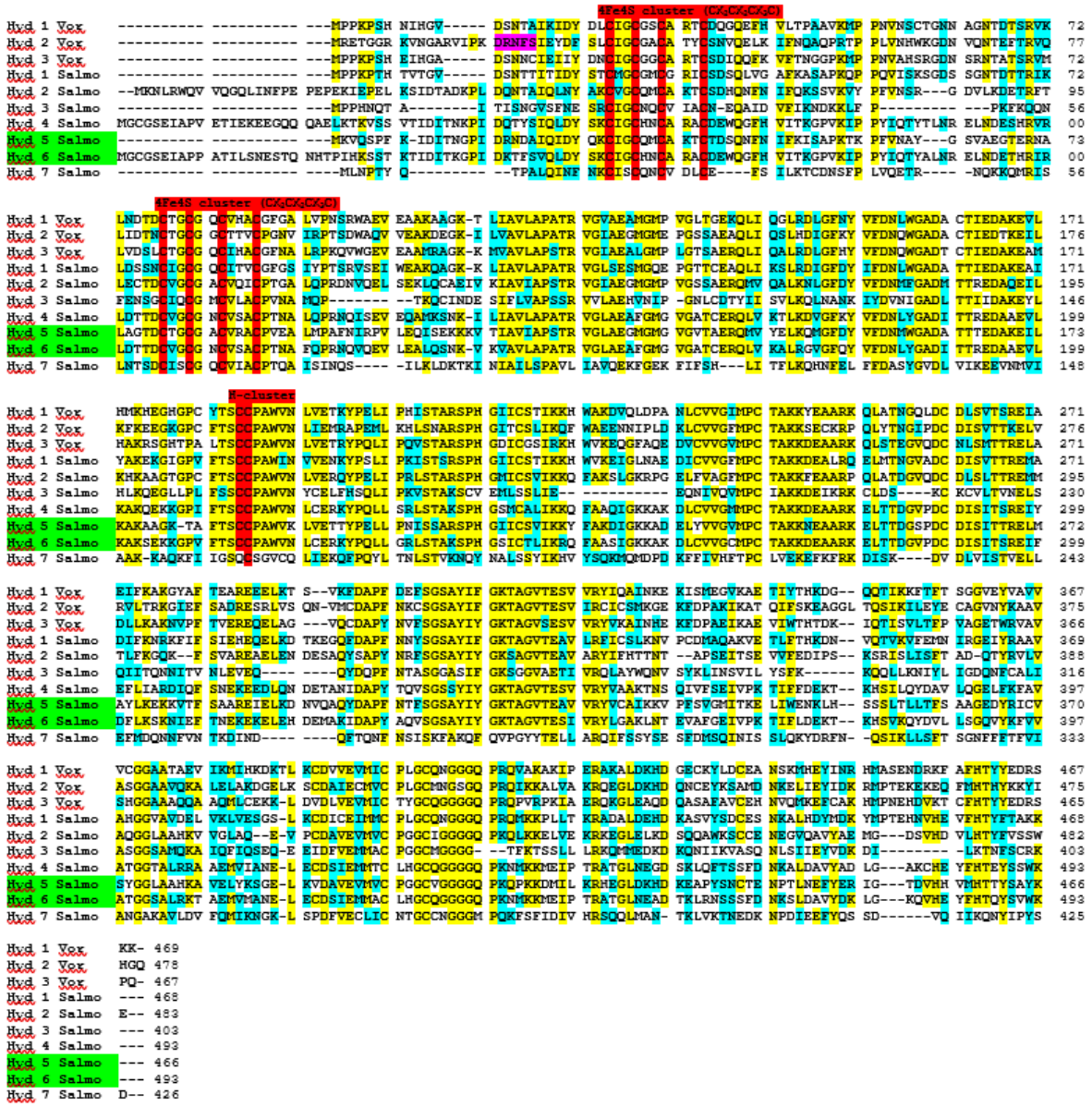

Figure 14. Protein sequence alignment of *S. vortens* and *S. salmonicida* hydrogenase. Three different hydrogenases of *S. vortens* were aligned to seven hydrogenase paralogs of *S. salmonicida*. [4Fe4S] cluster and H-cluster motifs are highlighted in red. Cleavage site prediction in Hydrogenase 2 of *S. vortens* is colored in purple. Similar amino acids are highlighted in blue, identical amino acids in yellow. Threshold for shading was set at 50%. Hydrogenosomal hydrogenases of *S. salmonicida* are highlighted in green. **Hyd Vor** = hydrogenase sequence in *S. vortens* **Hyd Salmo** = hydrogenase sequence in *S. salmonicida*.

	Hyd 1 Salmo	Hyd 2 Salmo	Hyd 3 Salmo	Hyd 4 Salmo	Hyd 5 Salmo	Hyd 6 Salmo	Hyd 7 Salmo
Hyd 1 Vor	55,7%	43,1%	27,6%	44,1%	48,4%	43,6%	24,9%
Hyd 2 Vor	49,1%	40,2%	27,3%	40,0%	46,1%	40,6%	22,8%
Hyd 3 Vor	51,0%	44,0%	28,7%	42,1%	47,3%	41,9%	22,2%

Table 1. Comparison of percentage identity of amino acid residues in hydrogenase sequences of *S. vortens* and *S. salmonicida* (analysis was performed by Geneious 8.0.5 software). **Hyd Vor** = hydrogenase sequence in *S. vortens*, **Hyd Salmo** = hydrogenase sequence in *S. salmonicida*.

	Hyd 1 Vor	Hyd 2 Vor	Hyd 3 Vor
Hyd 1 Vor		49,4%	59,5%
Hyd 2 Vor	49,4%		46,7%
Hyd 3 Vor	59,5%	46,7%	

Table 2. Comparison of percentage identity of amino acid residues in hydrogenase sequences of *S. vortens* (analysis was performed by Geneious 8.0.5 software). **Hyd Vor** = hydrogenase sequence in *S. vortens*.

5.1.3.2. Preparation of polyclonal anti-hydrogenase antibody

For the antibody preparation, 720 base pairs long partial sequence of hydrogenase (corresponding to Hydrogenase 3 in *S. vortens*) was selected (see Supplementary data 1). Hydrogenase gene fragment was subcloned into pJET1.2/blunt plasmid and then re-cloned into the expression vector pET42b. Plasmid with hydrogenase gene was used for transformation of BL21-DE3 *E. coli*. Four different clones were selected to test induction of protein expression using the IPTG. Ni-NTA-based affinity chromatography was used for the purification of the recombinant protein with 6x-HIS tag (Figure 15). Majority of the recombinant protein was released in E1-E4 elution fractions (pH 4,5). Altogether, 4 mg of purified protein were obtained in 8 M Urea, diluted into 4 M Urea and used for the rabbit immunization. Before the immunization, the pre-serum was tested for the nonspecific protein reaction on the lysate of *S. vortens* (Figure 16A). We received the final blood serum with desired antibody after the 4th immunization of the animal.

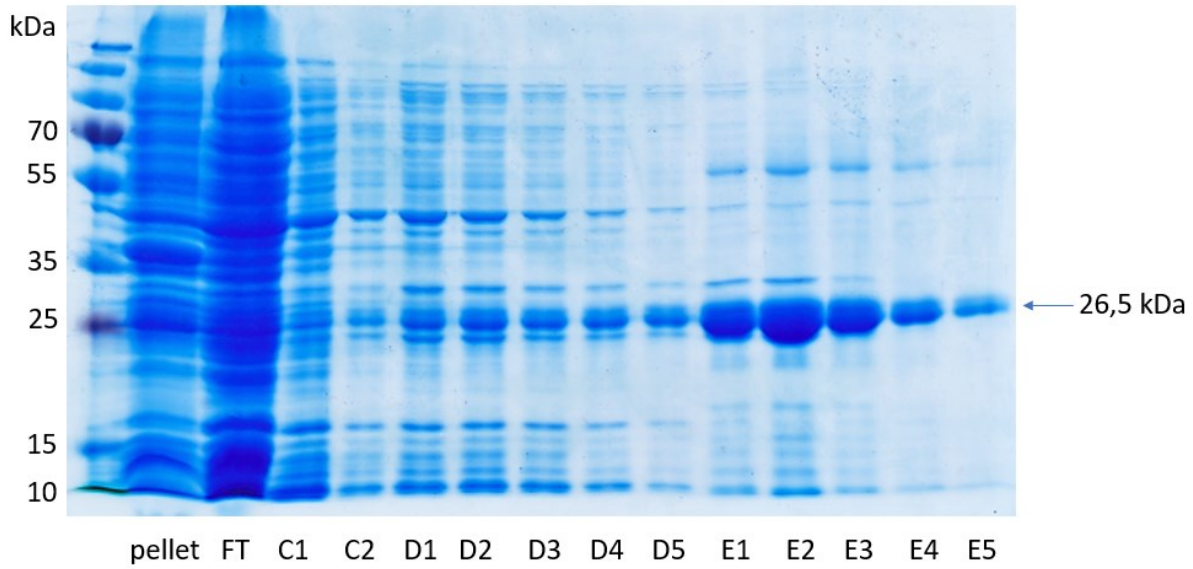

Figure 15. SDS-PAGE illustrating the purification of hydrogenase for the production of specific antibody. FT = flow through, **C1-C2** = wash buffer, **D1-E5** = elution buffers with released protein.

5.1.3.3. Cellular localization of hydrogenase in *S. vortens* using the western blot analysis

Western blot analysis was used for the detection of hydrogenase on subcellular fractions from *S. vortens*. The antibody recognized compete protein of expected size (52kDa) in the lysate and in the cytosolic fraction (Figure 16B). No signal was observed in the organellar fraction, which suggests only cytosolic localization of hydrogenase in *S. vortens*.

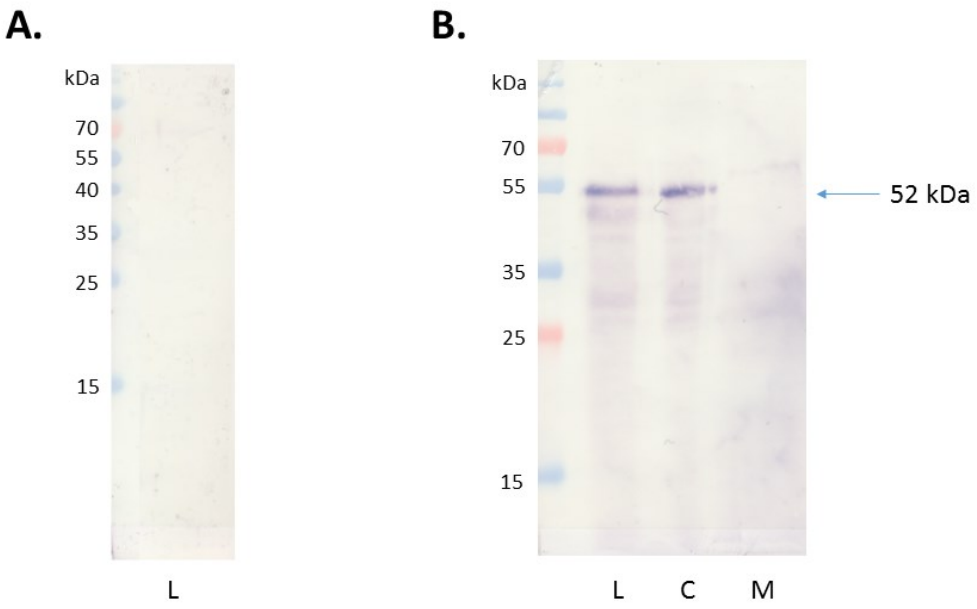

Figure16. Western blot analysis of pre-serum and serum after 4th immunization containing the anti-hydrogenase antibody. A. Test of preimmunized serum from selected rabbit as a primary antibody on a lysate of *S. vortens* **B.** Test of final serum after 4th immunization as a primary antibody on a subcellular fractions of *S. vortens*. **L** = total lysate, **C** = cytosolic fraction, **M** = organellar fraction containing mitochondrial organelles.

5.1.3.4. Cellular localization of hydrogenase in *S. vortens* using the immunofluorescence microscopy

Subsequently, the anti-hydrogenase antibody was used as a primary antibody for the hydrogenase detection in *S. vortens* using the immunofluorescence microscopy. The signal was observed in the large number of small dots that were evenly distributed throughout the cells, that most likely correspond to the cytosolic localization (Figure 17). These results are consistent with the western blot analysis of the cellular fractions.

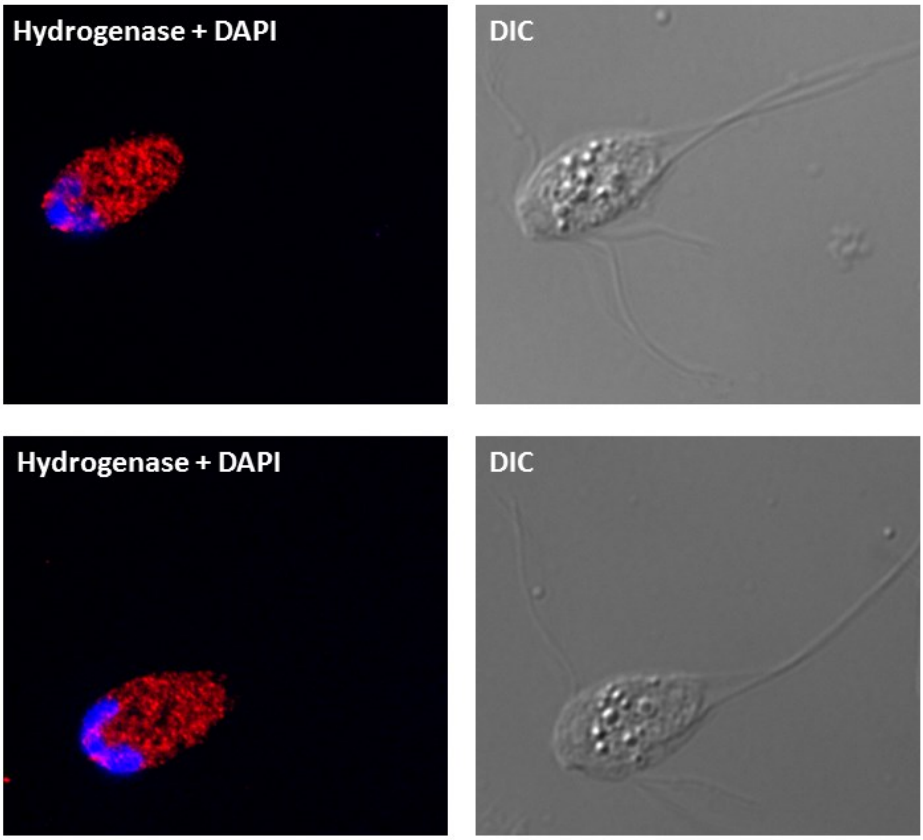

Figure 17. Detection of hydrogenase in *S. vortens* by polyclonal antibody (red). The nuclei were stained by DAPI (blue). Formaldehyde protocol was used for the slide preparation. **DIC** = differential interference contrast, **DAPI** = 4ˈ,6-diamidine-2ˈ-phenylindole dihydrochloride.

5.1.4. Preparation of polyclonal anti-HydE antibody

Partial sequence of HydE gene coding protein with total molecular weight of 22 kDa was selected (see Supplementary data 1). Although the sequence had one stop codon (in *S. vortens* coding glutamine) in the middle, the Taq polymerase caused a random mutation in this specific codon identified by sequencing in one of the bacterial colonies. During the HydE protein purification, high amount of protein remained in flow through fraction and did not bind to the NiNTA column (Figure 18). Despite of that, we were able to collect 2 mg of protein in E1-E4 elution fractions (pH 4,5). E1, E2, E3 and E4 samples containing HydE protein were loaded on the preparative SDS-PAGE for purification. Fragment of the gel was sent to Mass Spectrometry analysis that confirmed presence of HydE in the sample. 2 mg of purified HydE were used for the rat immunization in form of SDS-PAGE homogenate. The pre-serum of the rat was tested for the nonspecific reaction in subcellular fractions of *S. vortens* (Figure 19A). After the 4th immunization, the serum with antibody was harvested from the rat.

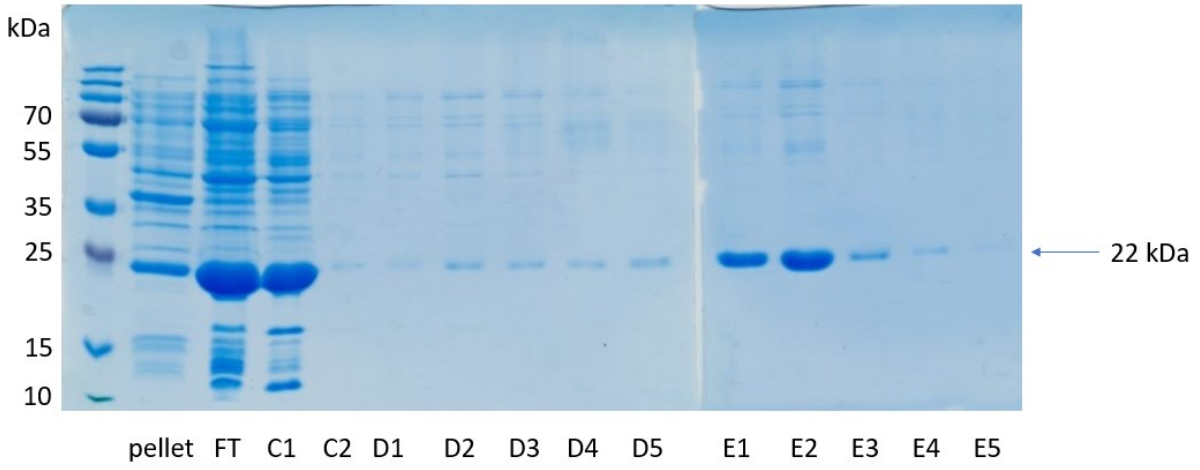

Figure 18. SDS-PAGE illustrating the purification of recombinant HydE protein for the production of specific antibody. FT = flow through, **C1-C2** = wash buffer, **D1-E5** = elution buffers with released protein.

5.1.4.1. Cellular localization of HydE using the western blot analysis

In order to investigate the cellular localization of HydE, I performed the cellular fractionation of *S. vortens* and tested the anti-HydE antibody on the western blot. Purified recombinant protein, lysate, cytosolic and organellar fraction containing mitochondrial organelles were tested (Figure 19B). Recombinant HydE with polyhis tag was used as a positive control. Anti-HydE as well as anti-His antibody recognized partial purified recombinant protein (22kDa). In cellular fractions, a protein with molecular weight of about 50 kDa was detected in lysate and in organellar fraction containing mitochondrial organelles using the anti-HydE antibody. These results indicate that HydE protein is most likely localized in mitochondrial organelles of *S. vortens*.

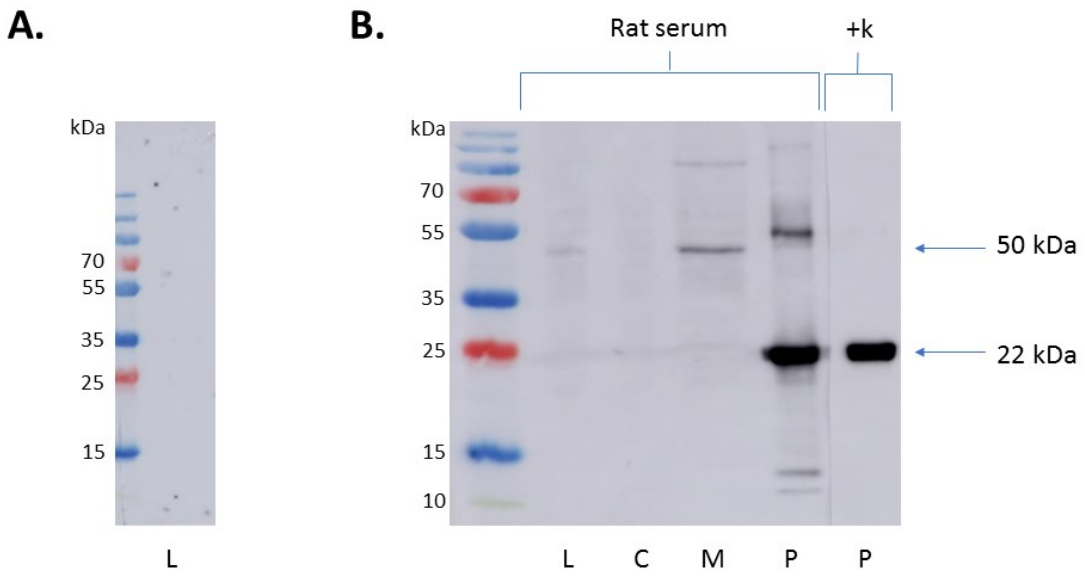

Figure 19. Western blot analysis of rat pre-serum and serum after 4th immunization containing the anti-HydE antibody. A. Test of preimmunized serum from selected rat as a primary antibody on a lysate of *S. vortens* **B.** Test of final serum after 4th immunization of selected rat as a primary antibody on a subcellular fractions of *S. vortens.* **+k** = anti-HIS primary antibody, **P** = partial purified recombinant protein, **L** = total lysate, **C** = cytosolic fraction, **M** = organellar fraction containing mitochondrial organelles.

5.1.4.2. Cellular localization of HydE using the immunofluorescence microscopy

Subsequently, the anti-HydE antibody was used for the protein detection in *S. vortens* using the immunofluorescence microscopy. Anti-HydE antibody labeled small number of vesicles (six to twelve) dispersed within the cell (Figure 20). Relative low number of labeled organelles and their distribution in the cell correspond with the results from TEM. Therefore, it is most likely that these vesicles represent the mitochondrial organelles of *S. vortens*.

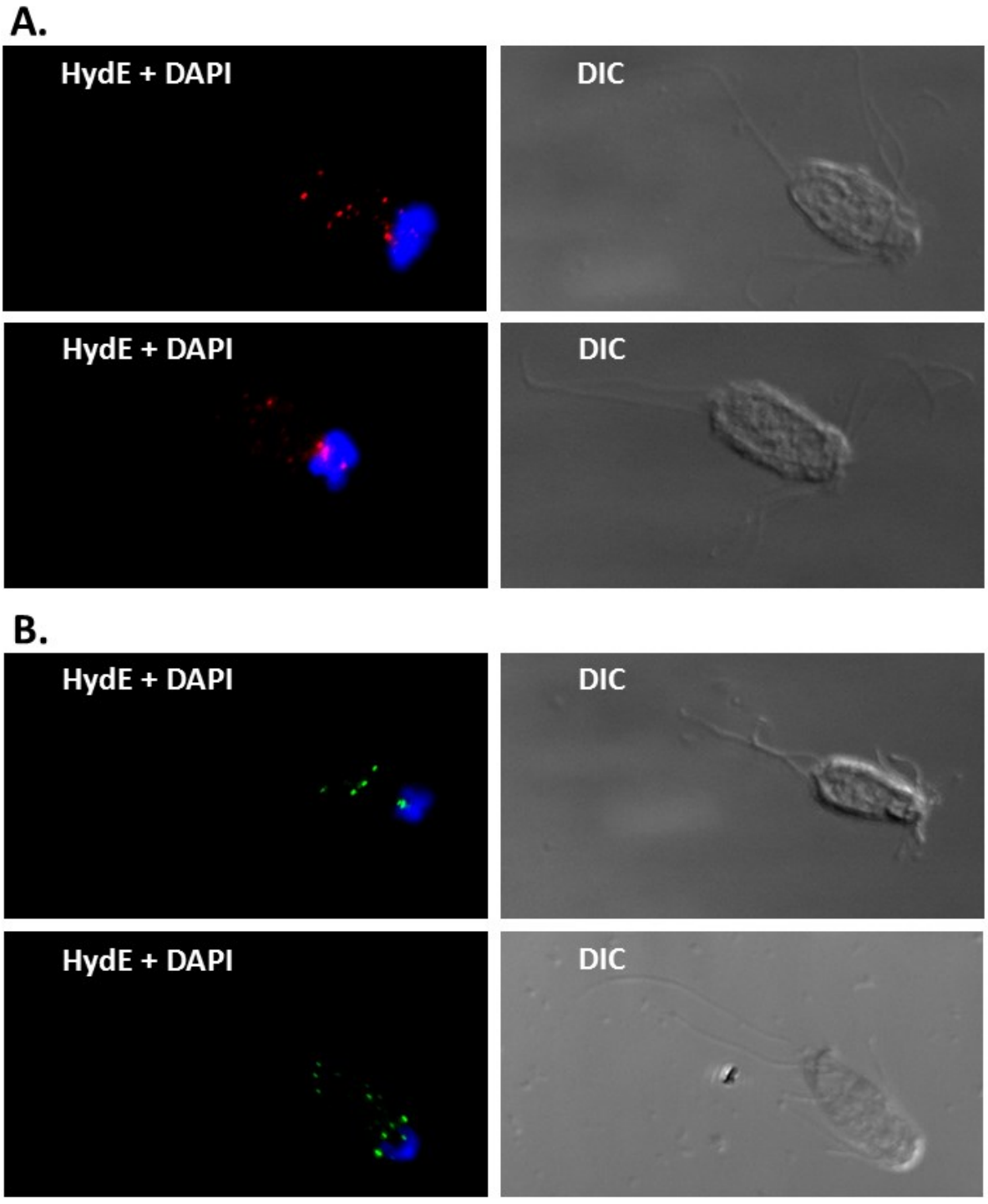

Figure 20. Detection of HydE antibody in the cells of *S. vortens*. A. HydE detection using rat polyclonal anti-HydE antibody and anti-rat IgG secondary antibody, Alexa Fluor 594 (red). **B.** HydE detection using rat polyclonal anti-HydE antibody and anti-rat IgG secondary antibody, Alexa Fluor 488 (green). The nuclei were stained by DAPI (blue). Methanol-acetone protocol was used for the slide preparation. **DIC** = differential interference contrast, **DAPI** = 4′,6-diamidine-2′-phenylindole dihydrochloride.

5.1.5. Preparation of polyclonal anti-HydG antibody

For the gene cloning, I used gene coding partial HydG protein of approximate molecular weight 28,5 kDa (see Supplementary data 1). Recombinant protein produced in *E. coli* was released from the NiNTA column in D and E elution buffer fractions (pH 5,9 and 4,5 respectively), with the highest yield in fraction E1 (Figure 21). Total amount of 2 mg was diluted in 2 M Urea and sent to Moravian Biotechnology (Brno, Czech Republic) for the rabbit immunization (two rabbits were used). Preimmune sera of the two selected animals were obtained after the start of the immunization process. Sera were tested on the purified recombinant protein and on the lysate and subcellular fractions of *S. vortens* (concentration 1:100) (Figure 22). Anti-HIS antibody was tested on the purified recombinant protein as a positive control. The estimated size of a complete HydG protein was 57,6 kDa. The sera recognized proteins of various sizes in all fractions. In the case of preimmune serum from rabbit 1, there was a strong bend with the same size as partial HydG protein in organellar fraction. Moreover, weak signal was detected around 58 kDa in lysate and cytosol. Rabbit 2 pre-serum visualized weak bends with the same size as complete HydG protein (57,6 kDa) in lysate, cellular fraction and also in the organellar fraction. The sera after the 4^{th} immunization were tested for the comparison (Figure 23). Serum from rabbit 1 recognized protein of the expected size in the lysate, however only slightly higher and slightly lower bend was detected in organellar fraction. In case of final serum from rabbit 2, protein of the approximate size 58 kDa was visualized in lysate, cytosolic and organellar fraction. We did not proceed to the antibody purification and further experiments due to the non-specific detection of protein of expected size by the pre-sera of both rabbits.

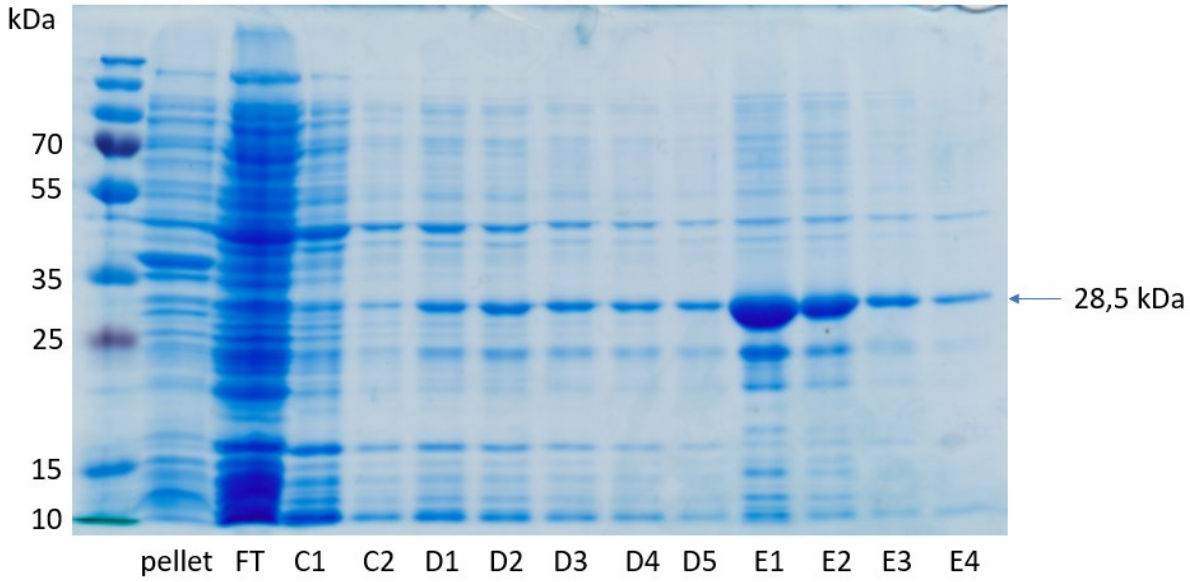

Figure 21. SDS-PAGE illustrating the purification of recombinant HydG protein for the production of polyclonal antibody. **FT =** flow through, **C1-C2** = wash buffer, **D1-E4** = elution buffers with released protein.

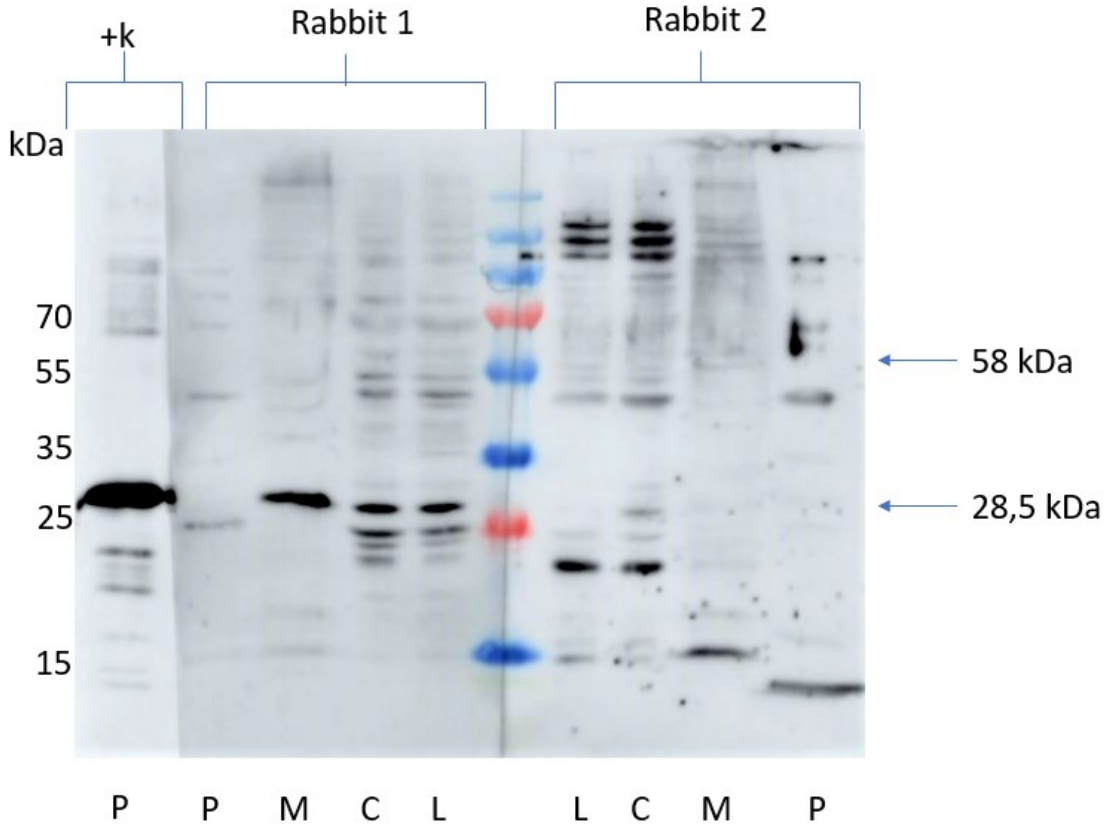

Figure 22. **Test of preimmune sera from two selected rabbits as a primary antibody on a subcellular fractions of *S. vortens.* +k** = anti-HIS primary antibody, **P** = purified recombinant HydG protein, **L** = total lysate, **C** = cytosolic fraction, **M** = organellar fraction containing mitochondrial organelles.

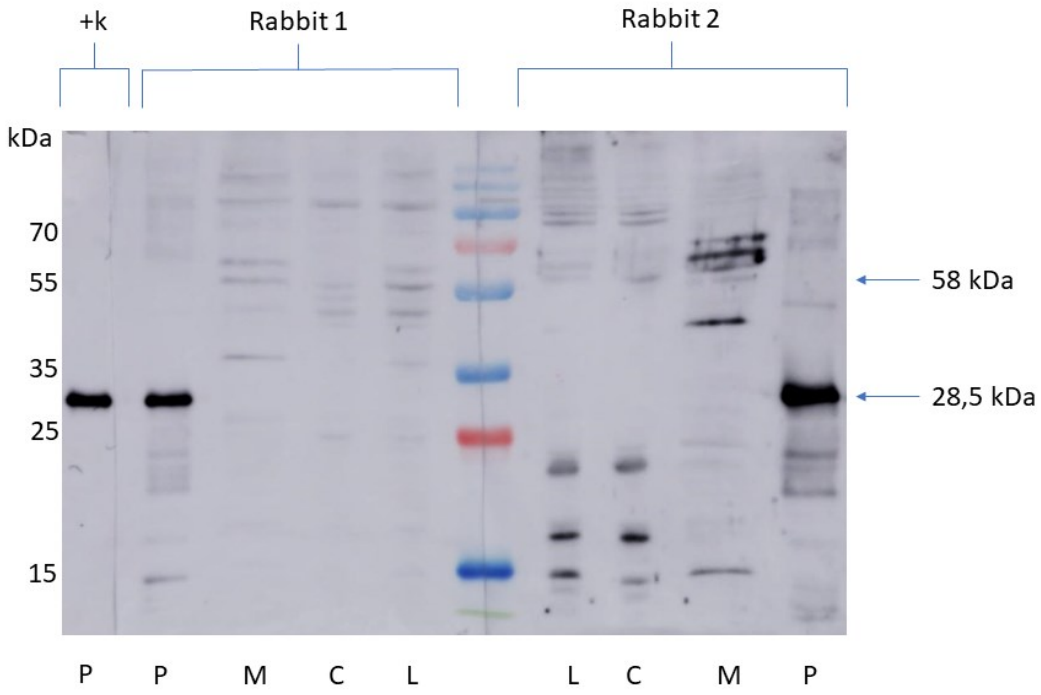

Figure 23. Test of the sera from two selected rabbits after 4th immunization as a primary antibody on a subcellular fractions of *S. vortens*. +k = anti-HIS primary antibody, **P** = purified protein, **L** = total lysate, **C** = cytosolic fraction, **M** = organellar fraction containing mitochondrial organelles

5.1.6. Cellular localization of Cpn60 in *S. vortens* using the western blot analysis and the immunofluorescence microscopy

Homologous antibody against Cpn60 in *S. vortens* has been developed by Eva Nývltová Ph.D. (Charles University, Laboratory of prof. J. Tachezy). Antibody was tested on the western blot using the *S. vortens* subcellular fractions. Slightly visible bend around the expected size (60kDa) was detected in lysate and organellar fraction. However, many of non-specific signals were repeatedly visualized (Figure 24A).

In addition to that, slides for the immunofluorescence microscopy were prepared. Anti-Cpn60 antibody labeled rather large number of unevenly distributed vesicles (Figure 24B). This observation does not correspond with the anti-HydE antibody results. It is unlikely that the anti-Cpn60 antibody labeled only mitochondrial organelles, therefore we believe that this antibody is not suitable for localization studies.

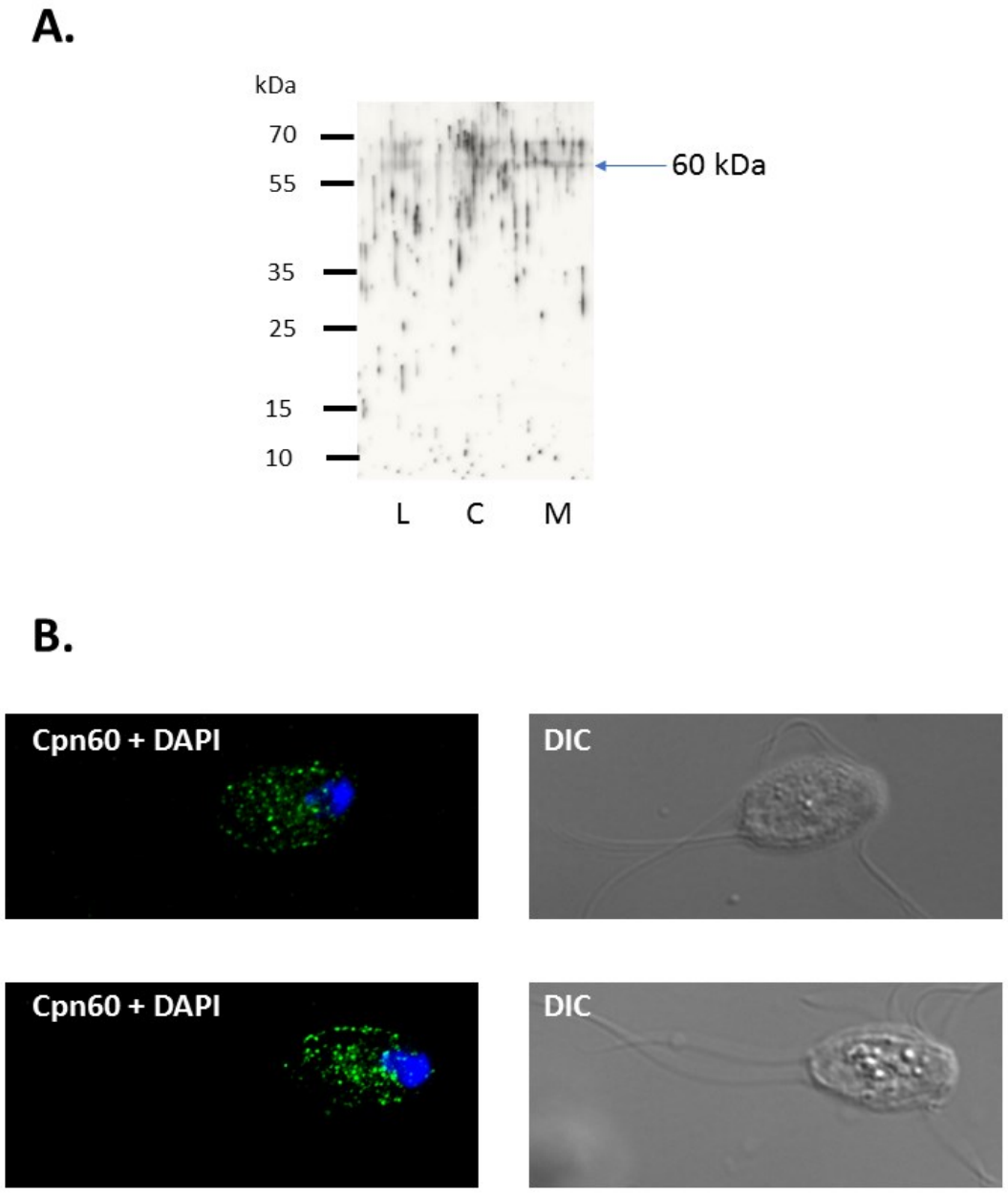

Figure 24. Test of anti-Cpn60 antibody in *S. vortens* A. Western blot analysis of Cpn60 antibody tested on subcellular fractions from *S. vortens* **B.** Detection of Cpn60 by rat anti-Cpn60 antibody (green). The nuclei were stained by DAPI (blue). **L** = total lysate, **C** = cytosolic fraction, **M** = organellar fraction containing mitochondrial organelles, **DIC** = differential interference contrast, **DAPI** = 4ˈ,6-diamidine-2ˈ-phenylindole dihydrochloride.

5.1.7. Test of antibodies against G. intestinalis mitosomal proteins in subcellular fractions of S. vortens and cellular localization via immunofluorescence microscopy

Four different heterologous antibodies developed against *G. intestinalis* mitosomal proteins (Tom40, IscU, IscS and Cpn60) were tested for labeling of the mitochondrial organelles in *S. vortens*. *G. intestinalis* (WB strain, ATCC_50803) lysate and subcellular

fractions were provided by the Laboratory of P. Doležal (Charles University, BIOCEV, Czech Republic) and used for experiments as positive control. (Figure 25).

Precursor of IscU protein in *G. intestinalis* (GenBank accession number AAM14634.1) with the expected molecular weight of approximately 17,7 kDa. was detected in the lysate and the cytosolic fraction. Maturated form with cleaved mitochondrial targeting sequence was visualized in the lysate and the organellar fraction. Tom40 (expected molecular weight 39 kDa, GenBank accession number EDX54229.1), IscS (expected molecular weight 47,6 kDa, GenBank accession number AAK39427.1) and Cpn60 (expected molecular weight 60,2 kDa, GenBank accession number AAC38821.1) were observed in the lysate and predominantly in the organellar fraction (Figure 25A).

Expected size of IscU protein in *S. vortens* is 21,3 kDa (see Supplementary data 1). Since we did not find complete sequences of IscS, Tom40 and Cpn60 in the genome of *S. vortens,* so we anticipated similar size of the protein bends as in *S. salmonicida* (43,9 kDa for IscS, 30,3 kDa for Tom40 and 60,2 kDa for Cpn60). IscU appeared as bend in all three fractions with approximate size of 17 kDa (Figure 25B). Anti-IscS antibody labeled several bends with the strongest signal for protein of approximate molecular weight 45 kDa, which correspond with our expectation. Antibody against Tom40 visualized two bends in the lysate and the cytosolic fraction (cca 40 and 35 kDa) and single bend in the organellar fraction (39 kDa). This antibody did not label any bend of anticipated molecular weight of 30 kDa. Finally, anti-Cpn60 antibody visualized a bend of 30 kDa in the lysate and the organellar fraction. In addition, a weak bend of expected molecular weight of 60 kDa was labeled by the antibody in the organellar fraction suggesting that the Cpn60 could be degraded. Overall, the results from the western blot analysis indicate that anti IscU and anti-IscS antibody from *G. intestinalis* might label the mitochondrial organelles of *S. vortens*.

Next, we tested antibodies against four *G. intestinalis* proteins using the immunofluorescence microscopy (Figure 26). IscU antibody was observed within *S. vortens* cell in about 8 to 14 small bright vesicles but was also detected in the cytosol. Tom40 signal was localized to approximately forty slightly bigger vesicles and IscS antibody signal was distributed over the whole cell. Cpn60 was detected mostly in one vesicle located in the apical part of the cells which is likely an artifact. Even though heterologous anti-IscU antibody detected bend in the cytosol on the western blot, results from the immunofluorescence microscopy suggest, that it might be a suitable mitochondrial marker. However, no further localization experiments were performed with this antibody yet.

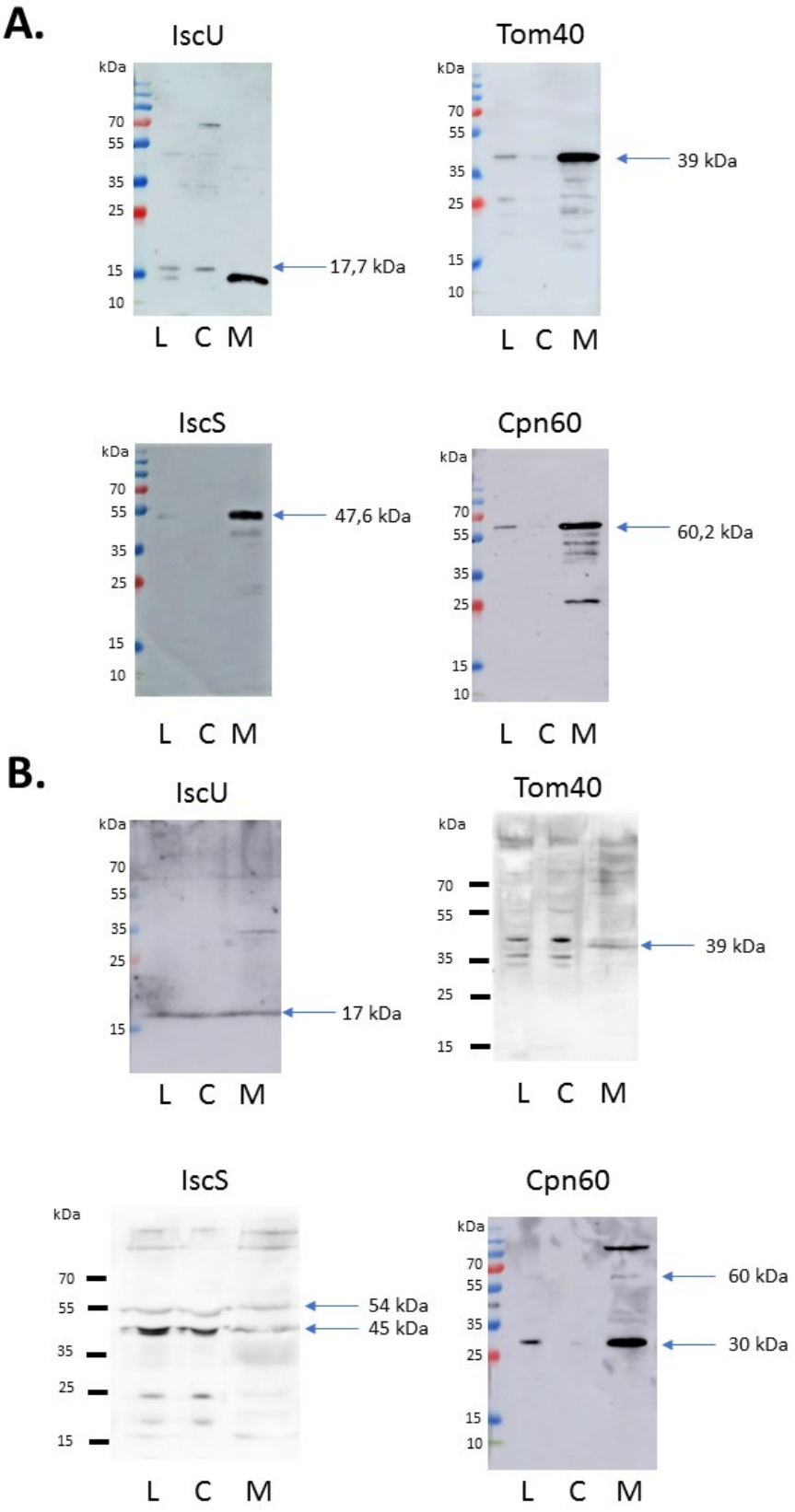

Figure 25. Test of anti-IscU, anti-Tom40, anti-IscS and anti-Cpn60 antibodies from *G. intestinalis* on the western blot A. Western blot analysis of *G. intestinalis* subcellular fractions using antibodies developed against four *Giardia* proteins **B.** Four *Giardia* antibodies tested on subcellular fractions of *S. vortens*. **L** = total lysate, **C** = cytosolic fraction, **M** = organellar fraction containing mitochondrial organelles.

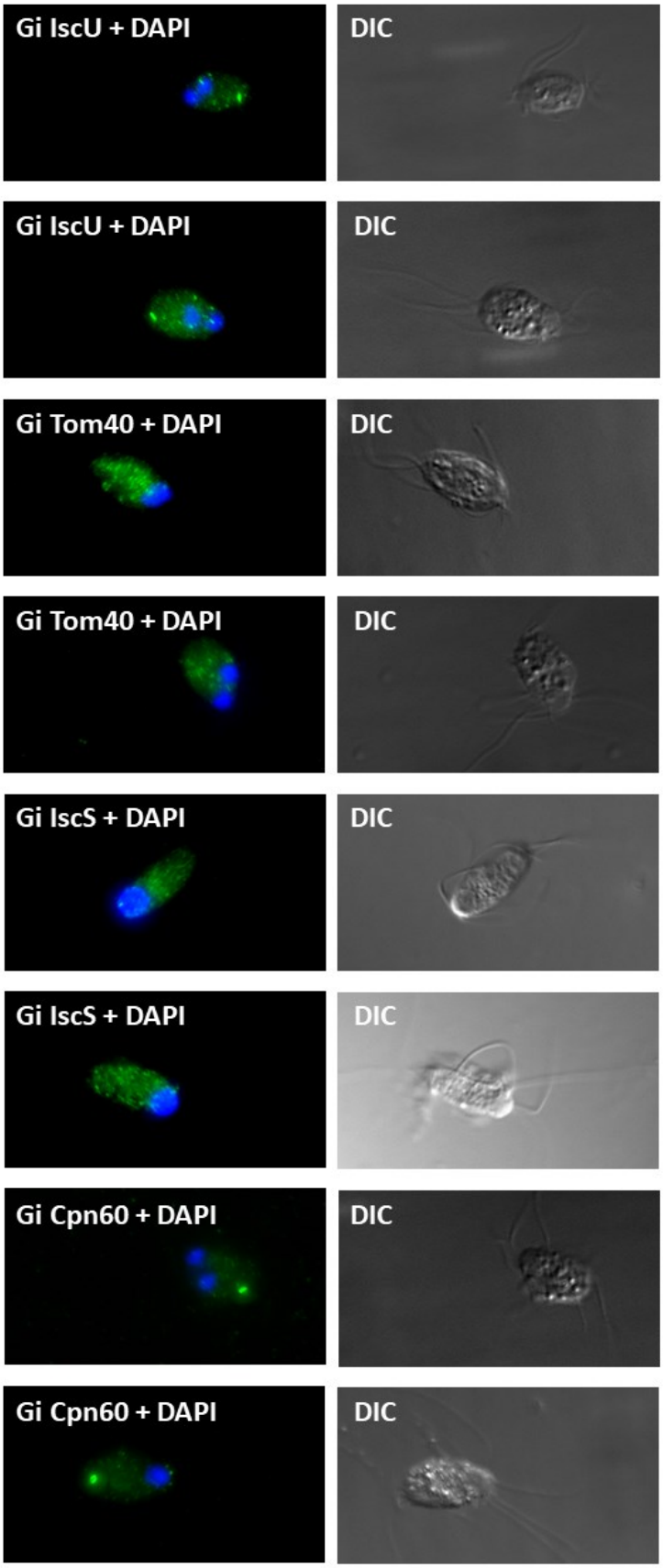

Figure 26. **Detection of IscU, Tom40, IscS and Cpn60 proteins in *S. vortens* (green).** Antibodies were raised against proteins of *G. intestinalis*. The nuclei were stained by DAPI (blue). Formaldehyde protocol was used for the slide preparation. **DIC** = differential interference contrast, **DAPI** = 4ˈ,6-diamidine-2ˈ-phenylindole dihydrochloride.

5.1.8. Expression of recombinant HydE, HydG and IscU proteins in *S. vortens*

5.1.8.1. Single-transfection

We used pSvor_PAC_3xHA_C plasmid for expression of HydE, HydG and IscU with C-terminal HA tag in *S. vortens* (see Chapter 4.4.8). Three different electroporation protocols were used and the transfectants grew under the puromycin selection pressure (concentration 50 µg/ml). After two weeks, stable tranfectant lineages were established from all three different electroporations, illustrating that the protocols were equally efficient. For the confirmation of the protein expression within the cells, the western bolt analysis on the subcellular fractions was performed using the anti-HA antibody (Figure 27). All three proteins were present in the lysate and organellar fraction. Expected molecular weight of IscU was approximately 21 kDa, which was confirmed on the western blot. Even though, molecular weight 43,1 kDa of complete HydE protein was calculated, anti-HA antibody labeled bends around 50 kDa. This observation corresponds with the test of anti-HydE antibody (see Chapter 5.1.4.1). Calculated molecular weight of HydG was 57,6 kDa. The anti-HA antibody labeled bends of approximate molecular weight of 54 kDa and 70 kDa. Lower bend was localized to the lysate and organellar fraction and the molecular weight was similar to the predicted one. Upper bend with molecular weight around 70 kDa was even slightly detected in the cytosol.

In addition to the western blot analysis, the anti-HA antibody was used for the detection of tagged IscU, HydE and HydG *S. vortens* transfectants using the immunofluorescence microscopy (Figure 28). All three proteins were localized to the small vesicles distributed in the cell. Number of vesicles (6 to 16) correspond to the results from anti-HydE antibody localization. We did not proceed to co-localization experiments due to the possible cross-reaction of anti-HA mouse antibody and anti-HydE rat antibody.

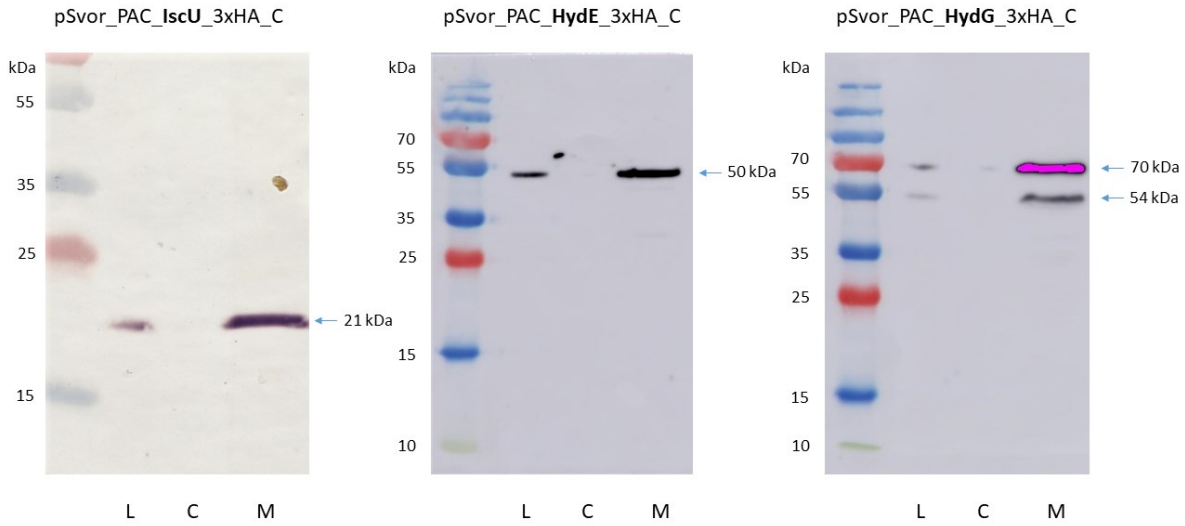

Figure 27. Western blot analysis of anti-HA mouse antibody tested on subcellular fractions from *S. vortens* expressing Iscu/HydE/HydG protein with HA tag. **L** = total lysate, **C** = cytosolic fraction, **M** = organellar fraction containing mitochondrial organelles.

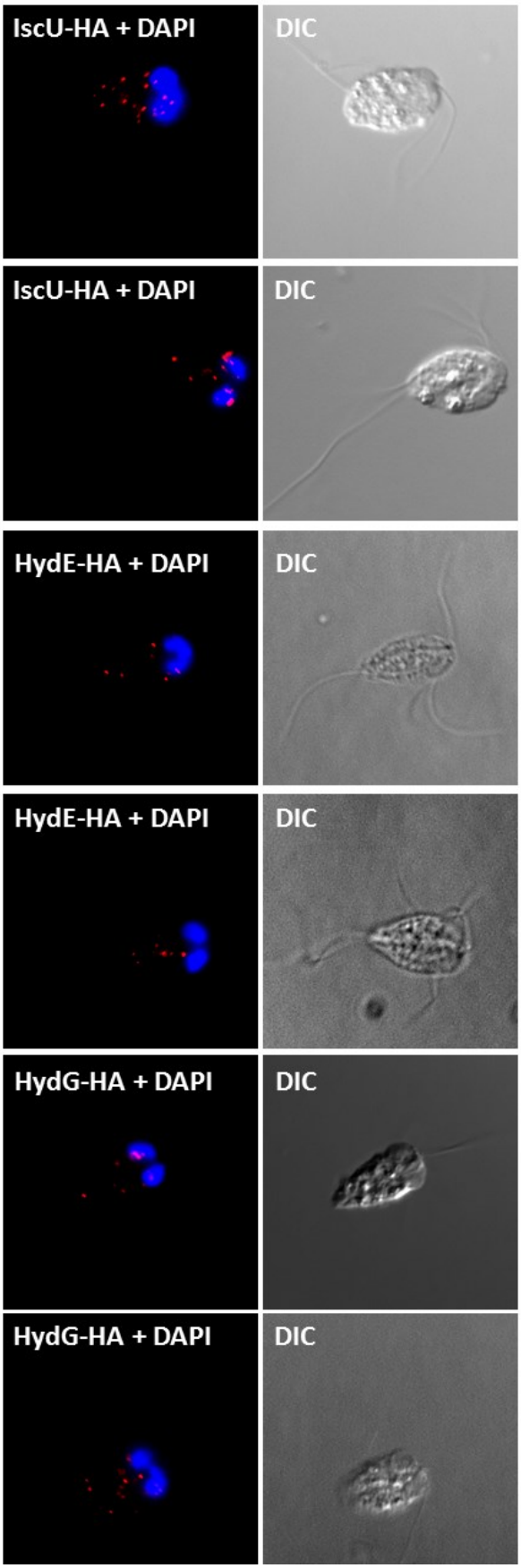

Figure 28. Detection of IscU, HydE and HydG proteins by mouse anti-HA antibody in *S. vortens* (red). The nuclei were stained by DAPI (blue). Formaldehyde protocol was used for the slide preparation. **DIC** = differential interference contrast, **DAPI** = 4ˈ,6-diamidine-2ˈ-phenylindole dihydrochloride.

5.1.8.2. Double-transfection

Empty pSpiro_NptII_NEO plasmid with HA tag for the double transfection experiments was obtained from laboratory of prof. S. Svard (Uppsala, Sweden). Cleavage of HA tag from the original vector was done by the ApaI and MluI restriction enzymes. I subcloned the IscU, HydE and HydG genes with the 5´UTR containing the native promotors. In case of HydG and IscU, V5 tag flanked by ApaI and NotI restriction sites was added to the reverse primer. pSpiro_NptII_HydG_NEO_V5 and pSpiro_NptII_IscU_NEO_V5 plasmids were successfully constructed. HydE gene had the restriction site for ApaI inside its gene sequence, therefore the V5 tag could not be directly added to the reverse primer. Because of that, HydG sequence from already constructed pSpiro_NptII_HydG_NEO_V5 plasmid was cut by MluI and NotI restriction enzymes. HydE sequence was inserted into this plasmid, therefore pSpiro_NptII_HydE_NEO_V5 plasmid was constructed.

pSpiro_NptII_NEO plasmids containing HydE, HydG and IscU sequences with V5 tag were used for the transfection of strains with confirmed expression of HydE, HydG and IscU cloned in pSvor_PAC_3xHA_C plasmid. Electroporation was performed, using all three different protocols, however, only transfectants established with protocol 1 (see Chapter 4.4.4) survived two weeks of antibiotic selection pressure (puromycin with concentration 50 µg/ml and geneticin G418 with concentration 100 µg/ml). Established double-transfected strains are listed in Figure 29. The subcellular fractionation and western blot analysis of the three established double-transfected strains were performed. Anti-HA antibody detected protein bend of expected size in organellar fraction of HydE_HA + IscU_V5 double transfectant. Signal in the lysate was not detected, however, it could be explained by lower concentration of HydE protein with HA-tag in total lysate. In IscU_HA + HydE_V5 and IscU_HA + HydG_V5 double-transfected strains, anti-HA antibody labeled IscU protein of expected molecular weight predominantly in lysate and organellar fraction (Figure 30). Anti-V5 antibody detected a bend in the organellar fraction of all three double-transfectants. Molecular weight of the bend was approximately 45 kDa which does not correspond with the size of IscU, HydE and HydG proteins verified by the anti-HA antibody in single and double-transfected strains. Because of that, I did not proceed to the immunofluorescence microscopy co-localization experiments.

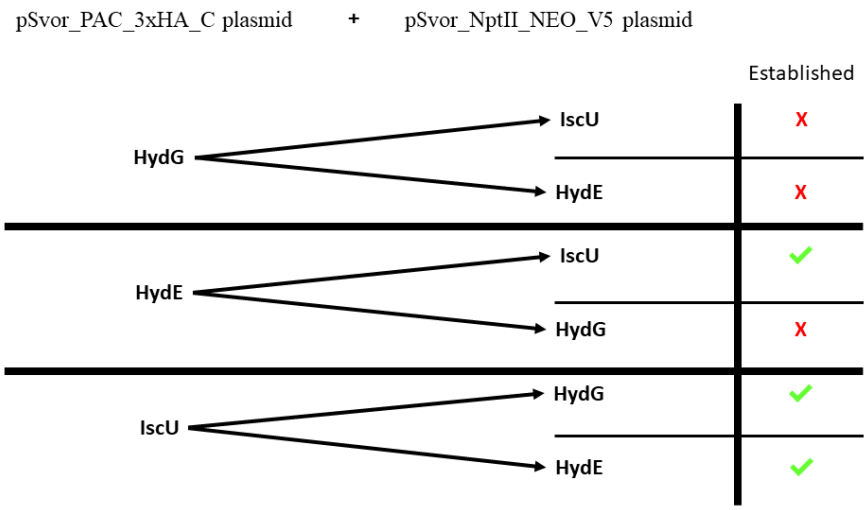

Figure 29. Schematic illustration of plasmid combinations we used for the double transfection of *S. vortens*. ✓ = strains which survived the antibiotic selection pressure, X = strains which died during selection process.

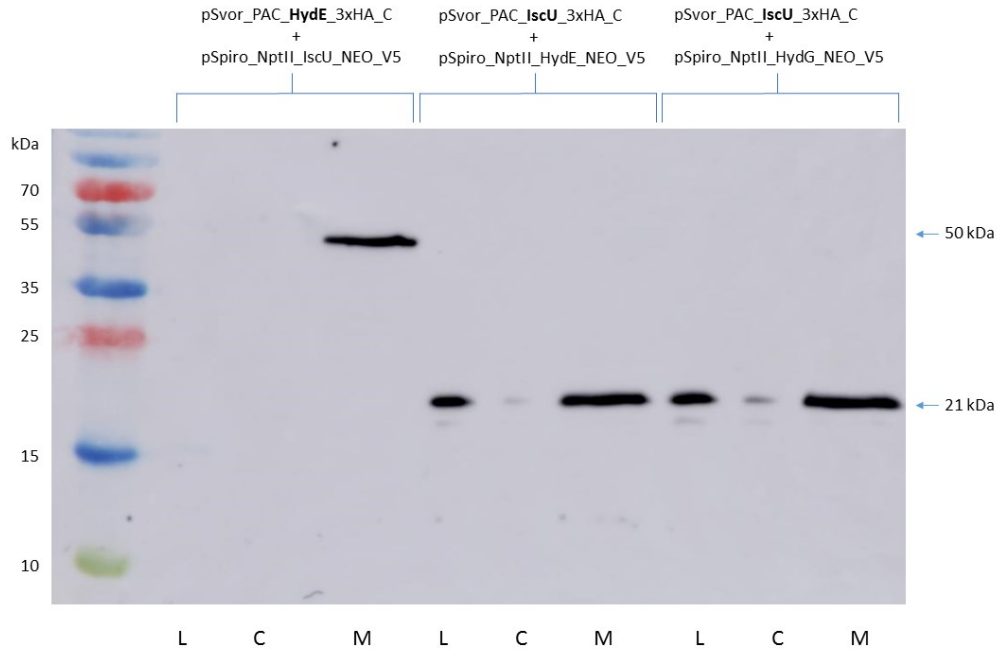

Figure 30. Western blot analysis of anti-HA mouse antibody tested on subcellular fractions from double-transfected strains of *S. vortens*. Detected proteins are highlighted in the title above the blot. **L** = total lysate, **C** = cytosolic fraction, **M** = organellar fraction containing mitochondrial organelles.

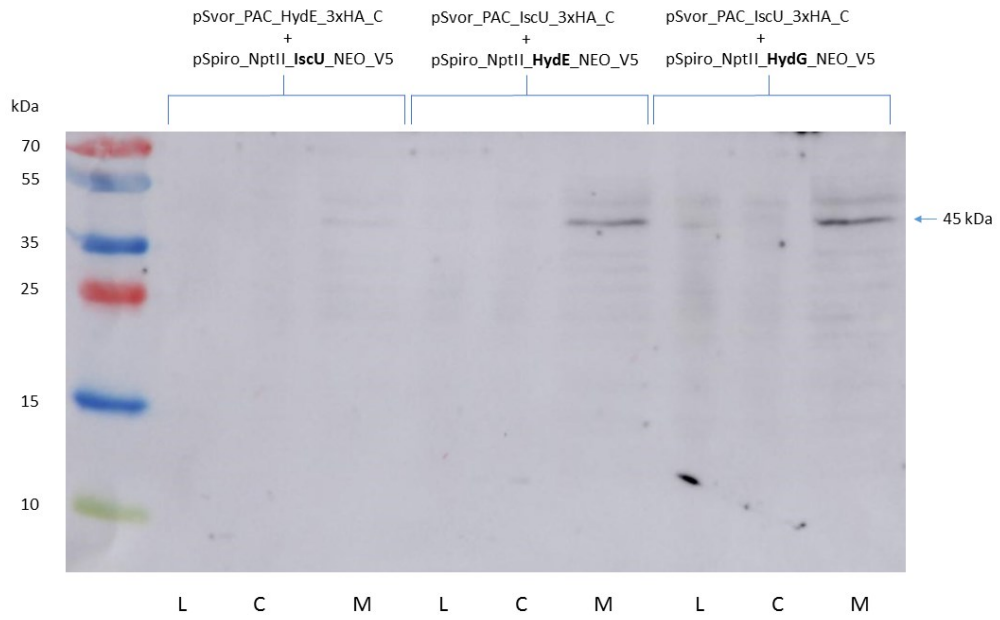

Figure 31. Western blot analysis of anti-V5 rabbit antibody tested on subcellular fractions from double-transfected strains of *S. vortens*. Tested proteins are highlighted in the title above the blot. **L** = total lysate, **C** = cytosolic fraction, **M** = organellar fraction containing mitochondrial organelles.

5.2. Characterization of mitochondrial organelle in *Hexamita sp.*

5.2.1. Transmission electron microscopy (TEM)

In the cells of *Hexamita sp.* (like in other diplomonads), two nuclei, endoplasmic reticulum, cytostomes, flagella and various vesicles were observed. Stacked rough endoplasmic reticulum was detected and localized to the both lateral parts of the *Hexamita* (Figure 32A and 32C). Only one double-membrane organelle (400 - 1000 nm in diameter) has been observed on the plane section in the cells (Figure 32B, 32D and 32F), suggesting even lower number of mitochondria-derived organelles present in comparison with *S. vortens*. Unlike the filamentous structure of mitochondria of *S. vortens*, matrix inside these mitochondrial organelles was rather densely dappled. The organelles were also much more electron-dense. Two membranes surrounding the vesicles had more space in between them (clearly depicted in Figure 32F).

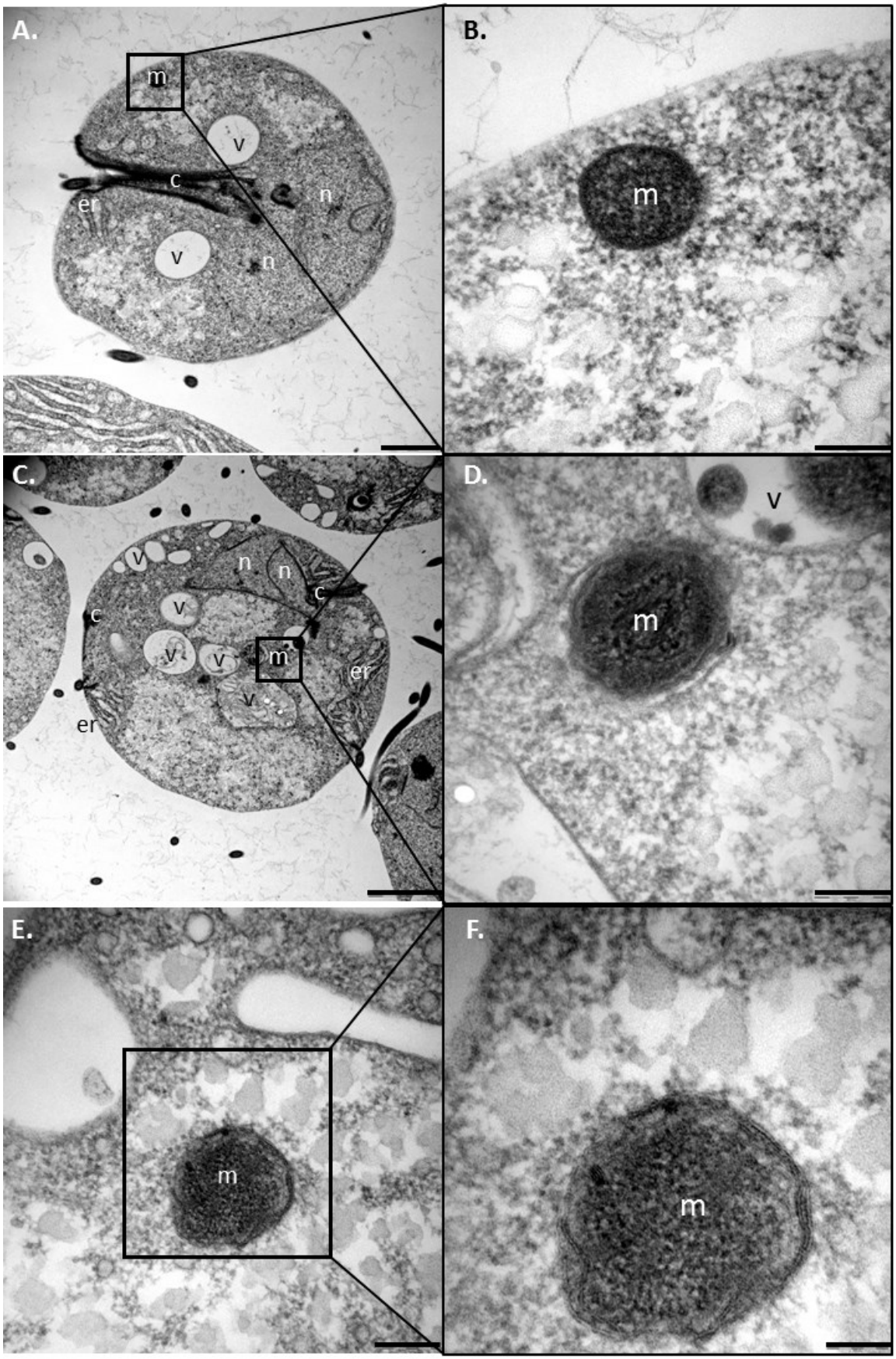

Figure 32. TEM of *Hexamita sp*. A.+C. *Hexamita sp.* cell overview (scale bar = 2000 nm). **B.+D.+E.+F.** Cell section with detail of double-membrane mitochondrial organelle (scale bar B.+D. = 500 nm; E. = 200 nm; F. = 100 nm) **n** = nucleus, **v** = vacuole, **c** = cytostome, **f** = flagellum, **er** = endoplasmic reticulum, **m** = double-membrane mitochondrial organelle.

5.2.2. Strategy of *Hexamita sp.* genome sequencing

Hexamita sp. DNA was isolated from 1 l of culture using the phenol-chloroform extraction. 700 µg of genomic DNA was sent to Uppsala University (Sweden) for Pacific Bioscience sequencing and another 700 µg were sequenced by Illumina method at Charles University (Czech Republic). Isolation of RNA was performed with NucleoSpin RNA extraction kit from 50 ml of *Hexamita* culture. 30 µg of DNA-free RNA was sequenced by Illumina method in Czech Republic, other 30 µg was sent to Sweden for PacBio sequencing. Original plan was to combine the genomic and transcriptomic data from Illumina and PacBio sequencing, however only genomic data from PacBio were used for the bioinformatic analysis so far.

5.2.3. Bioinformatic analysis of *Hexamita sp.* genome

Internal database containing sequences of mitochondrial proteins from *S. cerevisiae* and hydrogenosomal proteins from *S. salmonicida* was provided by C. Stairs (Uppsala University, Sweden) and was used as a query for searches in preliminary assembly of *Hexamita sp.* genome (sequences listed in Supplementary data 4). Putative mitochondrial protein sequences found in the genome are listed in Table 3, only the hits with e-value lower than $1x10^{-5}$ were considered as relevant. Several mitochondrial presequences were predicted by PSORTII, TargetP and MitoFates in some of the proteins, however, no mitochondrial processing peptidase was identified in the genome of *Hexamita sp.* (Supplementary data 5). Based on predictions and considering cellular localization of known orthologs, I predicted cellular localization of analyzed proteins as summarized in Table 3. Proteins which are part of Fe-S cluster synthesis or H cluster synthesis were considered as mitochondrial even without having any mitochondrial presequence. Protein not typically localized to hydrogenosomes or mitosomes were considered as cytosolic. I also predict dual localization of PFO, hydrogenase and CDP-diacylglycerol-glycerol-3-phosphate 3-phosphatidyltransferase (CDGPP). For the complete protein and nucleotide sequences and mitochondrial presequence prediction, see Supplementary data 5.

	Predicted mitochondrial localization	Predicted cytosolic localization
Acetyl-CoA synthetase 1		✓

Acetyl-CoA synthetase 2	✓	
Tom40	✓	
PFO	✓	✓
Malic enzyme		✓
IscS	✓	
IscU	✓	
HydE	✓	
HydF	✓	
HydG	✓	
Hydrogenase	✓	✓
SHMT	✓	
Frataxin	✓	
Nfu	✓	
[2Fe2S] ferredoxin	✓	
Cytosolic Hsp70		✓
Mitochondrial Hsp70	✓	
DnaJ	✓	

Cpn60	✓	
Alanine aminotransferase		✓
Aspartate aminotransferase		✓
Branched-chain amino acid aminotransferase		✓
Serine palmitoyltranferase		✓
Tryptophanase		✓
Pyruvate carboxylase fusion protein		✓
Nucleotide-binding protein 1		✓
Multidrug resistance-associated protein		✓
CDP-diacylglycerol-glycerol-3-phosphate 3-phosphatidyltransferase	✓	✓
Phosphatidylserine decarboxylase	✓	
3-ketoacyl-CoA reductase		✓
Peroxiredoxin		✓
Formate-acetyl transferase		✓

Table 3. Predicted localization of proteins found in the genome of *Hexamita sp.*

Three different hydrogenases were found in the genome of *Hexamita sp*. Percentage identity of amino acid residues indicate that Hydrogenase 1 from *Hexamita* is most related to the cytosolic Hydrogenase 1 from *S. salmonicida* (Table 4). However, Hydrogenase 3 of

Hexamita sp. displayed the highest percentage identity with hydrogenosomal Hydrogenase 5 from *S. salmonicida* even though it is just 26,9%. This suggest that the *Hexamita sp.* Hydrogenase 3 sequence is incomplete due to the insufficient genome assembly. Nevertheless, at least one of the hydrogenases might be present in the mitochondrial organelle of *Hexamita sp*. Moreover, one of the PFO paralogs and one of the acetyl-CoA synthetase (related to hydrogenosomal ACS2 in *S. salmonicida*) have the mitochondrial presequence suggesting that mitochondrial organelle of *Hexamita* could produce ATP.

	Hyd 1 Salmo	Hyd 2 Salmo	Hyd 3 Salmo	Hyd 4 Salmo	Hyd 5 Salmo	Hyd 6 Salmo	Hyd 7 Salmo
Hyd 1 Hexa	60,5%	42,9%	27,5%	41,8%	49,2%	42,4%	24,5%
Hyd 2 Hexa	48,0%	39,9%	27,4%	38,4%	44,8%	36,2%	22,1%
Hyd 3 Hexa	25,2%	25,2%	17,1%	23,8%	26,9%	24,7%	11,7%

Table 4. Comparison of percentage identity of amino acid residues in hydrogenase sequences of *Hexamita sp.* and *S. salmonicida* (analysis was performed by Geneious 8.0.5 software). **Hyd Hexa** = hydrogenase sequence in *Hexamita sp.* **Hyd Salmo** = hydrogenase sequence in *S. salmonicida*.

6. Discussion

6.1. Mitochondrial organelle of *S. vortens*

We have found three different paralogs of hydrogenase in the genome of *S. vortens*. PSORTII, TargetP and MitoFates programs were used for the prediction of N-terminal mitochondrial presequence and cleavage site. In hydrogenase 2, cleavage site was recognized by PSORTII program, however this prediction was not supported by other two prediction programs. Moreover, the cleavage site predicted in *S. vortens* Hydrogenase 2 was not unique just for this protein but was present with certain modifications in all other hydrogenases listed in the alignment (Figure 14). We compared the hydrogenase sequences of *S. vortens* with seven hydrogenases from *S. salmonicida*, including two paralogs that have been localized in hydrogenosomes. The three hydrogenases from *S. vortens* were the most similar to the cytosolic hydrogenase 1 of *S. salmonicida*.

Absence of N-terminal targeting sequences does not mean, that proteins could not be targeted to mitochondrial organelle. It has been shown, that all proteins experimentally localized in the hydrogenosome of *S. salmonicida* do not possess mitochondrial presequence (Jerlström-Hultqvist et al., 2013). This finding underlines the importance of experimental localization studies using specific antibodies or cell transfection systems to confirm *in silico* predictions.

Partial sequence of hydrogenase 3 from *S. vortens* has been subcloned into expression vector, recombinant protein was amplified in *E. coli* and purified. Homologous antibody against hydrogenase 3 from *S. vortens* has been developed. The experimental results strongly suggest that hydrogenase of *S. vortens* is present exclusively in cytosol, whereas there is no evidence for its localization in the mitochondrial organelle. Using the western blot analysis, specific anti-hydrogenase antibody raised against *S. vortens* hydrogenase 3 detected protein bend of expected molecular weight (52 kDa) in the lysate and the cytosolic fraction. This observation was supported by the immunofluorescence microscopy, where the antibody labeled large number of small dots evenly spread in the cells of *S. vortens*, resembling the cytosolic distribution. It is likely that this polyclonal antibody recognizes all three hydrogenase paralogs that have protein sequence identity ranging from 46,7 % to 59,5 %. However, because all three hydrogenases in *S. vortens* have similar molecular weight (around 52 kDa), it is not possible to distinguish hydrogenase 3 from other two paralogs based on their mobility in western blots. To exclude a

possibility that the antibody reacts specifically only with hydrogenase 3, comparing the reactivity of the antibody with all three recombinant hydrogenases will be necessary in the future.

Interestingly, heterologous antibody against the [FeFe] hydrogenase of *B. hominis* has been tested on the *S. vortens*, using the immunofluorescence microscopy (Millet et al., 2013). This antibody visualized vesicles, which have been interpreted as mitochondria-related organelles. However, western blot analysis of subcellular fractions to confirm organellar localization of hydrogenase have not been performed and the specificity of the heterologous antibody for *S. vortens* hydrogenase is unclear.

The cytosolic localization of hydrogenase in *S. vortens*, labeled in our experiments with homologous anti-hydrogenase antibody is consistent with the measuring of hydrogenase activity in cell fractions (E. Nývltová, unpublished). Hydrogenase activity was present exclusively in the cytosol of *S. vortens* whereas in *S. salmonicida*, the hydrogenase activity was found in the cytosolic and organellar fraction (E. Nývltová, unpublished).

Interestingly, it has been reported, that *S. vortens* produced significantly more hydrogen (77 nmol/min/10^7 cells) than *G. intestinalis* (2 nmol/min/10^7 cells) where hydrogen is produced exclusively in the cytosol or *T. vaginalis* (20 nmol/min/10^7 cells), organism containing hydrogenosomes (Millet et al., 2010). Because maturation of hydrogenase is dependent on the presence of specific hydrogenase maturases, we were interested in their cellular localization. Thus, we attempted to develop a polyclonal antibody against two maturases, HydE and HydG. Anti-HydE polyclonal antibody was successfully developed and used for the cell localization studies. HydE signal was detected in the cell lysate and organellar fraction. Immunofluorescence microscopy confirmed the localization of HydE to the small vesicles (possibly mitochondrial organelles) unevenly distributed in the cell. Unfortunately, development of anti-HydG antibody was not successful. To further support organellar localization of maturases we expressed HydE and HydG (and IscU as a mitochondrial marker) with C-terminal HA tag in *S. vortens* using pSvor_PAC_3xHA_C expression vectors. Plasmids were designed to facilitate the antibiotic selection of transformants with puromycin (50 µg/ml) and detection of proteins by the immunofluorescence and western blot analysis with anti_HA tag antibody. Western blot analysis and immunofluorescence microscopy confirmed organellar localization of HydE, HydG and IscU proteins. Unfortunately, we could not perform co-localization with the polyclonal anti-HydE antibody. This primary antibody was developed in the rat and HA tag was detected by the mouse antibody. Since secondary anti mouse and rat

antibodies could cross-react with the target primary antibody, these antibodies cannot be reliably used for co-localization studies. Therefore, we decided to establish double transfectants for the co-localization experiments. HydE, HydG and IscU genes with the native promotor and V5 tag were subcloned to pSpiro_NptII_NEO vector, enabling antibiotic selection with geneticin (100 μg/ml) and detection of the proteins by anti-V5 tag antibody. Even though some double transfectants survived the selective pressure of two different antibiotics (puromycin and geneticin), they were only expressing proteins with HA tag. These experiments need to be repeated.

Even though the double transfection experiment was not successful, we showed the cytosolic localization of hydrogenase and possibly organellar localization of HydE, HydG and IscU. There are other protists with specific localization of hydrogenase and its maturases to the cytosol or to the mitochondrial organelle. In *G. intestinalis*, no hydrogenase maturases have been discovered in the genome (Leger et al., 2017). However, hydrogenase is present and active in the cytosol, although the activity is rather low (2 nmol/min/10^7 cells) (Lloyd et al., 2002; Emelyanov and Goldberg, 2011). Another protist with cytosolic hydrogenase is *E. histolytica* (Nixon et al., 2003). Like in *Giardia*, no data for the presence of hydrogenase maturases in *E. histolytica* are available. In another amoeba, *M. balamuthi*, the hydrogenase activity was measured (Nyvltova et al., 2013). The activity was predominantly detected in the cytosol (approximately 1,351 μmol/min/mg), much lower activity was associated with hydrogenosomes (approximately 0,024 μmol/min/mg). Two hydrogenosomal (with N-targeting sequences), two cytosolic hydrogenases and HydE maturase were found in the genome. HydE maturase was localized to the hydrogenosomes of *M. balamuthi* via the immunofluorescence microscopy and western blot analysis (Nyvltova et al., 2013). *Naegleria gruberi* also possess hydrogenase which is localized exclusively in the cytosol. Surprisingly, HydE maturase has been also detected specifically in the cytosol (Tsaousis et al., 2014). Ten paralogs of hydrogenase have been discovered in the genome of *T. vaginalis*, however only five of them were found in the hydrogenosomal proteome (Carlton et al., 2007; Schneider et al., 2011). One paralog has been recently localized to the cytosol of *T. vaginalis* by immunofluorescence microscopy and western blot analysis (A. Dohnálková, Diploma thesis, 2015). However, all three hydrogenase maturases were specifically targeted to the hydrogenosomes of *T. vaginalis* (Pütz et al., 2006). In *S. salmonicida*, two paralogs of hydrogenase were localized to the hydrogenosome, other five are exclusively cytosolic (Jerlström-Hultqvist et al., 2013). All three hydrogenase maturases were detected specifically in the hydrogenosome of *S. salmonicida*

(Jerlström-Hultqvist et al., 2013). Overall, *S. vortens* is the first known organism with exclusively cytosolic localization of hydrogenase and organellar localization of all three hydrogenase maturases. How the organellar maturases can serve for the H-cluster formation of the cytosolic hydrogenases is therefore not clear.

Laboratory of prof. D. Lloyd proposed that *S. vortens* possess two different double membrane organelles, larger with the 200-1000 nm in diameter and smaller ones with 90-170 nm in diameter (Millet et al., 2013). Moreover, hydrogenase was supposedly detected in the larger organelles by heterologous anti-hydrogenase antibody from *B. hominis* using the immunofluorescence microscopy (Millet et al., 2013). I wanted to verify these observation by using the transmission electron microscopy (TEM). However, I observed only electron-dense double-membraned organelles of 400-500 nm in diameter. Furthermore, immunofluorescence microscopy experiments did not detect two distinct populations of vesicles as well.

Apart from the test of homologous antibodies against *S. vortens* hydrogenase, HydE and Cpn60 and expression of HydG, HydE and IscU recombinant proteins, I also tested heterologous antibodies against *G. intestinalis* proteins IscU, IscS, Tom40 and Cpn60 to identify another suitable mitochondrial marker for *S. vortens*. Anti-Tom40 antibody detected two bends in the lysate and the cytosolic fraction (cca 40 and 35 kDa) and single bend in the organellar fraction (39 kDa). However, the antibody did not label any protein of expected molecular weight of 30 kDa, therefore it might not be specific. Antobody against IscS detected bends of 45 and 54 kDa molecular weight in the cytosol and in the mitochondrial organelle, even though IscS typically resides in the mitochondria. Cpn60 antibody labeled protein of 30 kDa molecular weight in the lysate and organellar fraction, which might be degraded Cpn60. IscU was detected in both cytosolic and the organellar fraction, which did not correspond with the overexpression of IscU in the cells of *S. vortens*. Western blot analysis of heterologous antibodies was repeated four times always with the fresh cell fractionation samples and only the best western blots are presented in this thesis. I can definitely exclude the fractionation protocol failure since all other fractionation experiments were performed in the same way and the results were satisfactory. Overall, anti-IscS, anti-Cpn60 and anti-Tom40 heterologous antibodies were considered as not suitable for the mitochondrial labeling in *S. vortens*. Anti-IscU might label the mitochondrial organelles, however, further co-localization experiments have to be done.

Based on localization studies and analysis of *S. vortens* genome, I propose that the mitochondrial organelles contain all three hydrogenase maturases, two proteins of

mitochondrial import machinery Tom40 and Tim14, three chaperones Cpn60, Hsp70 and DnaK, proteins involved in the Fe-S cluster assembly (IscU, IscS, ferredoxin and frataxin) and SHMT enzyme responsible for conversion of serine into glycine. ATP synthesis probably occurs in the cytosol via the PFO and ACS1 enzymes. All the proteins with predicted or proved localization into the mitochondrial organelle of *S. vortens* are shown in Figure 33. Based on the cytosolic hydrogenase localization, I suggest that the mitochondrial organelles in *S. vortens* are most likely **the mitosomes**. The only possible functions of the *S. vortens* mitosomes are Fe-S cluster and H-cluster assembly and conversion of serine into glycine using the SHMT.

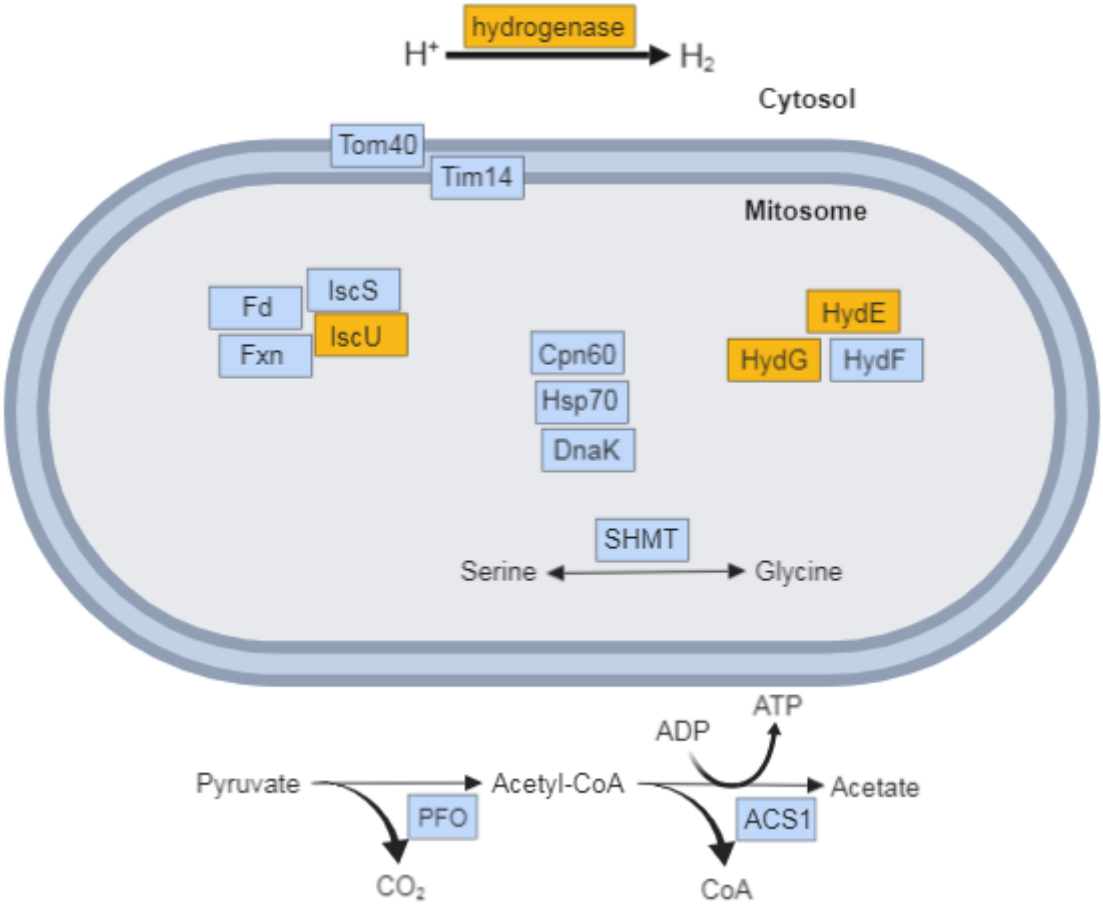

Figure 33. Mitosome of S. vortens. Proteins, which localization was verified by western blot analysis and immunofluorescence microscopy are highlighted in yellow. Proteins found in the genome of *S. vortens* with no experimental verification are highlighted in blue. **ACS** = acetyl-CoA synthetase, **Fd** = ferredoxin, **Fxn** = frataxin, **PFO** = pyruvate:ferredoxin oxidoreductase, **SHMT** = serine hydroxymethyltransferase

6.2. Mitochondrial organelle of *Hexamita sp.*

Genome of the *Hexamita sp.* was partially sequenced and preliminary assembly was searched for the mitochondrial proteins. Protein sequences (listed in Table 3 and Supplementary data 5) were analyzed by PSORTII containing Gavel program predicting the cleavage sites and by TargetP and MitoFates programs illustrating the probability of mitochondrial presequences.

Regarding the ATP synthesis in the *Hexamita sp*. mitochondrial organelle, pyruvate might be metabolized to acetyl-CoA by one of the four paralogs of PFO (in PFO 3, the predicted cleavage site by PSORTII was supported by the TargetP program prediction of mitochondrial presequence). ATP could be generated by one of the two paralogs of ACS through conversion of acetyl-CoA to acetate. In ACS2 from *Hexamita sp*., the predicted cleavage site was strongly supported by both TargetP and MitoFates programs. Localization of ACS2 has been experimentally detected in the hydrogenosome of diplomonad *S. salmonicida* and was predicted in H_2 producing mitochondrion of *C. marsupialis* (Jerlström-Hultqvist et al., 2013; Noguchi et al., 2015). Cytosolic ACS1 has been found in the genome of *Hexamita sp.* suggesting dual localization of ATP synthesis in both the cytosol and the mitochondrial organelle.

Three different paralogs of hydrogenase have been found in the genome of *Hexamita sp.* All of them have cleavage site motif (detected by PSORTII), however no mitochondrial presequence have been predicted by TargetP and MitoFates programs. Hydrogenase 1 and 2 from *Hexamita sp.* were the most similar to the cytosolic hydrogenase 1 from *S. salmonicida*. However, amino acid percentage identity of *Hexamita* hydrogenase 3 was the highest with the hydrogenosomal hydrogenase 5 from *S. salmonicida*, even though the number was just 26,9%. This might indicate that sequence of *Hexamita sp.* Hydrogenase 3 is incomplete due to the insufficient assembly. Nevertheless, I propose that the mitochondrial organelle of *Hexamita sp.* possess at least one hydrogenase paralog and consequently produce hydrogen. Specific hydrogenase localization could be proved by developing of the homologous polyclonal antibodies against all three paralogs of hydrogenase in *Hexamita* to observe, if any of them are targeted to the organelles. All three hydrogenase maturases are also present in the genome (HydE in three paralogs). Only HydF and one paralog of HydE (HydE 2) have the predicted mitochondrial presequence. However, I presume that HydG is also targeted to the organelle even without the targeting sequence.

The only biochemical pathway common to all mitochondrial organelles in diplomonads is Fe-S cluster assembly (Leger et al., 2017). In *Hexamita sp.* genome, genes for proteins that are responsible for the cluster assembly were identified: IscS (three paralogs), IscU (two paralogs), ferredoxin, frataxin (two paralogs, however both sequences were incomplete) and Nfu. None of them had the cleavage site or mitochondrial targeting sequence predicted. Since the mitochondrial processing peptidase was not found in the genome of *Hexamita sp.,* N-terminal targeting sequences might not be necessary for the organellar localization. Since the cleavage sites and mitochondrial presequences were predicted in some protein sequences, they might be cleaved by other enzyme than mitochondrial processing peptidase. Another possibility is that the genomic data are incomplete, therefore mitochondrial processing peptidase was not found. In *S. salmonicida* and *S. vortens*, no mitochondrial presequences were observed (Jerlström-Hultqvist et al., 2013). In *G. intestinalis*, only IscU and ferredoxin have the N-terminal targeting sequence for mitosome localization (Dolezal et al., 2005). Specific processing peptidase (GPP) is localized in *Giardia* mitosomes and is responsible for cleaving the mitochondrial presequences in these two proteins (Šmíd et al., 2008). *Hexamita sp.* mitochondrial proteins could also contain the internal targeting sequence, like IscS, Cpn60 and Hsp70 in *Giardia* (Dolezal et al., 2005).

Mitochondrial organelle of *Hexamita sp.* might have the metabolic function of converting serine molecule into glycine, since two paralogs of SHMT were found in the genome (without mitochondrial presequence). In *S. salmonicida*, SHMT has been localized to the hydrogenosome and in another diplomonad *Trepomonas sp.* was the gene for SHMT also found in the genome (Jerlström-Hultqvist et al., 2013; Leger et al., 2017).

Typical mitochondrial proteins responsible for the protein import (Tom40) and proper protein folding (Cpn60, Hsp70 and DnaJ) were predicted to reside in the mitochondria-related organelles of *Hexamita sp.* No N-terminal targeting sequence was predicted in these proteins.

Phosphatidylserine decarboxylase (PSD) and CDGPP are both typically localized in the inner mitochondrial membrane (Carman and Belunis, 1983; Zborowski et al., 1983). Mitochondrial presequence was predicted in both paralogs of PSD. This enzyme is responsible for conversion of phosphatidyl-L serine into phosphatidylethanolamine and CO_2 in the process of phospholipid metabolism (Satre and Kennedy, 1978). However, its localization into hydrogenosomes or mitosomes has not been previously observed. Another enzyme involved in the phospholipid synthesis, CDGPP has been also found in the genome of *Hexamita sp.* In one of the two paralogs, MitoFates program predicted N-terminal targeting sequence, therefore this

protein might be targeted to the mitochondria. I cannot exclude possible dual localization since the other paralog of CDGPP does not have the mitochondrial presequence predicted.

Glycine cleavage system was not found in the genome which corresponds with the absence of this system in all other diplomonads (Leger et al., 2017).

The scheme of predicted metabolic pathways in *Hexamita sp.* mitochondrial organelles is depicted in Figure 34. Main biochemical processes are probably ATP synthesis using the PFO and ACS2, production of hydrogen, conversion of serine into glycine using the SHMT, H-cluster synthesis and Fe-S cluster synthesis. Therefore, this organelle should be called **the hydrogenosome**. Furthermore, 3 chaperones, Tom40 channel and two enzymes of phospholipid metabolism were found in the genome of *Hexamita sp.* and they are possibly localized into this hydrogenosome.

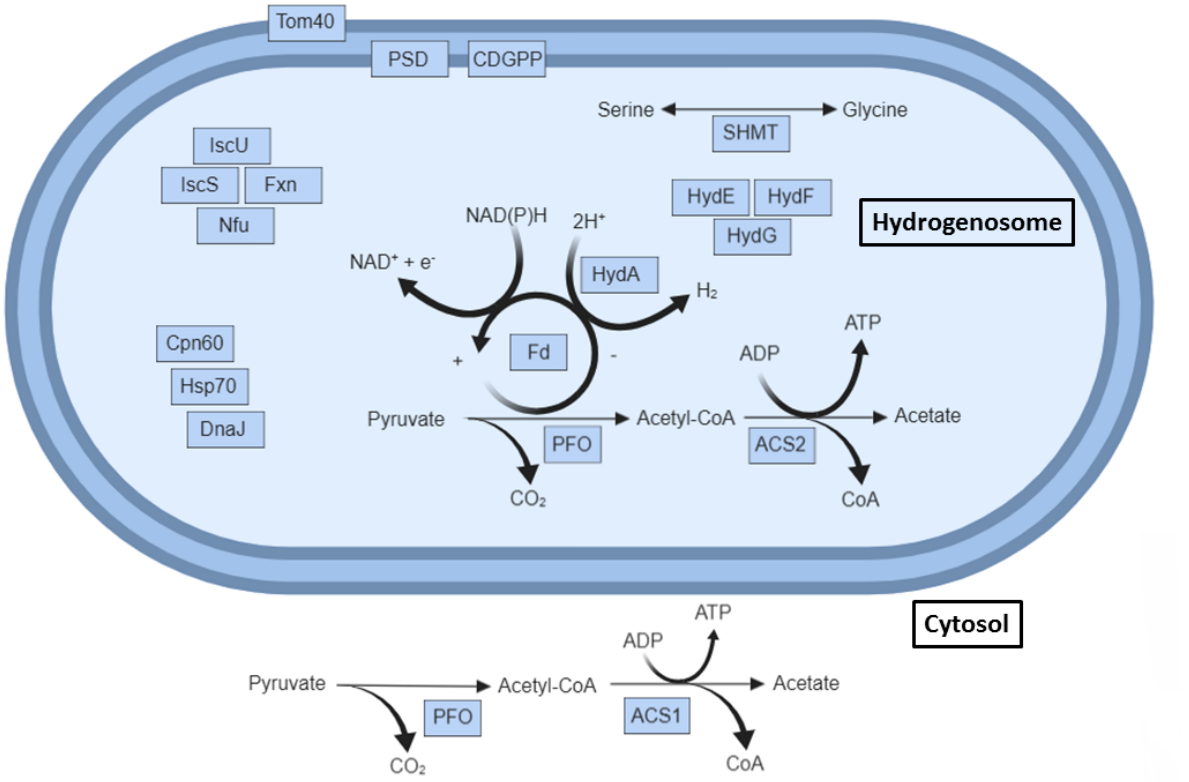

Figure 34. Hypothetical metabolism of *Hexamita sp.* hydrogenosome. ACS = acetyl-CoA synthetase, **CDGPP** = CDP-diacylglycerol-glycerol-3-phosphate 3-phosphatidylserine transferase, **Fd** = ferredoxin, **Fxn** = frataxin, **HydA** = hydrogenase, **PFO** = pyruvate:ferredoxin oxidoreductase, **PSD** = phosphatidylserin decarboxylase, **SHMT** = serine hydroxymethyltransferase.

6.3. Reductive evolution of diplomonads

In 2017, the hypothesis about reductive evolution in Diplomonadida group have been published (Leger et al., 2017). *D. brevis*, common diplomonad ancestor, *S. salmonicida* and *G. intestinalis* are included in this hypothesis. Apparently, mitochondrial organelle of the closest relative of diplomonads, *D. brevis* was able to produce hydrogen (which was not coupled with the pyruvate metabolism), it had glycine cleavage system and SHMT enzyme. *D. brevis* probably produces ATP exclusively in the cytosol using the ACS1. According to this hypothesis, diplomonad ancestor has lost glycine cleavage system and two subunits of complex I (NuoE and NuoF) found in *Dysnectes*. Interestingly, it has been proposed that *S. salmonicida* acquired the pyruvate metabolism secondarily during the taxon evolution. *G. intestinalis* is the last step of the reductive evolution, this parasite does not have SHMT and enzymes for hydrogen production and H-cluster assembly. Only function of *Giardia* mitochondrial organelle called mitosome is Fe-S cluster assembly.

Phylogenetic analysis of diplomonads based on SSU rRNA gene shows that two distinct lineages evolved from the common diplomonad ancestor, family *Giardiidae* and *Hexamitidae* (Kolisko et al., 2008, 2010). Therefore, it is necessary to put the reductive evolution of diplomonad mitochondrial metabolism into this context. It has been proposed that common diplomonad ancestor lacked ATP synthesis inside its mitochondrial organelle and only functions of the organelle were H-cluster and Fe-S cluster synthesis, hydrogen production and conversion of serine into glycine via SHMT enzyme (Leger et al., 2017). In *Giardiidae*, all mitochondrial functions were lost during the reductive evolution, except Fe-S cluster synthesis. However, in *Hexamitidae*, mitochondrial ATP synthesis has been acquired secondarily since the ACS2 is present in hydrogenosome of *S. salmonicida. Hexamita* and *Trimitus* are the most distant species on the diplomonad phylogenetic tree from the common ancestor (Kolisko et al., 2010). However, based on the genome analysis I predicted that *Hexamita sp.* might possess hydrogenosome with the same metabolic pathways which are also present in the hydrogenosome of *S. salmonicida*. On the other hand, *S. vortens* mitochondrial organelle has lost its ability to produce hydrogen and synthetize ATP during the reductive evolution and transformed into the mitosome, same organelle that is found in *Giardia* species. The only difference between the *Giardia* and *S. vortens* mitosomes is the absence of SHMT and hydrogenase maturases in *Giardia*. My hypothetical scheme of the reductive evolution in diplomonads is depicted in Figure 35. It might be interesting to analyze the genomes of

Octomitus, *Trimitus* or for example one of *Enteromonas* species, in order to better understand this mitochondrial reductive evolution processes. It might clarify, whether the mitochondrial organelle of *Octomitus* is the transitional state between the possible hydrogenosome-like organelle of common diplomonad ancestor and the mitosome of Giardia. Another question is, if *Trimitus* species possess the same mitochondrial organelle as *Hexamita sp.* since they are close relatives (according to the SSU rRNA phylogenetic tree). Also, genome sequencing of parasitic *Hexamita* species (for example *Hexamita salmonis* or *Hexamita meleagridis*) might uncover the interesting correlation between mitochondrial organelles of free-living and parasitic diplomonads.

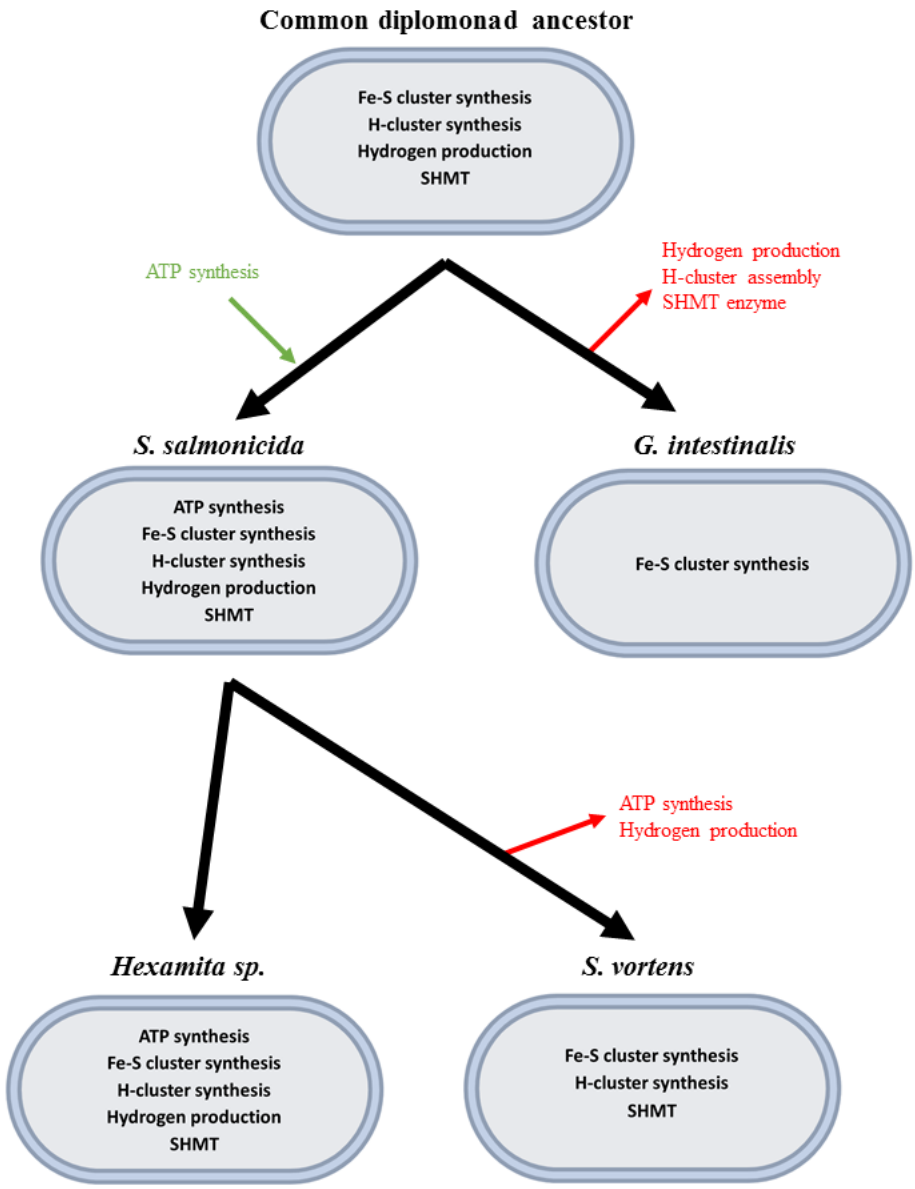

Figure 35. Proposed scheme of reductive evolution of mitochondrial organelle in diplomonads. Red arrows illustrate loss of described metabolic functions. Green arrow indicates the secondary acquisition of ATP synthesis.

7. Conclusion

This work was focused on determination of mitochondrion-related organelles in diplomonad species *S. vortens* and *Hexamita sp*. I detected double membrane bound organelles of both protist using TEM and described their structure. The homologous antibody against hydrogenase and HydE of *S. vortens* has been developed. Using the western blot analysis and immunofluorescence microscopy, cytosolic localization of hydrogenase in *S. vortens* has been suggested. HydE was experimentally localized to the possible mitochondrial organelle of *S. vortens.* In addition to that, overexpression of IscU, HydE and HydG was performed in the *S. vortens* transfected cells. All three proteins were detected in the vesicles that might be mitochondrial organelle using both the western blot analysis and immunofluorescence microscopy. Unfortunately, no double-transfected strains were established to perform co-localization studies.

Homologous anti-HydG antibody was not successfully developed. Available antibody against *S. vortens* Cpn60 was not considered as suitable for the labeling of the mitochondrion organelle. Four heterologous antibodies raised against IscU, IscS, Tom40 and Cpn60 of *G. intestinalis* were tested. Using the western blot analysis, none of them showed exclusive localization of the protein to the mitochondria of *S. vortens*. Results from the immunofluorescence microscopy showed that heterologous IscU antibody labeled small vesicles that might be considered as mitochondrial organelles. However, no co-localization experiments using the anti-IscU antibody from *G. intestinalis* were performed.

DNA and RNA from *Hexamita sp.* has been extracted and sequenced. Genomic data were used for the identification of mitochondrial proteins. ATP synthesis, production of hydrogen, conversion of serine into glycine using the SHMT, H-cluster synthesis and Fe-S cluster synthesis were predicted to the hypothetical mitochondrial organelle of *Hexamita.*

Based on the experimental data presented in this thesis, mitochondrial organelle of *S. vortens* was classified as the mitosome. *Hexamita sp.* mitochondria was proposed to be the hydrogenosome.

8. List of abbreviations

ACS = Acetyl-CoA synthetase

ASCT = Acetate:succinate CoA-transferase

ATCC = American Type Culture Collection

ATP = adenosine triphosphate

BIOCEV = Biotechnology and Biomedicine Center in Vestec

CBB = Coomassie Brilliant Blue solution

CDGPP = CDP-diacylglycerol-glycerol-3-phosphate 3-phosphatidyltransferase

CIA = Cytosolic Iron-sulfur cluster assembly pathway

DAPI = 4′,6-Diamidine-2′-phenylindole dihydrochloride

DHG = Dehydroglycine

DIC = Differential interference contrast

EDTA = Ethylenediaminetetraacetic acid

FBA = Fructose bisphosphate aldolase

GCS = Glycine cleavage system

ISC = Iron-sulfur cluster assembly pathway

JGI = Joint Genome Institute

LB = Luria-Bertani broth medium

NIF = Nitrogen fixation pathway

PacBio SMRT = Pacific Biosciences single molecule real time sequencing

PBS = Phosphate buffered saline

PDH = pyruvate dehydrogenase

PFL = pyruvate formate lyase

PFO = pyruvate:ferredoxin oxidoreductase

PNO = pyruvate:$NADP^+$ oxidoreductase

PSD = Phosphatidylserine decarboxylase

SAM = S-adenosylmethionine

SCS = Succinyl-CoA synthetase

SHMT = Serine hydroxymethyltransferase

ST = Sacharose-Tris buffer

SUF = Sulfur mobilization pathway

TEM = Transmission electron microscopy

TGS = Tris-Glycine-SDS buffer

TLCK = Tosyl-L-lysine-chlormethylketone

X-gal = 5-bromo-4-chloro-3-indolyl-β-D-galactoside

9. Literature

Adam, A.C., Bornhövd, C., Prokisch, H., Neupert, W., Hell, K., 2006. The Nfs1 interacting protein Isd11 has an essential role in Fe/S cluster biogenesis in mitochondria. The EMBO Journal **25**, 174–183.

Adam, R.D., 2001. Biology of *Giardia lamblia*. Clinical Microbiology Reviews **14**, 447-475.

Adrover, M., Howes, B.D., Iannuzzi, C., Smulevich, G., Pastore, A., 2015. Anatomy of an iron-sulfur cluster scaffold protein: Understanding the determinants of [2Fe–2S] cluster stability on IscU. Biochimica et Biophysica Acta (BBA) - Molecular Cell Research, SI: Fe/S proteins **1853**, 1448–1456.

Ajioka, R.S., Phillips, J.D., Kushner, J.P., 2006. Biosynthesis of heme in mammals. Biochimica et Biophysica Acta (BBA) - Molecular Cell Research, Cell Biology of Metals **1763**, 723–736.

Akhmanova, A., Voncken, F., van Alen, T., van Hoek, A., Boxma, B., Vogels, G., Veenhuis, M., Hackstein, J.H.P., 1998. A hydrogenosome with a genome. Nature **396**, 527–528.

Akhmanova, A., Voncken, F.G.J., Hosea, K.M., Harhangi, H., Keltjens, J.T., op den Camp, H.J.M., Vogels, G.D., Hackstein, J.H.P., 1999. A hydrogenosome with pyruvate formate-lyase: anaerobic chytrid fungi use an alternative route for pyruvate catabolism. Molecular Microbiology **32**, 1103–1114.

Alberts, B., Johnson, A.D., Lewis, J., Morgan, D., Raff, M., Roberts, K., Walter, P., 2014. Molecular Biology of the Cell, Sixth edition. ed. W. W. Norton & Company, New York, NY.

Ali, V., Shigeta, Y., Tokumoto, U., Takahashi, Y., Nozaki, T., 2004. An Intestinal Parasitic Protist, *Entamoeba histolytica*, Possesses a Non-redundant Nitrogen Fixation-like System for Iron-Sulfur Cluster Assembly under Anaerobic Conditions. Journal of Biological Chemistry **279**, 16863–16874.

Barberà, M.J., Ruiz-Trillo, I., Tufts, J.Y.A., Bery, A., Silberman, J.D., Roger, A.J., 2010. *Sawyeria marylandensis* (Heterolobosea) Has a Hydrogenosome with Novel Metabolic Properties. Eukaryotic Cell **9**, 1913–1924.

Beinert, H., 2000. Iron-sulfur proteins: ancient structures, still full of surprises. JBIC Journal of Biological Inorganic Chemistry **5**, 2–15.

Benchimol, M., 2009. Hydrogenosomes under microscopy. Tissue and Cell **41**, 151–168.

Bertani, G., 1951. STUDIES ON LYSOGENESIS I. Journal of Bacteriology **62**, 293–300.

Boxma, B., de Graaf, R.M., van der Staay, G.W.M., van Alen, T.A., Ricard, G., Gabaldón, T., van Hoek, A.H.A.M., Moon-van der Staay, S.Y., Koopman, W.J.H., van Hellemond, J.J., Tielens, A.G.M., Friedrich, T., Veenhuis, M., Huynen, M.A., Hackstein, J.H.P., 2005. An anaerobic mitochondrion that produces hydrogen. Nature **434**, 74–79.

Brancaccio, D., Gallo, A., Mikolajczyk, M., Zovo, K., Palumaa, P., Novellino, E., Piccioli, M., Ciofi-Baffoni, S., Banci, L., 2014. Formation of [4Fe-4S] Clusters in the Mitochondrial Iron–Sulfur Cluster Assembly Machinery. Journal of the American Chemical Society **136**, 16240–16250.

Braymer, J.J., Lill, R., 2017. Iron-sulfur cluster biogenesis and trafficking in mitochondria. Journal of Biological Chemistry **292**, 12754–12763.

Burki, F., Corradi, N., Sierra, R., Pawlowski, J., Meyer, G.R., Abbott, C.L., Keeling, P.J., 2013. Phylogenomics of the Intracellular Parasite *Mikrocytos mackini* Reveals Evidence for a Mitosome in Rhizaria. Current Biology **23**, 1541–1547.

Bych, K., Kerscher, S., Netz, D.J.A., Pierik, A.J., Zwicker, K., Huynen, M.A., Lill, R., Brandt, U., Balk, J., 2008. The iron–sulphur protein Ind1 is required for effective complex I assembly. The EMBO Journal **27**, 1736–1746.

Capozzi, F., Ciurli, S., Luchinat, C., 1998. Coordination sphere versus protein environment as determinants of electronic and functional properties of iron-sulfur proteins, in: Hill, H.A.O., Sadler, P.J., Thomson, A.J. (Eds.), Metal Sites in Proteins and Models Redox Centres. Springer Berlin Heidelberg, Berlin, Heidelberg, pp. 127–160.

Cardol, P., 2005. The Mitochondrial Oxidative Phosphorylation Proteome of *Chlamydomonas reinhardtii* Deduced from the Genome Sequencing Project. Plant Physiology **137**, 447–459.

Carlton, J.M., Hirt, R.P., Silva, J.C., Delcher, A.L., Schatz, M., Zhao, Q., Wortman, J.R., Bidwell, S.L., Alsmark, U.C.M., Besteiro, S., Sicheritz-Ponten, T., Noel, C.J., Dacks, J.B., Foster, P.G., Simillion, C., Peer, Y.V. de, Miranda-Saavedra, D., Barton, G.J., Westrop, G.D., Müller, S., Dessi, D., Fiori, P.L., Ren, Q., Paulsen, I., Zhang, H., Bastida-Corcuera, F.D., Simoes-Barbosa, A., Brown, M.T., Hayes, R.D., Mukherjee, M., Okumura, C.Y., Schneider, R., Smith, A.J., Vanacova, S., Villalvazo, M., Haas, B.J., Pertea, M., Feldblyum, T.V., Utterback, T.R., Shu, C.-L., Osoegawa, K., Jong, P.J. de, Hrdy, I., Horvathova, L., Zubacova, Z., Dolezal, P., Malik, S.-B., Logsdon, J.M., Henze, K., Gupta, A., Wang, C.C., Dunne, R.L., Upcroft, J.A., Upcroft, P., White, O., Salzberg, S.L., Tang, P., Chiu, C.-H., Lee, Y.-S., Embley, T.M., Coombs, G.H., Mottram, J.C., Tachezy, J., Fraser-Liggett, C.M., Johnson, P.J., 2007. Draft Genome Sequence of the Sexually Transmitted Pathogen *Trichomonas vaginalis*. Science **315**, 207–212.

Carman, G.M., Belunis, C.J., 1983. Phosphatidylglycerophosphate synthase activity in *Saccharomyces cerevisiae*. Canadian Journal of Microbiology **29**, 1452–1457.

Cavaliersmith, T., 1989. Molecular Phylogeny - Archaebacteria and Archezoa. Nature **339**, 100–101.

Cerkasov, J., Cerkasovová, A., Kulda, J., Vilhelmová, D., 1978. Respiration of hydrogenosomes of *Tritrichomonas foetus*. I. ADP-dependent oxidation of malate and pyruvate. Journal of Biological Chemistry **253**, 1207–1214.

Chomczynski, P., Sacchi, N., 1987. Single-step method of RNA isolation by acid guanidinium thiocyanate-phenol-chloroform extraction. Analytical Biochemistry **162**, 156–159.

Clemens, D.L., Johnson, P.J., 2000. Failure to detect DNA in hydrogenosomes of *Trichomonas vaginalis* by nick translation and immunomicroscopy. Molecular and Biochemical Parasitology **106**, 307–313.

Dean, D.R., Bolin, J.T., Zheng, L., 1993. Nitrogenase metalloclusters: structures, organization, and synthesis. Journal of Bacteriology **175**, 6737–6744.

Diamond, L.S., Harlow, D.R., Cunnick, C.C., 1978. A new medium for the axenic cultivation of *Entamoeba histolytica* and other *Entamoeba*. Transactions of the Royal Society of Tropical Medicine and Hygiene **72**, 431–432.

Dohnálková, A. 2015. Cytosolická hydrogenáza prvoka *Trichomonas vaginalis*. Diplomová práce (Mgr.). Univerzita Karlova, Přírodovědecká fakulta, Katedra Parazitologie. https://dspace.cuni.cz/handle/20.500.11956/74441.

Dolezal, P., Dagley, M.J., Kono, M., Wolynec, P., Likić, V.A., Foo, J.H., Sedinová, M., Tachezy, J., Bachmann, A., Bruchhaus, I., Lithgow, T., 2010. The Essentials of Protein Import in the Degenerate Mitochondrion of *Entamoeba histolytica*. PLOS Pathogens **6**, e1000812.

Dolezal, P., Smid, O., Rada, P., Zubacova, Z., Bursac, D., Sutak, R., Nebesarova, J., Lithgow, T., Tachezy, J., 2005. Giardia mitosomes and trichomonad hydrogenosomes share a common mode of protein targeting. Proceedings of the National Academy of Sciences of the United States of America **102**, 10924–10929.

Driesener, R.C., Challand, M.R., McGlynn, S.E., Shepard, E.M., Boyd, E.S., Broderick, J.B., Peters, J.W., Roach, P.L., 2010. [FeFe]-Hydrogenase Cyanide Ligands Derived From S-Adenosylmethionine-Dependent Cleavage of Tyrosine. Angewandte Chemie International Edition **49**, 1687–1690.

Emanuelsson, O., Brunak, S., von Heijne, G., Nielsen, H., 2007. Locating proteins in the cell using TargetP, SignalP and related tools. Nature Protocols **2**, 953–971.

Emelyanov, V.V., Goldberg, A.V., 2011. Fermentation enzymes of *Giardia intestinalis*, pyruvate:ferredoxin oxidoreductase and hydrogenase, do not localize to its mitosomes. Microbiology **157**, 1602–1611.

Fernandes, H.S., Ramos, M.J., Cerqueira, N.M.F.S.A., 2018. Catalytic Mechanism of the Serine Hydroxymethyltransferase: A Computational ONIOM QM/MM Study. ACS Catalysis **8**, 10096–10110.

Fontecave, M., Choudens, S.O. de, Py, B., Barras, F., 2005. Mechanisms of iron–sulfur cluster assembly: the SUF machinery. Journal of Biological Inorganic Chemistry **10**, 713–721.

Foury, F., Roganti, T., 2002. Deletion of the Mitochondrial Carrier Genes *MRS3* and *MRS4* Suppresses Mitochondrial Iron Accumulation in a Yeast Frataxin-deficient Strain. Journal of Biological Chemistry **277**, 24475–24483.

Fukasawa, Y., Tsuji, J., Fu, S.-C., Tomii, K., Horton, P., Imai, K., 2015. MitoFates: improved prediction of mitochondrial targeting sequences and their cleavage sites. Molecular & Cellular Proteomics **14**, 1113–1126.

Garcin, E., Vernede, X., Hatchikian, E., Volbeda, A., Frey, M., Fontecilla-Camps, J., 1999. The crystal structure of a reduced [NiFeSe] hydrogenase provides an image of the activated catalytic center. Structure **7**, 557–566.

Gawryluk, R.M.R., Chisholm, K.A., Pinto, D.M., Gray, M.W., 2014. Compositional complexity of the mitochondrial proteome of a unicellular eukaryote (*Acanthamoeba castellanii*, supergroup Amoebozoa) rivals that of animals, fungi, and plants. Journal of Proteomics **109**, 400–416.

Gawryluk, R.M.R., Kamikawa, R., Stairs, C.W., Silberman, J.D., Brown, M.W., Roger, A.J., 2016. The Earliest Stages of Mitochondrial Adaptation to Low Oxygen Revealed in a Novel Rhizarian. Current Biology **26**, 2729–2738.

Gelling, C., Dawes, I.W., Richhardt, N., Lill, R., Muhlenhoff, U., 2008. Mitochondrial Iba57p Is Required for Fe/S Cluster Formation on Aconitase and Activation of Radical SAM Enzymes. Molecular and Cellular Biology **28**, 1851–1861.

Gill, E.E., Diaz-Triviño, S., Barberà, M.J., Silberman, J.D., Stechmann, A., Gaston, D., Tamas, I., Roger, A.J., 2007. Novel mitochondrion-related organelles in the anaerobic amoeba *Mastigamoeba balamuthi*: Novel mitochondrion-related organelles in *M. balamuthi*. Molecular Microbiology **66**, 1306–1320.

Herzig, S., Raemy, E., Montessuit, S., Veuthey, J.-L., Zamboni, N., Westermann, B., Kunji, E.R.S., Martinou, J.-C., 2012. Identification and Functional Expression of the Mitochondrial Pyruvate Carrier. Science **337**, 93–96.

Higuchi, Y., Yagi, T., Yasuoka, N., 1997. Unusual ligand structure in Ni–Fe active center and an additional Mg site in hydrogenase revealed by high resolution X-ray structure analysis. Structure **5**, 1671–1680.

Hoffmeister, M., van der Klei, A., Rotte, C., van Grinsven, K.W.A., van Hellemond, J.J., Henze, K., Tielens, A.G.M., Martin, W., 2004. *Euglena gracilis* Rhodoquinone:Ubiquinone Ratio and Mitochondrial Proteome Differ under Aerobic and Anaerobic Conditions. Journal of Biological Chemistry **279**, 22422–22429.

Hrdy, I., Hirt, R.P., Dolezal, P., Bardonová, L., Foster, P.G., Tachezy, J., Martin Embley, T., 2004. *Trichomonas* hydrogenosomes contain the NADH dehydrogenase module of mitochondrial complex I. Nature **432**, 618–622.

Inui, H., Ono, K., Miyatake, K., Nakano, Y., Kitaoka, S., 1987. Purification and characterization of pyruvate:NADP+ oxidoreductase in *Euglena gracilis*. Journal of Biological Chemistry **262**, 9130–9135.

Jedelský, P.L., Doležal, P., Rada, P., Pyrih, J., Šmíd, O., Hrdý, I., Šedinová, M., Marcinčiková, M., Voleman, L., Perry, A.J., Beltrán, N.C., Lithgow, T., Tachezy, J., 2011. The Minimal Proteome in the Reduced Mitochondrion of the Parasitic Protist *Giardia intestinalis*. PLOS ONE **6**, e17285.

Jerlström-Hultqvist, J., Einarsson, E., Xu, F., Hjort, K., Ek, B., Steinhauf, D., Hultenby, K., Bergquist, J., Andersson, J.O., Svärd, S.G., 2013. Hydrogenosomes in the diplomonad *Spironucleus salmonicida*. Nature Communications **4**.

Johnson, D.C., Dean, D.R., Smith, A.D., Johnson, M.K., 2005. Structure, function, and formation of biological iron-sulfur clusters, in: Annual Review of Biochemistry. Annual Reviews, Palo Alto, pp. 247–281.

Jørgensen, A., Sterud, E., 2006. The Marine Pathogenic Genotype of *Spironucleus barkhanus* from Farmed Salmonids Redescribed as *Spironucleus salmonicida* n. sp. Journal of Eukaryotic Microbiology **53**, 531–541.

Karnkowska, A., Vacek, V., Zubáčová, Z., Treitli, S.C., Petrželková, R., Eme, L., Novák, L., Žárský, V., Barlow, L.D., Herman, E.K., Soukal, P., Hroudová, M., Doležal, P., Stairs, C.W., Roger, A.J., Eliáš, M., Dacks, J.B., Vlček, Č., Hampl, V., 2016. A Eukaryote without a Mitochondrial Organelle. Current Biology **26**, 1274–1284.

Katinka, M.D., Duprat, S., Cornillot, E., Méténier, G., Thomarat, F., Prensier, G., Barbe, V., Peyretaillade, E., Brottier, P., Wincker, P., Delbac, F., El Alaoui, H., Peyret, P., Saurin, W., Gouy, M., Weissenbach, J., Vivarès, C.P., 2001. Genome sequence and gene compaction of the eukaryote parasite *Encephalitozoon cuniculi*. Nature **414**, 450–453.

Kato, S. -i., Mihara, H., Kurihara, T., Takahashi, Y., Tokumoto, U., Yoshimura, T., Esaki, N., 2002. Cys-328 of IscS and Cys-63 of IscU are the sites of disulfide bridge formation in a covalently bound IscS/IscU complex: Implications for the mechanism of iron-sulfur cluster assembly. Proceedings of the National Academy of Sciences **99**, 5948–5952.

Keeling, P.J., Doolittle, W.F., 1997. Widespread and ancient distribution of a noncanonical genetic code in diplomonads. Molecular Biology and Evolution **14**, 895–901.

Keeling, P.J., Doolittle, W.F., 1996. A non-canonical genetic code in an early diverging eukaryotic lineage. EMBO Journal **15**, 2285–2290.

Kent, M., Ellis, J., Fournie, J., Dawe, S., Bagshaw, J., Whitaker, D., 1992. Systemic Hexamitid (protozoa, Diplomonadida) Infection in Seawater Pen-Reared Chinook Salmon *Oncorhynchus tshawytscha*. Diseases of Aquatic Organisms **14**, 81–89.

Kiley, P.J., Beinert, H., 1998. Oxygen sensing by the global regulator, FNR: the role of the iron-sulfur cluster. FEMS Microbiology Reviews **22**, 341–352.

Kim, K.-D., Chung, W.-H., Kim, H.-J., Lee, K.-C., Roe, J.-H., 2010. Monothiol glutaredoxin Grx5 interacts with Fe–S scaffold proteins Isa1 and Isa2 and supports Fe–S assembly and DNA integrity in mitochondria of fission yeast. Biochemical and Biophysical Research Communications **392**, 467–472.

Kispal, G., Csere, P., Guiard, B., Lill, R., 1997. The ABC transporter Atm1p is required for mitochondrial iron homeostasis. FEBS Letters **418**, 346–350.

Kispal, G., Csere, P., Prohl, C., Lill, R., 1999. The mitochondrial proteins Atm1p and Nfs1p are essential for biogenesis of cytosolic Fe/S proteins. The EMBO Journal **18**, 3981–3989.

Knoll, A.H., Javaux, E.J., Hewitt, D., Cohen, P., 2006. Eukaryotic organisms in Proterozoic oceans. Philosophical Transactions of the Royal Society B: Biological Sciences **361**, 1023–1038.

Kobayashi, M., Matsuo, Y., Takimoto, A., Suzuki, S., Maruo, F., Shoun, H., 1996. Denitrification, a Novel Type of Respiratory Metabolism in Fungal Mitochondrion. Journal of Biological Chemistry **271**, 16263–16267.

Kolisko, M., Cepicka, I., Hampl, V., Leigh, J., Roger, A.J., Kulda, J., Simpson, A.G., Flegr, J., 2008. Molecular phylogeny of diplomonads and enteromonads based on SSU rRNA, alpha-tubulin and HSP90 genes: Implications for the evolutionary history of the double karyomastigont of diplomonads. BMC Evolutionary Biology **8**, 205.

Kolisko, M., Silberman, J.D., Cepicka, I., Yubuki, N., Takishita, K., Yabuki, A., Leander, B.S., Inouye, I., Inagaki, Y., Roger, A.J., Simpson, A.G.B., 2010. A wide diversity of previously undetected free-living relatives of diplomonads isolated from marine/saline habitats. Environmental Microbiology **12**, 2700–2710.

Komuniecki, R., McCrury, J., Thissen, J., Rubin, N., 1989. Electron-transfer flavoprotein from anaerobic *Ascaris suum* mitochondria and its role in NADH-dependent 2-methyl branched-chain enoyl-CoA reduction. Biochimica et Biophysica Acta (BBA) - Bioenergetics **975**, 127–131.

Laemmli, U.K., 1970. Cleavage of Structural Proteins during the Assembly of the Head of Bacteriophage T4. Nature **227**, 680–685.

LaGier, M.J., 2003. Mitochondrial-type iron-sulfur cluster biosynthesis genes (IscS and IscU) in the apicomplexan *Cryptosporidium parvum*. Microbiology **149**, 3519–3530.

Lantsman, Y., Tan, K.S.W., Morada, M., Yarlett, N., 2008. Biochemical characterization of a mitochondrial-like organelle from *Blastocystis sp.* subtype 7. Microbiology **154**, 2757–2766.

Layer, G., Ollagnier-de Choudens, S., Sanakis, Y., Fontecave, M., 2006. Iron-Sulfur Cluster Biosynthesis: CHARACTERIZATION OF *ESCHERICHIA COLI* CYaY AS AN IRON DONOR FOR THE ASSEMBLY OF [2Fe-2S] CLUSTERS IN THE SCAFFOLD IscU. Journal of Biological Chemistry **281,** 16256–16263.

Leger, M.M., Kolisko, M., Kamikawa, R., Stairs, C.W., Kume, K., Čepička, I., Silberman, J.D., Andersson, J.O., Xu, F., Yabuki, A., Eme, L., Zhang, Q., Takishita, K., Inagaki, Y., Simpson, A.G.B., Hashimoto, T., Roger, A.J., 2017. Organelles that illuminate the origins of *Trichomonas* hydrogenosomes and *Giardia* mitosomes. Nature Ecology & Evolution **1**, 0092.

Leighton, J., Schatz, G., 1995. An ABC transporter in the mitochondrial inner membrane is required for normal growth of yeast. The EMBO Journal **14**, 188–195.

Lill, R., Diekert, K., Kaut, A., Lange, H., Pelzer, W., Prohl, C., Kispal, G., 2005. The Essential Role of Mitochondria in the Biogenesis of Cellular Iron-Sulfur Proteins. Biological Chemistry **380**, 1157–1166.

Lill, R., Mühlenhoff, U., 2005. Iron–sulfur-protein biogenesis in eukaryotes. Trends in Biochemical Sciences **30**, 133–141.

Lindmark, D.G., Müller, M., 1973. Hydrogenosome, a Cytoplasmic Organelle of the Anaerobic Flagellate *Tritrichomonas foetus*, and Its Role in Pyruvate Metabolism. Journal of Biological Chemistry **248**, 7724–7728.

Lloyd, D., Ralphs, J.R., Harris, J.C., 2002. *Giardia intestinalis*, a eukaryote without hydrogenosomes, produces hydrogen. Microbiology **148**, 727–733.

López-García, P., Eme, L., Moreira, D., 2017. Symbiosis in eukaryotic evolution. Journal of Theoretical Biology **434**, 20–33.

Maguire, F., Richards, T.A., 2014. Organelle Evolution: A Mosaic of 'Mitochondrial' Functions. Current Biology **24**, 1563.

Mai, Z., Ghosh, S., Frisardi, M., Rosenthal, B., Rogers, R., Samuelson, J., 1999. Hsp60 Is Targeted to a Cryptic Mitochondrion-Derived Organelle ("Crypton") in the Microaerophilic Protozoan Parasite *Entamoeba histolytica*. Molecular and Cellular Biology **19**, 2198–2205.

Martijn, J., Ettema, T.J.G., 2013. From archaeon to eukaryote: the evolutionary dark ages of the eukaryotic cell. Biochemical Society Transactions **41**, 451–457.

Martijn, J., Vosseberg, J., Guy, L., Offre, P., Ettema, T.J.G., 2018. Deep mitochondrial origin outside the sampled alphaproteobacteria. Nature **557**, 101.

Martin, W., Müller, M., 1998. The hydrogen hypothesis for the first eukaryote. Nature **392**, 37.

Martin, W.F., Garg, S., Zimorski, V., 2015. Endosymbiotic theories for eukaryote origin. Philosophical Transactions of the Royal Society B: Biological Sciences **370**, 20140330.

Martincová, E., Voleman, L., Najdrová, V., De Napoli, M., Eshar, S., Gualdron, M., Hopp, C.S., Sanin, D.E., Tembo, D.L., Van Tyne, D., Walker, D., Marcinčiková, M., Tachezy, J., Doležal, P., 2012. Live Imaging of Mitosomes and Hydrogenosomes by HaloTag Technology. PLoS One **7**.

Martincova, E., Voleman, L., Pyrih, J., Zarsky, V., Vondrackova, P., Kolisko, M., Tachezy, J., Dolezal, P., 2015. Probing the Biology of *Giardia intestinalis* Mitosomes Using In Vivo Enzymatic Tagging. Molecular and Cellular Biology **35**, 2864–2874.

Melber, A., Na, U., Vashisht, A., Weiler, B.D., Lill, R., Wohlschlegel, J.A., Winge, D.R., 2016. Role of Nfu1 and Bol3 in iron-sulfur cluster transfer to mitochondrial clients. eLife **5**, e15991.

Meyer, J., 2007. [FeFe] hydrogenases and their evolution: a genomic perspective. Cellular and Molecular Life Sciences **64**, 1063.

Mi-ichi, F., Makiuchi, T., Furukawa, A., Sato, D., Nozaki, T., 2011. Sulfate Activation in Mitosomes Plays an Important Role in the Proliferation of *Entamoeba histolytica*. PLoS Neglected Tropical Diseases **5**, e1263.

Mi-ichi, F., Yousuf, M.A., Nakada-Tsukui, K., Nozaki, T., 2009. Mitosomes in *Entamoeba histolytica* contain a sulfate activation pathway. Proceedings of the National Academy of Sciences **106**, 21731–21736.

Mikhailov, K.V., Simdyanov, T.G., Aleoshin, V.V., 2016. Genomic survey of a hyperparasitic microsporidian *Amphiamblys* sp. (Metchnikovellidae). Genome Biology and Evolution **9**, 454-467.

Miller, W.L., 1995. Mitochondrial specificity of the early steps in steroidogenesis. The Journal of Steroid Biochemistry and Molecular Biology, The Molecular and Cell Biology of Hydroxysteroid Dehydrogenases **55**, 607–616.

Millet, C.O.M., Cable, J., Lloyd, D., 2010. The Diplomonad Fish Parasite *Spironucleus vortens* Produces Hydrogen. Journal of Eukaryotic Microbiology **57**, 400–404.

Millet, C.O.M., Williams, C.F., Hayes, A.J., Hann, A.C., Cable, J., Lloyd, D., 2013. Mitochondria-derived organelles in the diplomonad fish parasite *Spironucleus vortens*. Experimental Parasitology **135**, 262–273.

Mooberry, S.L., Tien, G., Hernandez, A.H., Plubrukarn, A., Davidson, B.S., 1999. Laulimalide and isolaulimalide, new paclitaxel-like microtubule-stabilizing agents. Cancer Research **59**, 653–660.

Mühlenhoff, U., Richter, N., Pines, O., Pierik, A.J., Lill, R., 2011. Specialized Function of Yeast Isa1 and Isa2 Proteins in the Maturation of Mitochondrial [4Fe-4S] Proteins. Journal of Biological Chemistry **286**, 41205–41216.

Muller, M., 1993. The Hydrogenosome. Journal of General Microbiology **139**, 2879–2889.

Muller, M., Mentel, M., van Hellemond, J.J., Henze, K., Woehle, C., Gould, S.B., Yu, R.-Y., van der Giezen, M., Tielens, A.G.M., Martin, W.F., 2012. Biochemistry and Evolution of Anaerobic Energy Metabolism in Eukaryotes. Microbiology and Molecular Biology Reviews **76**, 444–495.

Mus, F., Dubini, A., Seibert, M., Posewitz, M.C., Grossman, A.R., 2007. Anaerobic Acclimation in *Chlamydomonas reinhardtii*: ANOXIC GENE EXPRESSION, HYDROGENASE INDUCTION, AND METABOLIC PATHWAYS. Journal of Biological Chemistry **282**, 25475–25486.

Nachin, L., Hassouni, M.E., Loiseau, L., Expert, D., Barras, F., 2001. SoxR-dependent response to oxidative stress and virulence of *Erwinia chrysanthemi*: the key role of SufC, an orphan ABC ATPase. Molecular Microbiology **39**, 960–972.

Nakai, K., Horton, P., 1999. PSORT: a program for detecting sorting signals in proteins and predicting their subcellular localization. Trends in Biochemical Sciences **24**, 34–36.

Nakamura, M., Saeki, K., Takahashi, Y., 1999. Hyperproduction of Recombinant Ferredoxins in *Escherichia coli* by Coexpression of the ORF1-ORF2-iscS-iscU-iscA-hscB-hscA-fdx-ORF3 Gene Cluster. Journal of Biochemistry **126**, 10–18.

Neupert, W., Herrmann, J.M., 2007. Translocation of Proteins into Mitochondria. Annual Review of Biochemistry **76**, 723–749.

Nicolet, Y., Fontecilla-Camps, J.C., Fontecave, M., 2010. Maturation of [FeFe]-hydrogenases: Structures and mechanisms. International Journal of Hydrogen Energy, Indo-French Workshop on Biohydrogen: from Basic Concepts to Technology **35**, 10750–10760.

Nicolet, Y., Rubach, J.K., Posewitz, M.C., Amara, P., Mathevon, C., Atta, M., Fontecave, M., Fontecilla-Camps, J.C., 2008. X-ray Structure of the [FeFe]-Hydrogenase Maturase HydE from *Thermotoga maritima*. Journal of Biological Chemistry **283**, 18861–18872.

Nixon, J.E.J., Field, J., McArthur, A.G., Sogin, M.L., Yarlett, N., Loftus, B.J., Samuelson, J., 2003. Iron-Dependent Hydrogenases of *Entamoeba histolytica* and *Giardia lamblia*: Activity of the Recombinant Entamoebic Enzyme and Evidence for Lateral Gene Transfer. The Biological Bulletin **204**, 1–9.

Noguchi, F., Shimamura, S., Nakayama, T., Yazaki, E., Yabuki, A., Hashimoto, T., Inagaki, Y., Fujikura, K., Takishita, K., 2015. Metabolic Capacity of Mitochondrion-related Organelles in the Free-living Anaerobic Stramenopile *Cantina marsupialis*. Protist **166**, 534–550.

Nývltová, E., Stairs, C.W., Hrdý, I., Rídl, J., Mach, J., Pačes, J., Roger, A.J., Tachezy, J., 2015. Lateral Gene Transfer and Gene Duplication Played a Key Role in the Evolution of *Mastigamoeba balamuthi* Hydrogenosomes. Molecular Biology and Evolution **32**, 1039–1055.

Nyvltova, E., Sutak, R., Harant, K., Sedinova, M., Hrdy, I., Paces, J., Vlcek, C., Tachezy, J., 2013. NIF-type iron-sulfur cluster assembly system is duplicated and distributed in the mitochondria and cytosol of *Mastigamoeba balamuthi*. Proceedings of the National Academy of Sciences **110**, 7371–7376.

Ogden, R.C., Adams, D.A., 1987. Electrophoresis in agarose and acrylamide gels. Methods in Enzymology **152**, 61–87.

Pandey, A., Gordon, D.M., Pain, J., Stemmler, T.L., Dancis, A., Pain, D., 2013. Frataxin Directly Stimulates Mitochondrial Cysteine Desulfurase by Exposing Substrate-binding Sites, and a Mutant Fe-S Cluster Scaffold Protein with Frataxin-bypassing Ability Acts Similarly. Journal of Biological Chemistry **288**, 36773–36786.

Parent, A., Elduque, X., Cornu, D., Belot, L., Le Caer, J.-P., Grandas, A., Toledano, M.B., D'Autréaux, B., 2015. Mammalian frataxin directly enhances sulfur transfer of NFS1 persulfide to both ISCU and free thiols. Nature Communications **6**.

Parvatham, K., Veerakumari, L., 2013. Drug target prediction using elementary mode analysis in *Ascaris lumbricoides* energy metabolism. Biotechnology and Bioprocess Engineering **18**, 491–500.

Pastore, C., Franzese, M., Sica, F., Temussi, P., Pastore, A., 2007. Understanding the binding properties of an unusual metal-binding protein − a study of bacterial frataxin: Metal-binding properties of CyaY. FEBS Journal **274**, 4199–4210.

Paull, G.C., Matthews, R.A., 2001. *Spironucleus vortens*, a possible cause of hole-in-the-head disease in cichlids. Diseases of Aquatic Organisms **45**, 197–202.

Peña-Diaz, P., Lukeš, J., 2018. Fe–S cluster assembly in the supergroup Excavata. Journal of Biological Inorganic Chemistry **23**, 521–541.

Pilak, O., Mamat, B., Vogt, S., Hagemeier, C.H., Thauer, R.K., Shima, S., Vonrhein, C., Warkentin, E., Ermler, U., 2006. The Crystal Structure of the Apoenzyme of the Iron–Sulphur Cluster-free Hydrogenase. Journal of Molecular Biology **358**, 798–809.

Posewitz, M.C., King, P.W., Smolinski, S.L., Zhang, L., Seibert, M., Ghirardi, M.L., 2004. Discovery of Two Novel Radical *S* -Adenosylmethionine Proteins Required for the Assembly of an Active [Fe] Hydrogenase. Journal of Biological Chemistry **279**, 25711–25720.

Pütz, S., Dolezal, P., Gelius-Dietrich, G., Bohacova, L., Tachezy, J., Henze, K., 2006. Fe-Hydrogenase Maturases in the Hydrogenosomes of *Trichomonas vaginalis*. Eukaryotic Cell **5**, 579–586.

Py, B., Gerez, C., Angelini, S., Planel, R., Vinella, D., Loiseau, L., Talla, E., Brochier-Armanet, C., Garcia Serres, R., Latour, J.-M., Ollagnier-de Choudens, S., Fontecave, M., Barras, F., 2012. Molecular organization, biochemical function, cellular role and evolution of NfuA, an atypical Fe-S carrier: Role of NfuA in Fe-S biosynthesis. Molecular Microbiology **86**, 155–171.

Pyrih, J., Pyrihová, E., Kolísko, M., Stojanovová, D., Basu, S., Harant, K., Haindrich, A.C., Doležal, P., Lukeš, J., Roger, A., Tachezy, J., 2016. Minimal cytosolic iron-sulfur cluster assembly machinery of *Giardia intestinalis* is partially associated with mitosomes. Molecular Microbiology **102**, 701–714.

Pyrihová, E., Motyčková, A., Voleman, L., Wandyszewska, N., Fišer, R., Seydlová, G., Roger, A., Kolísko, M., Doležal, P., 2018. A Single Tim Translocase in the Mitosomes of *Giardia intestinalis* Illustrates Convergence of Protein Import Machines in Anaerobic Eukaryotes. Genome Biology and Evolution **10**, 2813–2822.

Rada, P., Šmíd, O., Sutak, R., Doležal, P., Pyrih, J., Žárský, V., Montagne, J.-J., Hrdý, I., Camadro, J.-M., Tachezy, J., 2009. The Monothiol Single-Domain Glutaredoxin Is Conserved in the Highly Reduced Mitochondria of *Giardia intestinalis*. Eukaryotic Cell **8**, 1584–1591.

Rodríguez-Ezpeleta, N., Embley, T.M., 2012. The SAR11 Group of Alpha-Proteobacteria Is Not Related to the Origin of Mitochondria. PLOS ONE **7**, e30520.

Roger, A.J., Muñoz-Gómez, S.A., Kamikawa, R., 2017. The Origin and Diversification of Mitochondria. Current Biology **27**, R1177–R1192.

Rout, S., Zumthor, J.P., Schraner, E.M., Faso, C., Hehl, A.B., 2016. An Interactome-Centered Protein Discovery Approach Reveals Novel Components Involved in Mitosome Function and Homeostasis in *Giardia lamblia*. PLOS Pathogens **12**.

Sagan, L., 1967. On the origin of mitosing cells. Journal of Theoretical Biology **14**, 225-IN6.

Santos, H.J., Makiuchi, T., Nozaki, T., 2018. Reinventing an Organelle: The Reduced Mitochondrion in Parasitic Protists. Trends in Parasitology **34**, 1038–1055.

Satre, M., Kennedy, E.P., 1978. Identification of bound pyruvate essential for the activity of phosphatidylserine decarboxylase of *Escherichia coli*. Journal of Biological Chemistry **253**, 479–483.

Schneider, R.E., Brown, M.T., Shiflett, A.M., Dyall, S.D., Hayes, R.D., Xie, Y., Loo, J.A., Johnson, P.J., 2011. The *Trichomonas vaginalis* hydrogenosome proteome is highly reduced relative to mitochondria, yet complex compared with mitosomes. International Journal for Parasitology **41**, 1421–1434.

Schwartz, R.M., Dayhoff, M.O., 1978. Origins of Prokaryotes, Eukaryotes, Mitochondria, and Chloroplasts. Science **199**, 395–403.

Sheftel, A.D., Wilbrecht, C., Stehling, O., Niggemeyer, B., Elsässer, H.-P., Mühlenhoff, U., Lill, R., 2012. The human mitochondrial ISCA1, ISCA2, and IBA57 proteins are required for [4Fe-4S] protein maturation. Molecular Biology of the Cell **23**, 1157–1166.

Shepard, Eric M., Duffus, B.R., George, S.J., McGlynn, S.E., Challand, M.R., Swanson, K.D., Roach, P.L., Cramer, S.P., Peters, J.W., Broderick, J.B., 2010. [FeFe]-Hydrogenase Maturation: HydG-Catalyzed Synthesis of Carbon Monoxide. Journal of the American Chemical Society **132**, 9247–9249.

Shepard, E. M., McGlynn, S.E., Bueling, A.L., Grady-Smith, C.S., George, S.J., Winslow, M.A., Cramer, S.P., Peters, J.W., Broderick, J.B., 2010. Synthesis of the 2Fe subcluster of the [FeFe]-hydrogenase H cluster on the HydF scaffold. Proceedings of the National Academy of Sciences **107**, 10448–10453.

Shomura, Y., Yoon, K.-S., Nishihara, H., Higuchi, Y., 2011. Structural basis for a [4Fe-3S] cluster in the oxygen-tolerant membrane-bound [NiFe]-hydrogenase. Nature **479**, 253–256.

Šmíd, O., Matušková, A., Harris, S.R., Kučera, T., Novotný, M., Horváthová, L., Hrdý, I., Kutějová, E., Hirt, R.P., Embley, T.M., Janata, J., Tachezy, J., 2008. Reductive Evolution of the Mitochondrial Processing Peptidases of the Unicellular Parasites *Trichomonas vaginalis* and *Giardia intestinalis*. PLOS Pathogens **4**, e1000243.

Spang, A., Saw, J.H., Jørgensen, S.L., Zaremba-Niedzwiedzka, K., Martijn, J., Lind, A.E., van Eijk, R., Schleper, C., Guy, L., Ettema, T.J.G., 2015. Complex archaea that bridge the gap between prokaryotes and eukaryotes. Nature **521**, 173–179.

Srinivasan, V., Pierik, A.J., Lill, R., 2014. Crystal Structures of Nucleotide-Free and Glutathione-Bound Mitochondrial ABC Transporter Atm1. Science **343**, 1137–1140.

Stairs, C.W., Eme, L., Brown, M.W., Mutsaers, C., Susko, E., Dellaire, G., Soanes, D.M., van der Giezen, M., Roger, A.J., 2014. A SUF Fe-S Cluster Biogenesis System in the Mitochondrion-Related Organelles of the Anaerobic Protist *Pygsuia*. Current Biology **24**, 1176–1186.

Stechmann, A., Hamblin, K., Pérez-Brocal, V., Gaston, D., Richmond, G.S., van der Giezen, M., Clark, C.G., Roger, A.J., 2008. Organelles in *Blastocystis* that Blur the Distinction between Mitochondria and Hydrogenosomes. Current Biology **18**, 580–585.

Sterud, E., Poynton, S.L., 2002. *Spironucleus vortens* (Diplomonadida) in the Ide, *Leuciscus idus* (L.) (Cyprinidae): a Warm Water Hexamitid Flagellate Found in Northern Europe. Journal of Eukaryotic Microbiology **49**, 137–145.

Tachezy, J., Sánchez, L.B., Müller, M., 2001. Mitochondrial Type Iron-Sulfur Cluster Assembly in the Amitochondriate Eukaryotes *Trichomonas vaginalis* and *Giardia intestinalis*, as Indicated by the Phylogeny of IscS. Molecular Biology and Evolution **18**, 1919–1928.

Takahashi, Y., Tokumoto, U., 2002. A Third Bacterial System for the Assembly of Iron-Sulfur Clusters with Homologs in Archaea and Plastids. Journal of Biological Chemistry **277**, 28380–28383.

Takamiya, S., Matsui, T., Taka, H., Murayama, K., Matsuda, M., Aoki, T., 1999. Free-Living Nematodes *Caenorhabditis elegans* Possess in Their Mitochondria an Additional Rhodoquinone, an Essential Component of the Eukaryotic Fumarate Reductase System. Archives of Biochemistry and Biophysics **371**, 284–289.

Takishita, K., Kolisko, M., Komatsuzaki, H., Yabuki, A., Inagaki, Y., Cepicka, I., Smejkalová, P., Silberman, J.D., Hashimoto, T., Roger, A.J., Simpson, A.G.B., 2012. Multigene Phylogenies of Diverse Carpediemonas-like Organisms Identify the Closest Relatives of 'Amitochondriate' Diplomonads and Retortamonads. Protist **163**, 344–355.

Tielens, A.G.M., 1994. Energy generation in parasitic helminths. Parasitology Today **10**, 346–352.

Tielens, A.G.M., Rotte, C., van Hellemond, J.J., Martin, W., 2002. Mitochondria as we don't know them. Trends in Biochemical Sciences **27**, 564–572.

Tovar, J., Fischer, A., Clark, C.G., 1999. The mitosome, a novel organelle related to mitochondria in the amitochondrial parasite *Entamoeba histolytica*. Molecular Microbiology **32**, 1013–1021.

Tovar, J., León-Avila, G., Sánchez, L.B., Sutak, R., Tachezy, J., van der Giezen, M., Hernández, M., Müller, M., Lucocq, J.M., 2003. Mitochondrial remnant organelles of *Giardia* function in iron-sulphur protein maturation. Nature **426**, 172–176.

Tsaousis, A.D., Nyvltova, E., Sutak, R., Hrdy, I., Tachezy, J., 2014. A Nonmitochondrial Hydrogen Production in *Naegleria gruberi*. Genome Biology and Evolution **6**, 792–799.

Tsaousis, A.D., Ollagnier de Choudens, S., Gentekaki, E., Long, S., Gaston, D., Stechmann, A., Vinella, D., Py, B., Fontecave, M., Barras, F., Lukes, J., Roger, A.J., 2012. Evolution of Fe/S cluster biogenesis in the anaerobic parasite *Blastocystis*. Proceedings of the National Academy of Sciences **109**, 10426–10431.

Urbina, H.D., Silberg, J.J., Hoff, K.G., Vickery, L.E., 2001. Transfer of Sulfur from IscS to IscU during Fe/S Cluster Assembly. Journal of Biological Chemistry **276**, 44521–44526.

Uzarska, M.A., Dutkiewicz, R., Freibert, S.-A., Lill, R., Mühlenhoff, U., 2013. The mitochondrial Hsp70 chaperone Ssq1 facilitates Fe/S cluster transfer from Isu1 to Grx5 by complex formation. Molecular Biology of the Cell **24**, 1830–1841.

Van Vranken, J.G., Jeong, M.-Y., Wei, P., Chen, Y.-C., Gygi, S.P., Winge, D.R., Rutter, J., 2016. The mitochondrial acyl carrier protein (ACP) coordinates mitochondrial fatty acid synthesis with iron sulfur cluster biogenesis. eLife **5**, e17828.

Vignais, P.M., Billoud, B., 2007. Occurrence, Classification, and Biological Function of Hydrogenases: An Overview. Chemical Reviews **107**, 4206–4272.

Vignais, P.M., Billoud, B., Meyer, J., 2001. Classification and phylogeny of hydrogenases. FEMS Microbiology Reviews **25**, 455–501.

Voleman, L., Najdrová, V., Ástvaldsson, Á., Tůmová, P., Einarsson, E., Švindrych, Z., Hagen, G.M., Tachezy, J., Svärd, S.G., Doležal, P., 2017. *Giardia intestinalis* mitosomes undergo synchronized fission but not fusion and are constitutively associated with the endoplasmic reticulum. BMC Biology **15**.

Wang, Z., Wu, M., 2015. An integrated phylogenomic approach toward pinpointing the origin of mitochondria. Scientific Reports **5**, 7949.

Wiedemann, N., Urzica, E., Guiard, B., Müller, H., Lohaus, C., Meyer, H.E., Ryan, M.T., Meisinger, C., Mühlenhoff, U., Lill, R., Pfanner, N., 2006. Essential role of Isd11 in mitochondrial iron–sulfur cluster synthesis on Isu scaffold proteins. The EMBO Journal **25**, 184–195.

Williams, B.A.P., Hirt, R.P., Lucocq, J.M., Embley, T.M., 2002. A mitochondrial remnant in the microsporidian *Trachipleistophora hominis*. Nature **418**, 865–869.

Williams, C.F., Millet, C.O.M., Hayes, A.J., Cable, J., Lloyd, D., 2013. Diversity in mitochondrion-derived organelles of the parasitic diplomonads *Spironucleus* and *Giardia*. Trends in Parasitology **29**, 311–312.

Xu, F., Jerlström-Hultqvist, J., Kolisko, M., Simpson, A.G.B., Roger, A.J., Svärd, S.G., Andersson, J.O., 2016. On the reversibility of parasitism: adaptation to a free-living lifestyle via gene acquisitions in the diplomonad *Trepomonas sp.* PC1. BMC Biology **14**, 62.

Yaffe, M.P., Ohta, S., Schatz, G., 1985. A yeast mutant temperature-sensitive for mitochondrial assembly is deficient in a mitochondrial protease activity that cleaves imported precursor polypeptides. The EMBO Journal **4**, 2069–2074.

Yagi, T., Higuchi, Y., 2013. Studies on hydrogenase. Proceedings of the Japan Academy, Series B **89**, 16–33.

Yang, D., Oyaizu, Y., Oyaizu, H., Olsen, G., Woese, C., 1985. Mitochondrial Origins. Proceedings of the National Academy of Sciences of the United States of America **82**, 4443–4447.

Youssef, N.H., Couger, M.B., Struchtemeyer, C.G., Liggenstoffer, A.S., Prade, R.A., Najar, F.Z., Atiyeh, H.K., Wilkins, M.R., Elshahed, M.S., 2013. The Genome of the Anaerobic Fungus *Orpinomyces sp.* Strain C1A Reveals the Unique Evolutionary History of a Remarkable Plant Biomass Degrader. Applied and Environmental Microbiology **79**, 4620–4634.

Zaremba-Niedzwiedzka, K., Caceres, E.F., Saw, J.H., Bäckström, D., Juzokaite, L., Vancaester, E., Seitz, K.W., Anantharaman, K., Starnawski, P., Kjeldsen, K.U., Stott, M.B., Nunoura, T., Banfield, J.F., Schramm, A., Baker, B.J., Spang, A., Ettema, T.J.G., 2017. Asgard archaea illuminate the origin of eukaryotic cellular complexity. Nature **541**, 353–358.

Zborowski, J., Dygas, A., Wojtczak, L., 1983. Phosphatidylserine decarboxylase is located on the external side of the inner mitochondrial membrane. FEBS Letters **157**, 179–182.

Zheng, L., White, R.H., Cash, V.L., Dean, D.R., 1994. Mechanism for the Desulfurization of L-Cysteine Catalyzed by the nifS Gene Product. Biochemistry **33**, 4714–4720.

Zheng, L., White, R.H., Cash, V.L., Jack, R.F., Dean, D.R., 1993. Cysteine desulfurase activity indicates a role for NIFS in metallocluster biosynthesis. Proceedings of the National Academy of Sciences **90**, 2754–2758.